



### This is to certify that the

### thesis entitled

# AN AUTOMATED REAGENT PREPARATION SYSTEM FOR FAST REACTION-RATE ANALYSES

presented by

Rytis Tomas Balciunas

has been accepted towards fulfillment of the requirements for

Ph.D. degree in Chemistry

Major professor

Date\_\_\_\_5/19/81

**O**-7639

**U**-/638



#### OVERDUE FINES: 25¢ per day per item

# RETURNING LIBRARY MATERIALS: Place in book return to remove charge from circulation records

# AN AUTOMATED REAGENT PREPARATION SYSTEM FOR FAST REACTION-RATE ANALYSES

Ву

Rytis Tomas Balciunas

#### A DISSERTATION

Submitted to
Michigan State University
in partial fulfillment of the requirements
for the degree of

DOCTOR OF PHILOSOPHY

Department of Chemistry

1981

Mamytei ir Tėtukui

#### **ABSTRACT**

# AN AUTOMATED REAGENT PREPARATION SYSTEM FOR FAST REACTION-RATE ANALYSES

Βv

#### Rytis Tomas Balciunas

The design, operation, and evaluation of an automated system for fast reaction-rate measurements that utilizes a microcomputer-controlled reagent preparation device is described.

The modular, stepper motor-driven syringe-based reagent preparation system features a dilution range of up to five orders of magnitude from a single stock solution, with 0.1% RSD or better. Reagents are prepared from up to three different stock solutions and a diluent. Reproducibility of the delivered stock solutions and of the dilution process is better than Class A glassware in all cases tested. The operational hardware and software descriptions are presented, with detailed circuitry and timing of the microcomputer operations. The results of several chemical complexation studies are presented as a demonstration of the precision and utility of the system. The reagent preparation device offers some improvement in the time required for the preparation of solutions and a significant increase in the precision and reliability of preparation of working reagents.

The reconstruction, documentation, and evaluation details of the automated stopped-flow instrument used for

fast reaction-rate studies are presented. The instrument is capable of a throughput rate of 50-60 samples per hour and can be used for rate measurements for periods of 100 ms (1 ms resolution) or greater. The results of several kinetics studies that establish the performance specifications of the instrument are presented. The automated stopped-flow device is used with the automated reagent preparation system for several reaction characterization studies.

Preliminary results of the characterization of the chemiluminescence reaction of luminol and hypochlorite are presented. A potentially useful method for indirectly determining ammonia in solution using the chemiluminescence reaction is described.

#### **ACKNOWLEDGEMENTS**

First and foremost, I would like to thank Dr. Stan Crouch for the opportunity to experience the joys and frustrations of independent research. Also, my thanks to the machine shop personnel, Russ Geyer, Dick Menke, and Len Eisle, for their patience and advice during the construction phase of the reagent prenaration system. I am also grateful to Ron Haas of the electronics shop for the many helpful consultations concerning practical electronics throughout the course of various projects.

A special note of thanks goes to Dr. Tom Atkinson for many days and weeks of work on the plotting packages available on the department's CemComGraf. Without these, the graphics in this thesis would not have been possible.

My thanks to the chemistry department for providing monetary support in the form of teaching assistanships and to Dr. Crouch for financial assistance in the form of research support.

I am grateful to the Moose Farm, the Tammany House, and the Crouch group members past and present for their friendship: without them, life in this winter wonderland would have been indeed very dull. A special thanks to Chasmo, Phil, and Tieck for being good friends and always ready to bend an elbow or two.

Finally, my deepest and sincerest gratitude goes to my parents. Without them, without their help and support, I would have never had a life worth living.

# TABLE OF CONTENTS

	age
LIST OF TABLES	vi
LIST OF FIGURES	vii
CHAPTER I - THE PHILOSOPHY AND PRACTICE OF AUTOMATED  CHEMICAL ANALYSIS	. 1
CHAPTER II - OVERVIEW OF AUTOMATED REAGENT PREPARATION	•
SYSTEMS DEVELOPED IN THE 1970's	. 4
A. Designs of Pardue and Co-Workers	. 6
B. Designs of the Malmstadt Group	. 7
C. Design of Stieg and Nieman	. 8
D. Early Designs of Crouch Group Workers	9
CHAPTER III - AN AUTOMATED REAGENT PREPARATION SYSTEM	. 11
A. An Overview	11
B. Considerations in the Mechanical Design	11
C. System Description-Mechanical Components	12
1. Reagent Delivery Syringes	13
	18
2. Flow Control Valves and Dilution System	22
D. System Electronics	
1. The Microcomputer	23
2. Processor Timing States	25
3. The Interface-Controller Board	32
a. Device Decoder Circuit	33
b. Valve Controls and Status Testing	34
c. Stepper Motor Waveform Generation	39
E. The Controlling Software	41
F. Sequence of Operation for a Dilution Series:	
	45
G. Reagent Preparation Sequence: Mechanical Actions	49
H. Component Evaluation	51
1. Calibration of the Syringes	53
2. Dilution Vessel Evaluation	55
3. Carry-Over of Reagents and Diluted Solution	57
	59
I. System Performance	
1. Chemical Complexation Reactions-Mole Ratio Study	. 59
2. Continuous Variations Study	61
INSTRUMENT	68
A. General Considerations	70
B. Automated Stopped-Flow System Description	75
1. The Valve Controller Module	/5
2. The Flow-Stopped Status Generator	. 77
3. The Computer Interface Module	77
4. The Data Acquisition System	. 82

					Į	age
С.	Operational Software Description					85
D.	Stopped-Flow Instrument Characteristics					91
	1. Observation Cell Path Length					91
	2. Stopped-Flow Dead Time					92
E.	Evaluation of the Performance of the Automated Reager	nt				
	Preparation System Using Reaction-Rate Methods of Ana		'si	s		92
	1. Iron-Thiocyanate Kinetics Study					93
	a. Reagents					93
	b. Procedures					94
	c. Results of Initial Rate Measurements					95
	2. Phospho-Molybdate Reaction					
	a. Reagents					
	b. Results					
CHAPTER	R V - ANALYTICAL APPLICATIONS OF THE STOPPED-FLOW					
	INSTRUMENT					105
Α.	Phosphate in Blood Serum					
	1. Reagents					
	2. Results					
В.	Determination of Ascorbic Acid by Initial Rates					
	1. Reagents					
	2. Results					
С.	Characterization of the Luminol-Hypochlorite	•			•	
	Chemiluminescence Reaction	_	_	_	_	117
	1. Reaction Mechanisms					
	2. General Procedures					
	3. Working Range for Hypochlorite Solutions					
	a. Results					
	4. Linearity of Calibration Curves	•	•			126
	5. Detection Limits for Ammonia					
	6. Stability of Hypochlorite Solutions					
	a. Hypochlorite Stability Study	•	•	•	•	137
	1) Theories Concerning Reaction Species					
	b. Stability of Hypochlorite-Ammonia Solutions					
	7. Conclusions					
СНАРТЕР	R VI - CONCLUSIONS AND FUTURE PERSPECTIVES	•	•	•	•	161
APPENDI						
	REFERENCES					

# LIST OF TABLES

		Page
Table	1.	Summary of Control Line Functions
Table	2.	Software Commands for Reagent Preparation System 35
Table	3.	Syringe Calibration Data 54
Table	4.	Volumetric Flask Delivery Precision
Table	5.	Data for Carry-Over Experiment
Table	6.	Stopped-Flow Instrument Controller Software Commands 81
Table	7.	Software Commands for Data Acquisition
		and Display System 84
Table	8.	Functions of Stopped-Flow Controller Software
		Modules
Table	9.	Phospho-Molybdate Reaction Kinetics Study Data 104
Table	10.	Results of Initial Rate Measurements of the Reaction
		of Ascorbic Acid with DCPI
Table	11.	Extended Concentration Range of Ascorbic Acid Study 115
Table	12.	Sensitivity Study Data for Luminol-Hypochlorite
		CL Reaction
Table	13.	Calibration Data for the Determination of Ammonia
		using the Luminol-Hypochlorite CL Reaction 128
Table	14.	Peak Flash Intensities of Hypochlorite Solutions
		Containing Ammonia. Solutions Prepared Manually.
		$[OC1^{-}] = 100 \ \mu M$
Table	15.	Peak Flash Intensities of Hypochlorite Solutions
		Containing Ammonia. Solutions Prepared Automatically.
		$[OC1^{-}] = 100 \ \mu M$
Table	16.	Data for Detection Limits of Ammonia. [OC1] = 10 µM.
		Solutions Prepared Automatically
Table	17.	Peak Flash Intensities of Luminol-Hypochlorite
		CL Reaction as a Function of pH

# LIST OF FIGURES

			F	age
Figure	1.	Block diagram of automated reagent preparation		
		system	•	14
Figure	2.	1 mL stepper motor-driven syringe		16
Figure	3.	Schematic of the optical meniscus detector		21
Figure	4.	Major timing states of the Intersil IM6100 microprocessor		26
Figure	5.	Input/output instruction timing of the		29
Figure	6.	IM6100 microprocessor		
		preparation system	•	33
Figure				36
Figure	8.	Stepper motor waveform generator circuit	•	40
Figure	9.	Stepper motor driver circuit	•	42
Figure	10.	Sequence of operations for automatic reagent		
Figure	11.	preparation	•	46
115410		sequence		50
Ei aumo	12	Absorbance vs. mole-ratio EDTA/Cu(II)		62
		Absorbance vs. mole-fraction 1,10-phenanthroline		64
			•	04
rigure	14.	Test of syringe interchangeability using the Fe(II)-1,10-phenanthroline reaction		66
Figure	15.	Block diagram of the automated stopped-flow	-	
Ü		instrument		74
Figure	16.	Schematic of the stopped-flow valve controller		76
Figure	17.	Schematic of the flow-stopped status signal		
		generator	•	78
Figure	18.	Schematic of the valve controller-to-minicomputer		
		interface	•	79
Figure	19.	Schematic of the 8-channel data acquisition		
		system	•	83
Figure	20.	Sequence of operations for a typical		0.0
	••	stopped-flow analysis	•	88
Figure	21.	Initial rate vs. thiocyanate concentration.		06
г.	22	Solutions prepared manually	•	96
Figure	22.	Initial rate vs. Fe(III) concentration.  Solutions prepared manually		97
Ei auma	27		•	31
rigure	23.	Initial rate <u>vs.</u> thiocyanate concentration.  Solutions prepared automatically		98
Figure	24	Initial rate vs. Fe(III) concentration.	•	50
riguic	27.	Solutions prepared automatically		99
Figure	25	Initial rate vs. phosphate concentration.	•	55
TRULE	23.	Solutions prepared manually		102
Figure	26.	Initial rate vs. phosphate concentration.	•	
0		Solutions prepared automatically		103

		Page
Figure	27.	Reaction of ascorbic acid with DCPI
		indicator solution
Figure	28.	Initial rate vs. ascorbic acid concentration 112
Figure	29.	Initial rate vs. ascorbic acid concentration.
		Extended range of ascorbic acid concentration
		study
Figure	30.	Proposed mechanism for luminol-hypochlorite
•		CL reaction (Isacsson et al. (75))
Figure	31.	Peak flash intensity of luminol as a function
ζ.		of hypochlorite concentration
Figure	32.	Reduction of CL intensity as a function of
0	-	NH <sub>z</sub> concentration
Figure	33.	Peak flash intensity of CL reaction of luminol and
-6	•	hypochlorite as a function of time
Figure	34.	Peak flash intensity vs. time, Hypochlorite
6		solution contains 3 $\mu \overline{M}$ ammonia
Figure	35.	Peak profiles of luminol-hypochlorite reaction.
6		pH = 9.0, 9.5, and 10.0
Figure	36.	Peak profiles of luminol-hypochlorite reaction.
		pH = 10.5, 11.0, and 11.5
Figure	37.	Peak profiles of luminol-hypochlorite reaction.
5	•,•	pH = 12.0 and 12.4
Figure	38.	Stability of the peak flash intensity of
60	•••	hypochlorite-luminol solutions with time
Figure	39.	Average peak flash intensity vs. pH
		Logarithmic concentration diagram for species
. 18410		present in mixed luminol-hypochlorite solutions 146
Figure	41.	Peak flash intensity as a function of pH for
. 16410	• •	solutions used in the hypochlorite-ammonia
		mixture stability study
Figure	42.	Peak profiles of the CL reaction of luminol
. 15410		solutions and solutions containing hypochlorite
		(upper curve) and solutions containing hypochlorite
		and ammonia (lower curve), pH = 9.0, 9.5 151
Figure	43.	Peak profiles of the CL reaction of luminol
. 16410	,	solutions and solutions containing hypochlorite
		(upper curve) and solutions containing hypochlorite
		and ammonia (lower curve), pH = 10.0, 10.5 152
Figure	44.	Peak profiles of the CL reaction of luminol
	• • •	solutions and solutions containing hypochlorite
		(upper curve) and solutions containing hypochlorite
		and ammonia (lower curve), pH = 11.0, 11.5 153
Figure	45	Peak profiles of the CL reaction of luminol
. 15416	73.	solutions and solutions containing hypochlorite
		(upper curve) and solutions containing hypochlorite
		and ammonia (lower curve), pH = 12.0, 12.4 154
		with dissipation (rounds out to); pir = 12:0; 12:1

					I	Page
Figure	46.	Time-stability study of ammonia-hypochlorite				
		solutions at pH 9.0, 9.5, and 10.0	•	•	•	156
Figure	47.	Time stability of ammonia-hypochlorite				
		solutions at pH 10.5 and 11.0			•	157
Figure	48.	Time stability of ammonia-hypochlorite				
_		solutions at pH 11.5, 12.0, and 12.4				158
Figure	49.	Logarithmic concentration diagram of the species				
Ü		present in luminol-hypochlorite-ammonia mixtures	•		•	159

#### CHAPTER T

THE PHILOSOPHY AND PRACTICE OF AUTOMATED CHEMICAL ANALYSIS

Advances in the development of microcircuitry in the 1970's have had a major impact on instrumental design and classical chemical analysis. Through automation the tedious and time-consuming tasks of data acquisition, data calculations, drawing of graphs, etc., have been the first to be removed from the list of manual tasks the analyst must perform. Most analytical instrumentation developed for commercial and academic research is also capable of controlling many or all of the parameters involved in a given experiment without user intervention. At first glance, it seems that the analytical chemist may be relegated to the status of button pusher or sample handler. However, as methods become more automated, the analyst's detailed knowledge of the chemical and physical processes occurring in an experiment becomes critical in the interpretation of the results produced. Ideally, an automated system that performs routine operations will leave more time for the chemist to evaluate the processes occurring rather than have him worry if the light source shutter is open or if there is enough reagent left to do a particular study. The quality and the relevance of results obtained from an experiment can be improved through automation only if

the analyst fully understands the procedures used to produce the results and is able to interpret them correctly.

The development of an automated method or the improvement of an existing technique through automation involves several choices. The designer can fit the new method to work with existing instrumental techniques, define a totally new system that uses available techniques in the solution of the problem in the most effective manner, or design a system from scratch, in which manual procedures are broken down into a number of individual operations. Each of the approaches has its own merit. Ultimately, the chemical advantages of the method and possible financial constraints will determine which approach is used.

The projects described in this thesis encompass automated systems that were designed or improved with the last two criteria mentioned above in mind. The research group already had a working stopped-flow instrument that required modifications in hardware and software to make it more flexible and generally useable. Most of the stopped-flow kinetics studies required minimal amounts of time for the date collection and reduction steps, but were limited by the preparation time of solutions to be used in the study. Therefore, a totally unique reagent preparation system with an accurate, reproducible, and flexible dilution procedure was designed from scratch. The system was designed for general use in cases where the concentration of the reagents used was the precision-limiting step in the

analysis as well as where the reduction of labor involved in reagent preparation was desired.

Due to the many sub-projects that were required to create or modify the instrumentation described herein, the thesis is divided into chapters according to the major projects of the design and characterization of the reagent preparation system and the modification and evaluation of the stopped-flow instrument. These chapters include all of the necessary detail of the hardware used as well as documentation of the operations and the characterization of the systems.

#### CHAPTER II

# OVERVIEW OF AUTOMATED REAGENT PREPERATION SYSTEMS DEVELOPED IN THE 1970's

Most chemical analyses are comprised of the operations of sampling, sample treatment, measurement of the sample characteristics, performance of standardization procedures, control of instrumental parameters, calculation of the analytical and sample results, and finally, report generation, distribution and archiving. The automation of most of these procedures has minimized the time required for an experiment or analysis and has also enabled optimization of procedures and higher precision measurements. Although the computer technology was present in the early 70's, the sometimes prohibitive cost of purchasing a system and dedicating it to on-line control of any device may have kept many workers from extensive experimentation with simple automated devices. With the advent of relatively inexpensive microcomputer systems in the latter part of the decade, the experimenter had at last found a cost-effective medium for assembling simple automated systems. However, the automation of the most error-prone and time-consuming task of reagent preparation has received little attention in the literature during the early part of the past decade. The fact that reagent preparation requires a great deal of time is painfully evident in the computer-controlled,

stopped-flow kinetics studies done in our research group. Quite often, a series of ten or more solutions at a constant ionic strength or pH are required for a study. The preparation of the reagents easily requires much more time and manual manipulations than the data acquisition and analysis requires.

Automating the reagent preparation sequence should lead to several advantages. Reagents could be prepared rapidly, accurately, and reproducibly. Activity corrections for dilute solutions could be calculated via the computer prior to reagent preparation. In cases where constant ionic strength or pH are critical, the computer would be able to do the required calculations. The feature of rapid solution preparation would also enable the preparation of unstable solutions just prior to use and allow accurate control of the addition times of reagents to a reaction mixture. Finally, a well-designed mechanical system would exhibit long-term reproducibility and stability. In many analyses, the automation of the reagent preparation sequence would maintain optimum precision in a given experiment by reducing the level of uncertainty of reagent concentration to below that of the measurement of the physical or chemical property of the sample.

Aliquoting and mixing devices have been classified

(1,2) on the basis of reagent delivery methods as continuousflow or discrete-manipulation systems. The dilution ratio
in continuous-flow systems is determined by the ratio of

reagent flow rate to diluent flow rate, which is in turn determined by the duty cycle of the proportioning valve or the pumping rate of solution. Discrete-manipulation systems essentially mimic the manual operations of pipetting and dilution and are further classified as volume-based or weight-based reagent and diluent delivery systems.

Several authors, primarily workers in the research groups headed by Pardue at Purdue University and by Malmstadt at the University of Illinois, have recognized the utility of an automated reagent preparation system within the boundaries of their specific applications. A summary of the features and applications of systems developed by these groups as well as in our group will be described herein.

#### A. Designs of Pardue and Co-Workers

Deming and Pardue initially developed a discretemanipulation reagent preparation system based on stepper
motor-driven syringes (3) that achieved good success in the
preparation and delivery of reagents. This system probably
was an evolution of an "automated" sample handling system
developed by Pardue and Malmstadt in 1962 (4). Electrical
pulses from a hardware controller were converted to mechanical motion of the stepper motors that were used to deliver
up to three reagents and a diluent to a spectrophotometer
cell. The largest dilution factor available was 1:80 with
0.1% precision. Severe problems with the mechanical link-

ages between the stepper motors and the micrometer syringes detracted from the utility of the system. Even though several automated titration systems were making their appearance at this time (5-7), this system was one of the first to utilize a computer to emulate the manual task of reagent preparation with any kind of success.

Mieling et al. later developed an automated continuous-flow reagent preparation system that was used with their stopped-flow analyzer (8-9). This system utilized a timed peristaltic pump to deliver up to five reagents and a diluent into a mixing vessel. The diluted reagent was then drawn up into a reagent loop in the stopped-flow apparatus for use in an experiment. The calibrated pump was found to have good long-term stability (0.14%), but lacked precision (1% at 1 mL dilution volume and 0.5% at 11 mL) and was limited by a rather narrow dilution range.

## B. Designs of the Malmstadt Group

One of the more prolific contributers to the development of automated analysis systems is the research group of Malmstadt at the University of Illinois. The automated reagent preparation device developed in the group (10-13) was a discrete-manipulation system based on measuring the exact weights of reagents and diluent delivered. Desired weights of the reagents are gravity-fed into a sample cup, which sits on a programmable turntable that may be raised or lowered. The sample cup itself rests upon an electronic

weight sensor when the turntable is lowered. The diluted solution is then mixed and is available for further use in an experiment. The operation and the components of the system are quite simple, and in most cases, the preparation of solutions is quite rapid with nominal reproducibility of 0.1% (dilution to 1 gram). The system is limited by the weight-sensor resolution on the low end of the dilution range and by the total beaker size on the high end. A maximum of 1:30 dilution factor with a 10 gram sample size has a dilution precision of ±1 mg. The reagent preparation device was the first to exhibit the flexibility and integrity to operate in a manner similar to a good technician without incurring common error sources such as operator bias.

A dilution unit that is part of a stopped-flow analyzer was developed by Krottinger et al. (14). The system aliquots a sample, mixes it with a suitable diluent, and transfers the resulting mixture to a stopped-flow mixer.

Despite the excellent precision of dilution of 0.1%, the system is very limited by its narrow dilution range of 1:4.

## C. Design of Steig and Nieman

A simple approach to reagent preparation utilizing a continuous-flow method was recently developed by Stieg and Nieman (2). The reagent preparation device consists of three-way proportioning valves and mixers in line with sample loops of a stopped-flow instrument. The amount of

reagent and diluent delivered to the homogenizing mixer, and hence the dilution ratio, is determined by the duty cycle of the proportioning valve. All of the mechanical and pneumatic operations are under microcomputer control. Along with a 0.2% to 0.5% precision of a typical dilution, the system is compact and relatively inexpensive in terms of cost per channel. The system is limited by a relatively narrow dilution range of 1:91, dependent upon solution flow rate. It is prone to errors due to solution viscosity changes, and is not generally applicable to the preparation of solutions to be used other than in the stopped-flow instrument.

# D. Early Designs of Crouch Group Workers

Previous workers in the Crouch group have designed and partially tested various components of a dilution system (15,16) based on stepper motor-driven syringes. A working system was never constructed, but some of the components, i.e. a 50 mL syringe, were used as automatic titrators (16,17). A crude dilution vessel utilizing an optical meniscus detector was constructed and partially evaluated (16). Basically, the automated system was to consist of two stepper motor-driven micrometer syringes similar in design to those of Deming and Pardue (3) that were to be connected in a line common with the dilution stream and dilution flask. All of the motor control, valve sequencing, and dilution level sensing functions were to be done by a

dedicated computer. From initial studies of the precision of the dilution flask and syringes as stand-alone devices, a theoretical maximum dilution factor of 1:100000 with 0.1% precision was found feasible (16).

#### CHAPTER III

#### AN AUTOMATED REAGENT PREPARATION SYSTEM

#### A. An Overview

Although the automated reagent preparation system was first conceived by Johnson (18), the actual design and construction details of the device detailed in this chapter were done by the author. The physical development of the system required the consideration of several alternative approaches to mechanical design, to controlling hardware design, and to operational software development. The discussion of these approaches as well as the details of the operational characteristics of the microcomputer and the particular designs used are presented. The goal of the construction of the system was to develop a device with a large dilution range that is capable of handling several reagents at once, that needs minimal operator intervention, and above all, that is accurate and precise in the dilution process.

This chapter covers the details of the mechanical components, the electronic hardware, and the controlling software used in the automated reagent preparation system.

# B. Considerations in the Mechanical Design

Several methods for reagent delivery were available at the inception of the project, including those described by workers in the Pardue and Malmstadt research groups. It was decided to improve upon the existing design of the stepper motor-driven syringe, one of which was already in use as a titrator at the time (16,17), and to attempt to minimize the problems of the mechanical linkage of the motor to the syringe plunger experienced by the Pardue group (3). The primary advantage in using stepper motor-driven syringes lies in their capability to precisely deliver relatively small volume increments from large syringes. This is due to the inherent high resolution of the stepper motor (1.8 degrees per step) and to the fine pitch on the lead screw thread.

The detection of solution volumes presented more of a problem because the diluent flow rate could not be reliably controlled without slowing down the dilution process to unacceptably long time periods. In addition, flow control valves have relatively slow response times. The choice of an appropriate dilution vessel also was critical: the flexibility of having different dilution volumes was one of the criteria in the design of the system. It was decided to use the existing design of the optical meniscus detector (16) for sensing the dilution volume, provided that the diluent flow rate would be slow enough to allow for reproducible shearing of solution by the flow control valves without compromising the time required to prepare a solution. dilution vessel was chosen to be easily interchangeable and to mate with the high pressure liquid chromatography (HPLC) fittings of the flow control valves.

# C. System Description-Mechanical Components

The block diagram of the automated reagent preparation

system is shown in Figure 1. The heart of the system consists of three stepper motor-driven syringes A. B. and C. that have total capacities of 1. 5. and 50 mL, respectively. Reagents are drawn into the syringes through check valves (19) and selectively dispensed through a zero dead volume, rotary six-port valve (20) into a common line. The fourth channel of the six-port valve is connected to a pressurized diluent reservoir. The common channel of the valve is connected through two pairs of Kel-F three-way slider valves (21) into the volumetric flask. The slider valves control the flow of solution, venting, pressure, and vacuum through the dilution vessel. Two meniscus detectors are attached to the top neck of the flask. All of the tubing connections are made with 1.5 mm inner diameter (i.d.) Teflon HPLC tubing. All of the valve and motor control functions and the dilution limit sensing functions are done by microcomputer-resident controlling instructions that are decoded by a hardware interface. The minicomputer is used for program development, data storage, and routine calculations. Information is exchanged between the two computers via a serial link. a typical dilution series, all of the parameters and controlling routines reside in microcomputer memory, which leaves the minicomputer free for other tasks.

# 1. Reagent Delivery Syringes

The 50 mL syringe was constructed and evaluated by previous workers (15,17). Volumetric uptake and delivery of fluids are carried out by a Teflon plunger that moves

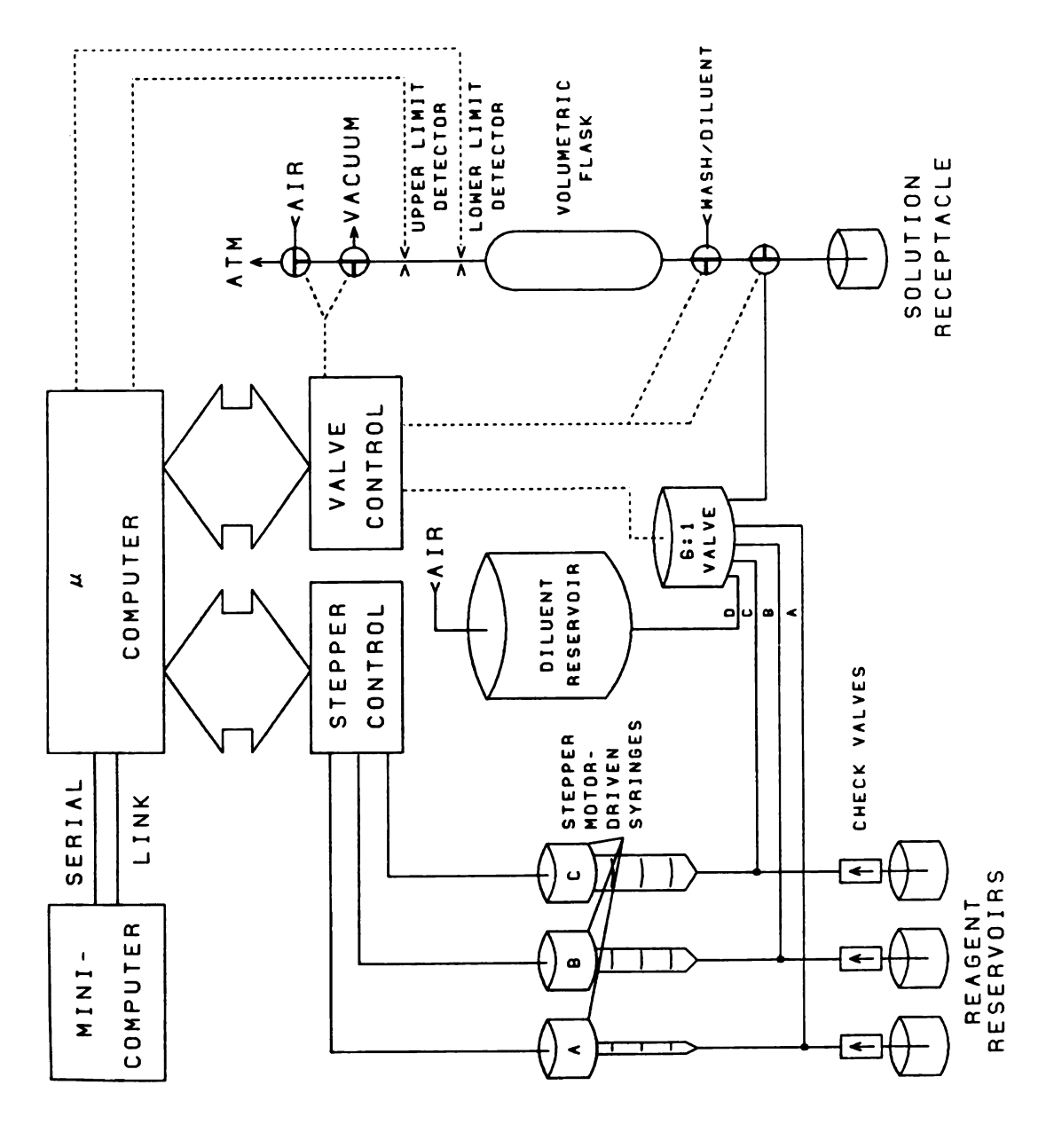


Figure 1. Block diagram of automated reagent preparation system.

inside a sleeve made of heavy wall, precision-bore glass tubing. The plunger is linked to the stepping motor shaft by a threaded aluminum tube that mates with a threaded stainless steel rod by means of a brass collar. Rotary motion of the motor is translated into linear motion of the plunger by this arrangement. Exact details concerning the construction and performance of this syringe are found elsewhere (15).

A unique, adjustable syringe drive unit was designed to accommodate any size commercial gas-tight syringe barrel from 0.1 to 5 mL capacity. A picture of the unit is shown in Figure 2. Linear plunger movement occurs through connection of the stepper motor shaft to a high precision dovetail slider (22), pitched at 40 threads per inch, with a mechanical tolerance of ±0.0015 inches per linear foot of travel. The resolution of the stepper motors (23) is 1.8 degrees per step, ±3.0% non-cumulative error. In theory. the smallest volume increment delivered by the syringes is determined by the resolution of the stepper motor and the pitch of the lead screw. In practice, the smallest volume increment delivered is determined by the amount of mechanical play in the dovetail slider-syringe plunger linkage. reproducibility of delivering a given volume is determined by the weighing uncertainty in the calibration process.

No alteration to the commercial gas-tight syringes was necessary before mounting them in the plexiglass holders, which are slotted at one end to accept the syringe collar.

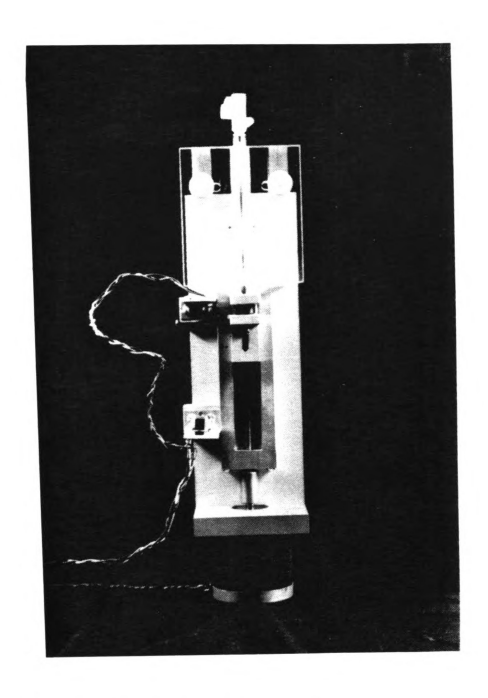


Figure 2. 1 mL stepper motor-driven syringe.

This method of holding the syringe eliminates any free play of the syringe during plunger motion changes. The syringe plunger is fixed to a vertical aluminum holder that is attached to the dovetail slider. Plumbing connections from the syringe tip to the check valves and the appropriate channel of the six-way valve are made by means of a Kel-F "tee" fitting drilled to accept HPLC connectors. The 1 mL and 5 mL commercial gas-tight syringes used (24) are also conveniently threaded to fit HPLC connectors. Initial studies of the characteristics of the system indicated that the 5 mL and 1 mL syringes provided sufficiently small volume resolution and reproducibility to meet the design criteria for a wide dynamic dilution range.

Some problems were encountered with the quality of the glass seals of the syringe tips to the barrel: the tips had a tendency to break off when the "tee" fitting was screwed onto them. Further experimentation with a silicone sealant on the threads and a light touch when tightening the "tee" onto the syringe tip proved to be successful in making a leak-free connection.

Optical interrupter modules (25) were installed on the extrema of travel of the dovetail sliders to ensure that the syringe plunger would not be drawn out of the barrel at one end and would not blow out the tip of the syringe at the other. The positioning of the optointerrupter modules entails moving the dovetail slider manually to the desired limit, loosening the retaining screw of the module, and

moving the module until the bar on the vertical plunger mount crosses the detector light path and the limit indicator light emitting diode (LED) turns off.

## 2. Flow Control Valves and Dilution System

The requirement of rapid dilution created another unique approach to the process. The volumetric flask initially used had a capacity of approximately 100 mL, a relatively large volume to fill by gravity-fed diluent. Since all of the reagents and diluent had to be dispensed through 0.8 mm bore tubing on the six-port valve, the flow rate of solution was very slow. The stepping rate of the syringe motors was adjusted to give fairly rapid flow rates of solution without any undo stress on the tubing or the syringe barrels. A situation in which the flow of solution was blocked was encountered with no damage to the motors or syringes. However, pressurizing the diluent reservoir in a manner that would allow rapid diluent flow would have required very thick-walled glass to avoid explosion of the vessel. A moderately low pressure (~ 1 psi) was eventually used to deliver small aliquots of diluent slowly in order to flush reagents from the common line on the six-port valve into the volumetric flask and eventually complete the dilution process. An auxiliary diluent is rapidly drawn up through another port in the flow-control valves by means of a slight vacuum. The vacuum level was adjusted by changing the water flow rate of the faucet aspirator to give a fairly rapid solution uptake without degassing. A pair of dual three-way valves were designed to sit in a vertical line with the dilution vessel. These valves switch air pressure, vacuum, venting to the atmosphere, auxiliary diluent solution, or drain into the volumetric flask making in effect, a closed system.

Various-sized dilution vessels were conveniently made from 10, 50, and 100 mL pipets with the tips removed. Eventually, similar sized vessels were made in the glass shop with necks for #6 glass tubing. This size tubing fits commercial HPLC fittings after the connector threads are reamed out. A strong, inert, and leakproof seal with the connector was made by roughing up the last inch of the glass neck on both ends of the flask with 400 grit sandpaper followed by application of a commercial epoxy resin glue and attachment of the drilled-out connector. Connectors are used at both ends of the dilution vessel, one for attachment to the solution input valve line and the other for connection to the air, vent, and vacuum selector valve. It is important to note that the dead volume of the system is not determined by the length of tubing connected from the six-port common line to the flow selector valves. Rather, the dead volume is determined by how efficiently the rotary valve can shear off solution segments.

Switching the valves and turning the rotary six-way selector valve requires a supply of compressed air at  $\sim$  70 psi. A separate air supply is used to deliver diluent

through the six-way valve and to expel diluted solution from the volumetric flask. The stepper motor-driven syringe modules, the valve solenoids, and the six-way valve are mounted on a central column. The flow-control valves, volumetric flask, and meniscus detectors are mounted on a platform fixed to the central column. This vertical configuration provides minimal tubing connections to the valves and volumetric flask as well as to the modularity of all of the mechanical components of the system.

Optical meniscus detectors sense the fluid levels in the dilution vessel. The design used in this project is slightly modified and improved over that conceived by Rothman (16) and Johnson (18) and is detailed in Figure 3. Light from a tungsten bulb passes through a 1/4 inch long, 0.7 mm diameter hole, through the neck of the volumetric flask, through another hole of the same dimensions as described above, and onto an infrared-sensitive detector. The detector consists of the photodarlington transistor half of a commercial optical interruptor device (25). The sensor is fixed directly onto the opening on the side of the holder and is completely illuminated by the impinging light. output of the transistor is the input of the window comparator circuit shown in Figure 3. The comparators (26) were chosen to operate from a single +5 VDC power source. Resistor R1 is adjusted to give a voltage level at test point 2 that is  $\sim$  0.30 volts below the output of the detector measured at test point 1. This adjustment for a detection

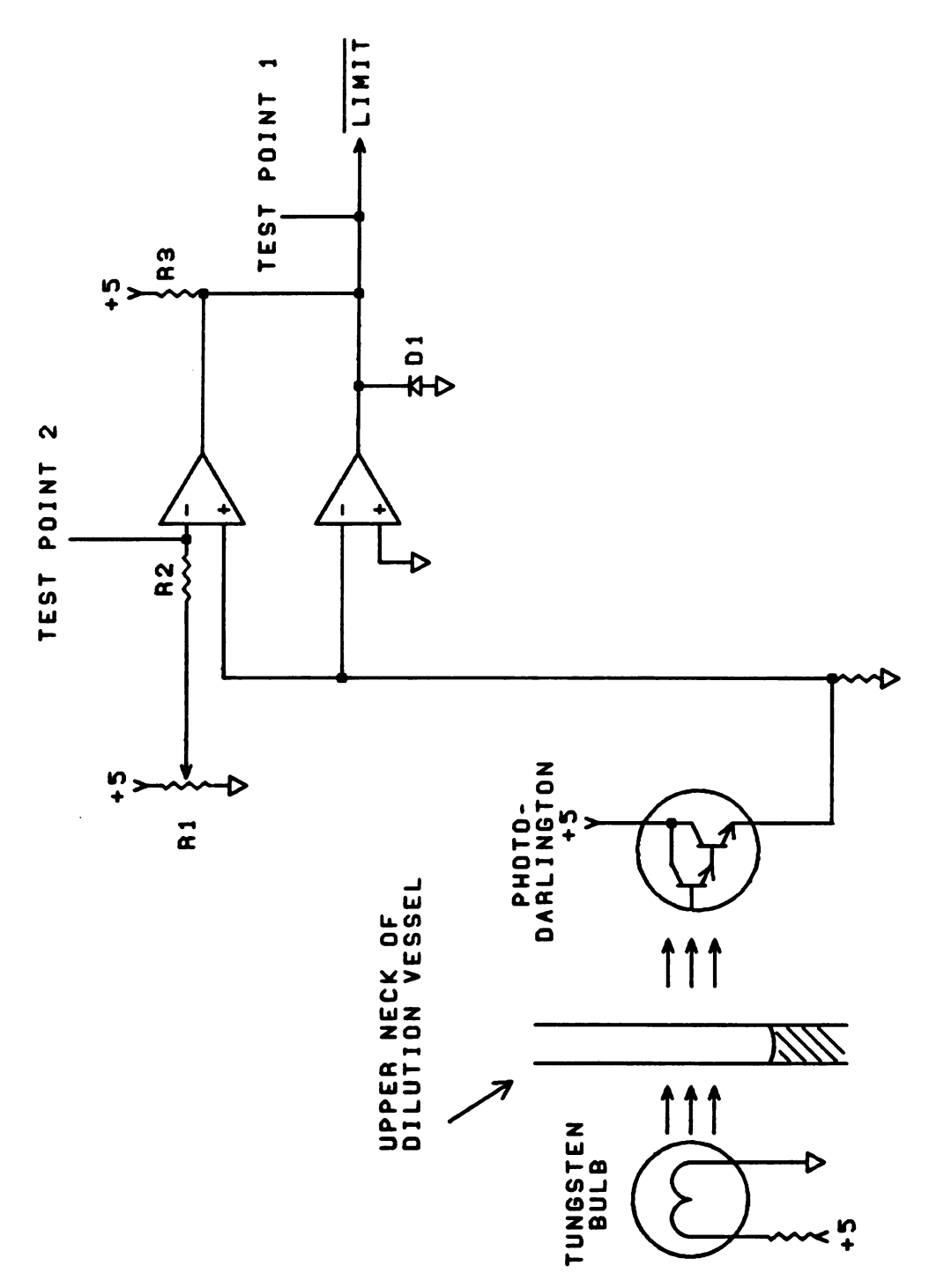


Figure 3. Schematic of the optical meniscus detector.

window gives immunity of the circuit from bulb intensity fluctuations and from random noise from the power supply. With no solution in the light path, the output of the circuit is a HI logic level. When the solution meniscus crosses the light path, the intensity of the impinging light is reduced sufficiently to cause the detector output to drop below the lower threshold set by Rl, with a subsequent change of the comparator output to a LO logic level. Because the solution is flowing past the detector beam, the change in logic level is a short duration pulse, and a JK flip-flop is required to store the logic level change. circuitry in the interface to the solution preparation device handles the changes in logic levels of the comparator circuit in a different manner for each detector and is discussed in a later section. In essence, when the solution meniscus crosses the detector light path, appropriate valves are switched to slow down or stop diluent flow, depending upon which detector's light beam is broken. the reference voltage is set close to the output voltage level of the detector, the control valves may not open. Conversely, if the reference level is set near zero volts, the comparator circuit may not respond to the solution meniscus.

# D. System Electronics

The interface of the reagent preparation device to the microcomputer is contained on a single wire-wrap board that

plugs directly onto the microcomputer bus, with all of the control and sensing lines led out to the various devices on 24 lines. The microcomputer is powered by a +5 VDC, 6 A (27), and a  $\pm 15$  VDC 100 mA power supply (28). The meniscus detectors are powered by a separate +5 VDC, 3 A power supply (27) for the tungsten bulbs. This power supply is enclosed along with the home-built stepper motor power supply, which is rated at +25 VDC, 8 A. The 25 V of the supply is dropped to 5 V across a series pair of 10  $\Omega$ , 20 W resistors before being supplied to the motor coils.

### 1. The Microcomputer

At the time the system was in the design phase, the most convenient and efficient choice of a controller was a microprocessor. If the minicomputer were to be used for the control of the solution preparation system, its use would be restricted. The reagent preparation system does not require any sophisticated feedback control or many on-line calculations, so using the minicomputer would be a gross waste of computer power. Microprocessor technology was relatively inexpensive at design time, so dedication of a microcomputer system to the reagent preparation system was an ideal choice. The decision to use the IM6100 microprocessor (29) was made because the processor recognizes the instruction set of the PDP 8/e minicomputer (30) in use at the time. This feature eliminated the tedium of cross-assembly and debugging of programs written for other microprocessors before use.

The controlling software could be run in the minicomputer and errors could be immediately corrected. Cross-assembly and debugging of programs written in other machine languages would involve more time because the program would have to be tested externally to the minicomputer; this involves the additional steps of downloading the cross-assembled program and writing diagnostic messages within the body of the program.

A custom-built software front panel board was designed and tested in conjunction with other work in progress (31). The front panel enables operation of the microcomputer in either a transparent mode, in which the microcomputer passes characters bidirectionally between the user and the minicomputer, or in a local mode, in which the user can examine and/or modify memory locations or initiate program execution. User routines are first developed and compiled in the minicomputer and then are downloaded into the microcomputer memory via a serial link. Further details on the construction and use of the various versions of the front panel board are found elsewhere (31,32).

The Intersil IM6100 is a single address, fixed word length, parallel transfer microprocessor that uses 12-bit, two's complement arithmetic. The processor clock runs at 4 MHz, with a 5  $\mu$ s execution time for a 12-bit memory accumulator add instruction and an 8.5  $\mu$ s execution time for input/output (I/O) instructions. Memory addressing is the same as for the PDP 8/e: direct, indirect, and autoindexing.

The processor has excellent noise immunity due to its use of CMOS technology in its construction. The microcomputer system consists of 4096 words of static memory, two universal asynchronous receive-transmit (UART) boards (one for communication with the operator console, the other for communication with the minicomputer), and a front panel board.

### 2. Processor Timing States

Interfacing to the IM6100 processor is facilitated by having a single, 12-bit bidirectional data bus that handles many types of information, including memory addresses, memory contents, peripheral instructions and data, and incoming or outgoing signals to the processor. The major timing states of the processor are shown in Figure 4.

During the major timing state T1, a 12-bit address is sent onto the DataX (DX) lines to be used as a memory reference instruction. The Load eXternal Memory Address Register (LXMAR) signal is used to clock an external register in order to store the address information, if required. If an I/O instruction is to be executed, the instruction is sent on the DX lines to be stored externally to the central processing unit (CPU) board. The external address register then contains the device address and control information. Various CPU request lines are priority sampled during T1 if the next machine cycle is an Instruction FETCH (IFETCH) cycle. The current state of the CPU is

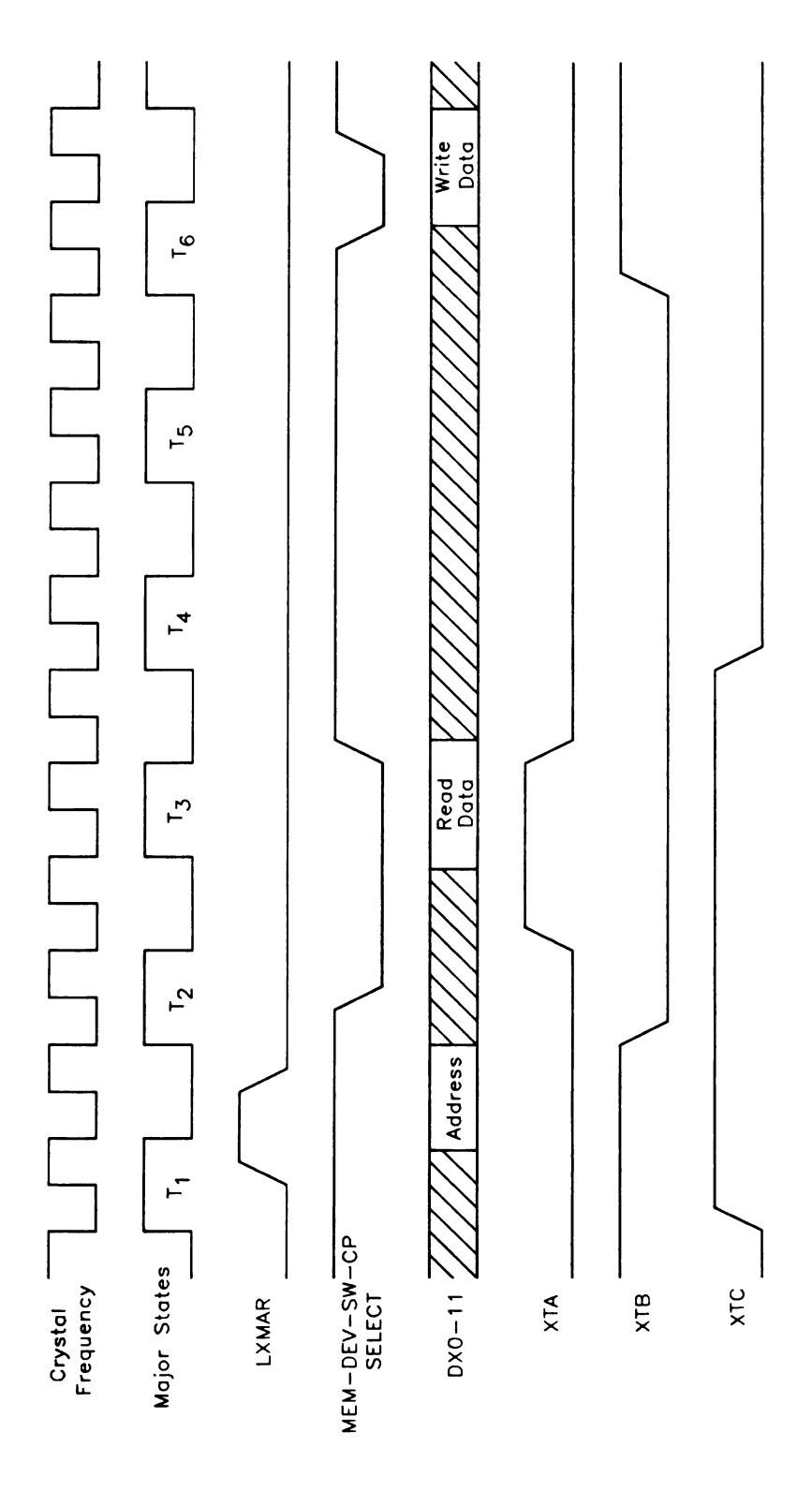


Figure 4. Major timing states of the Intersil IM6100 microprocessor.

available externally at this time on lines XTA, XTB, and XTC.

The memory and device control unit in the CPU provides external control signals to communicate with peripherals (DEVSEL), with memory (MEMSEL), with control-panel memory (CPSEL), and to read a switch register (SWSEL). During major state T2, memory or peripheral data are read by the CPU for an input transfer (READ) operation, with a WAIT control line available for slow-access memory or peripherals. If the WAIT state is activated, the CPU remains in the T2 state until the recognition of the device is complete. The CPU asserts the XTA line to indicate a read-bus-information operation by the CPU. External device sense lines CO, Cl, C2, and  $\overline{SKP}$  are sampled during this interval to determine if the instruction being executed is an I/O transfer, and if so, to determine the destination of the data read by the CPU. If the  $\overline{SKP}$  line is asserted, the processor skips the next instruction in the program sequence. The data transfer from the device to the CPU occurs during major state T3, with arithmatic and logical unit (ALU) and internal CPU register transfer operations occurring during the states T4 and T5.

Timing state T6 occurs when an output transfer (WRITE) operation is to be executed by the 'CPU, with the data destination being memory or a peripheral device. The address of the instruction is defined during major state T1. At this point XTB is asserted to indicate a WRITE operation

by the CPU to the data bus. The CPU also samples the WAIT line at this interval and extends state T6 an integral number of system clock cycles if the line is asserted. The CPU also asserts the appropriate SELect line for the destination of the data.

Input/output transfer (IOT) instructions are used to initiate the operation of peripheral devices and to transfer data between the peripherals and the CPU; these operations are classified as programmed data transfer, interrupt transfer, or direct memory access (DMA). Programmed data transfer is the simplest method of moving data to and from peripherals such as CRT's, cassettes, and teletypes, but is limited in the rate of transfer because the processor must hang up in a WAIT state while the I/O device completes the last transfer and prepares for the next one. Interrupt transfer operations service several peripheral devices nearly simultaneously and permit computational operations to be performed concurrently with the data transfer operation. Both programmed data and interrupt transfer operations use the CPU accumulator register as a buffer. Direct memory access transfers variably-sized blocks of data between high-speed peripherals and the memory with minimal control of the operation by the CPU.

The interface described in this thesis makes use of programmed data transfers. More information about the other types of data transfer operations is found elsewhere (33). Figure 5 shows the details of IOT instruction timing.

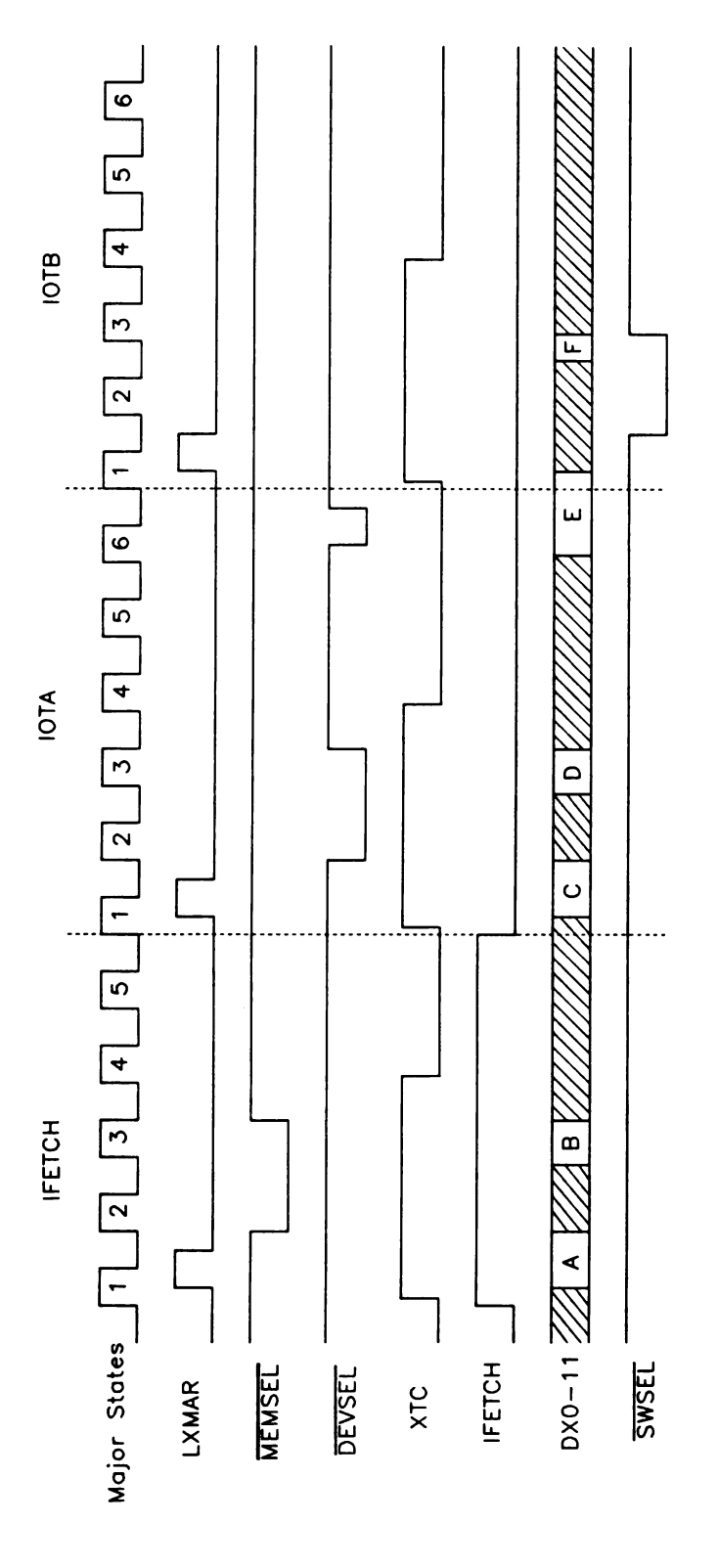


Figure 5. Input/output instruction timing of the IM6100 microprocessor.

The CPU issues an IOT instruction when the most significant three bits of the instruction are set to an octal 6. Bits 3-8 contain the device selection code used to specify the I/O device for which the instruction is intended. Bits 9-11 contain the specific operation that is to be performed by the peripheral for a given device code. The nature of any given IOT instruction depends entirely upon the circuitry designed into the I/O device interface.

Data transfers begin when the CPU fetches an instruction from memory (MEMSEL asserted) and recognizes it as an IOT.

This cycle is referred to as IFETCH and consists of five major states. The CPU then sequences the IOT instruction through a two-cycle execution phase, IOTA and IOTB. The IOT instruction is latched into the external address register during IOTA at the trailing edge of LXMAR. At this point, DEVSEL is asserted to enable data transfer to enable data transfer from the peripheral to the CPU. The destination of the data is determined by asserting the control lines, as described earlier, and the results of these operations are outlined in Table 1.

When the  $\overline{SKP}$  control line is asserted during IOTA, the CPU will skip the next sequential operation. This feature is useful for sensing the status of various devices. The CO, Cl, and C2 lines are treated independently from the  $\overline{SKP}$  line. During IOTA, the input signals to the CPU, the DX lines, and the control lines are sampled when  $\overline{DEVSEL}$  and XTC are asserted. Data from the CPU are available to the

Table 1. Summary of Control Line Functions.

CONTROL LINE	OPERATION
<u>C0 C1 C2</u>	
HI HI HI LO HI HI LO LO HI x HI LO x LO LO	Contents of accumulator (AC) sent to device. Contents of AC sent to device; AC cleared. Data from device is OR'ed with data in AC. Data from device is jam-transferred into AC. Data from device is added to program counter (PC). Data from device is jam-transferred into PC.

<sup>&</sup>quot;x" = don't care

peripheral when DEVSEL and XTC are asserted. The IOTB cycle is internal to the CPU and is used to perform the operations requested during IOTA. If the CPU recognizes the instruction "read a switch register" during IFETCH, the SWSEL line is asserted during IOTB and the data are transferred into the accumulator. For I/O instructions that do not involve transfer of data, such as turning a valve on or off, it is sufficient to have the CPU address the device during IFETCH, even though the processor still goes through the IOTA and IOTB cycles.

## 3. The Interface-Controller Board

All handling of bus signals, instruction decoding, conditional testing, and stepper motor waveform generation is provided by the controller board. The integrated circuits (IC's) used were mounted on wire-wrap sockets for debugging purposes. The wire-wrap design has proved to be durable with no problems of deterioration in the connections. In addition, minor changes and additions to the control functions are facilitated by this design.

a. <u>Device Decoder Circuit</u> - Figure 6 shows the circuitry used to decode device control instructions. All of the device control signals are decoded as IOT instructions with no data transfer involved. The DX lines are buffered through permanently enabled tri-state buffers. The IOT instruction is latched during LXMAR by a pair of six-bit

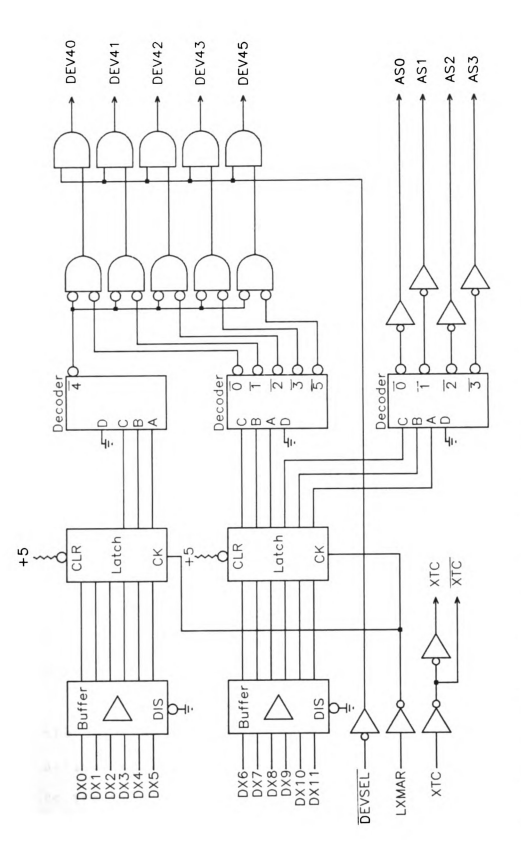


Figure 6. Device decoder circuit for automated reagent preparation system.

latches and is decoded into DEVice and ASsignment pulses by an octal decoder circuit. A two-digit device code is enabled by combining the decoded number from bits 3-5 and the number from bits 6-8 with the asserted DEVSEL signal. The device code signals were wired to be asserted in a HI logic state. The final three bits of the latched instruction are used to distinguish among eight additional commands available for any given device code. The XTC line is buffered and used in the actual execution of the control function by being asserted along with the device code, assignment code, and DEVSEL. A summary of the executable commands for control and sensing functions are presented in Table 2.

b. Valve Controls and Status Testing - Details of the circuitry used to generate specific actions in the reagent preparation system are presented in Figure 7. The soft-ware commands are divided into active control commands and status testing commands. The following section details the action of each instruction. In general, a given command is recognized when DEVxx, ASx, and XTC are simultaneously asserted.

The opening and closing of the flow control valves and the positioning of the six-port rotary valve are done by activating solid state relays (34) that switch line current to the valve air solenoids (35). These solenoids control the air pressure available to the pneumatic actuator/spring

<u>Table 2</u>. Software Commands for Reagent Preparation System.

MNEMONIC	OPCODE	OPERATION
FILL1	6400	Draw solution up into syringe #1.
FILL2	6410	Draw solution up into syringe #2.
FILL3	6420	Draw solution up into syringe #3.
PUSH1	6401	Deliver solution from syringe #1.
PUSH2	6411	Deliver solution from syringe #2.
PUSH3	6421	Deliver solution from syringe #3.
FLIM1	6402	Skip next instruction if fill travel limit reached for #1.
FLIM2	6412	Skip next instruction if fill travel limit reached for #2.
FLIM3	6422	Skip next instruction if fill travel limit reached for #3.
PLIM1	6403	Skip next instruction if deliver limit for #1 reached.
PLIM2	6413	Skip next instruction if deliver limit for #2 reached.
PLIM3	6423	Skip next instruction if deliver limit for #3 reached.
STEP6	6431	Turn the 6-port valve to the next position.
CK6	6432	Skip next instruction if 6-port valve is not in motion.
WASHOP	6430	Set upper pair of flow-control valves to wash position.
WASHCL	6433	Set upper pair of flow-control valves for dilution/dump.
DILUTE	6450	Set lower pair of flow-control valves for dilution.
DILLIM	6451	Skip next instruction if upper meniscus detector reached.
DUMP	6452	Set lower pair of flow-control valves for delivery.
LOLIM	6453	Skip next instruction if lower meniscus detector reached.

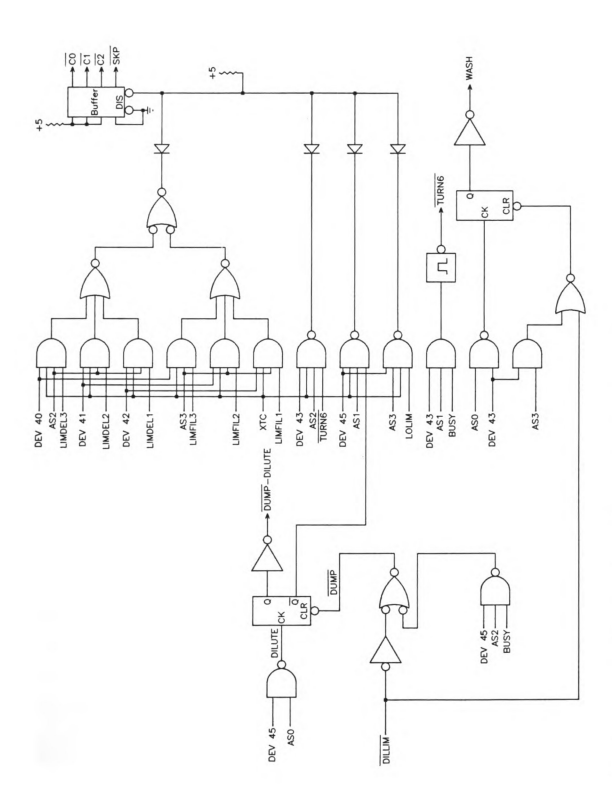


Figure 7. Valve control and status testing circuitry.

return mechanism of the flow control valves; they also control the push-pull action of the piston used to turn the six-port valve. Device codes 43 and 45 are used for controlling the valves and testing their status.

Two JK flip-flops are used to store the desired state of the flow control valve. The DILUTE command (instruction 6450) sets the DUMP/DILUTE control line to a LO logic level, which is inverted to an active HI signal on the control signal distribution board. This signal energizes the lower pair of flow control valves so that the volumetric flask is connected to the common line of the six-way valve and is vented to the atmosphere. The DILLIM command (code 6451) checks the status of the upper meniscus detector. A HI logic level from the detector circuitry indicates that no solution is in the detector light path. As the meniscus crosses the detector, the LO-going pulse clears the flipflop to set the Q output to a HI logic level and the  $\overline{\mathsf{Q}}$ output to a LO level. This immediately deenergizes the valve solenoid and causes the program to skip the next instruction (which is a "jump back one location" instruction), and test the status of the detector. The dilution flow control valve may also be closed by the DUMP instruction (code 6452), which is ORed with the dilution limit status line shown in Figure 7. The operation of the auxiliary diluent/wash control valve is similar to that of the dilution flow control valve. The WASHOP (code 6430) instruction is used to open the upper pair of flow control valves to pull

a slight vacuum in the dilution vessel and draw up diluent through the auxiliary diluent line. The control flip-flop for this valve is cleared to a LO state when the upper meniscus detector line is asserted LO or when the lower meniscus detector circuit is asserted LO during a status checking instruction (LOLIM, code 6453) and is followed by a WASHCL (code 6433) instruction.

Two control functions are required by the rotary six-port selector valve: one to energize the piston solenoid, the other to read the position of the valve. A TURN6 (code 6431) instruction fires a monostable for  $\sim 1$  s. This action ensures that the piston solenoid is actuated long enough to allow the piston to travel its full length and turn the valve. The TURN6 line is simultaneously monitored by the CK6 instruction (code 6432). When the output of the monostable returns to a HI logic level, the piston solenoid is deenergized and the piston is latched onto the drive tooth of the valve, ready to turn it to the next position. The  $\overline{SKP}$  line is also asserted at this time. The instruction following the status test reads the position of the six-port valve, which is encoded by three optical interruptor modules and an encoder wheel attached to the center shaft of the rotary valve. Rather than provide a separate instruction on the interface board to read the valve position, the processor's ability to read a switch register is used. Data encoding the position of the six-way valve are driven onto the data bus by the FETCH instruction

(code 7604), which asserts the SWSEL line during IOTB. The position information is contained in data bits 9-11 and is converted into an ASCII number by addition of octal 260. The position data are then stored in memory and displayed on a 7-segment LED display on the front panel of the control signal distribution rack.

The fill and push travel limits of the syringe plungers are monitored by the FLIMx and DLIMx instructions respectively. The "x" indicates the syringe identification number. Status checking is done in the same manner as for the meniscus detectors. When any of the limits are reached, the appropriate syringe plunger movement instruction is skipped, (i.e. the  $\overline{SKP}$  line is asserted), and a warning is issued on the console.

All of the status monitoring lines are in a wired-OR configuration connected to the processor status control-tri-state buffer chip enable line. When any of the status lines are asserted, control lines CO-C2 are asserted HI and the  $\overline{\rm SKP}$  line is asserted LO on the bus.

c. Stepper Motor Waveform Generation - Figure 8 shows the controlling circuitry for the stepper motors used to move the syringe plungers. The design is a full-wave, fourphase waveform generator of commercial origin (36). The motor direction is latched into the driver circuit flipflop during a FILLx or PUSHx instruction. When XTC goes LO during IOTA, the WRITE data pulse of DEVSEL causes

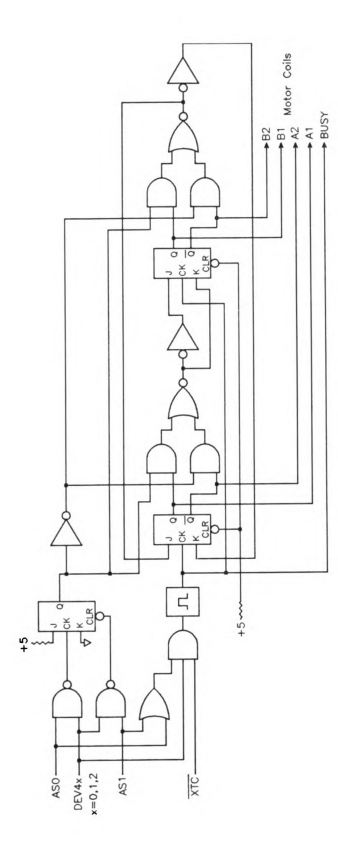


Figure 8. Stepper motor waveform generator circuit.

triggering of the monostable to generate a 22 µs step pulse to the motor, which turns 1.8 degrees. This configuration allows for any settling time of the motor direction information before the actual movement takes place. Each of the four phases of the motor is controlled by lines Al, A2, Bl, and B2.

The schematic of the stepper motor driver circuit is shown in Figure 9. Four identical units of the type illustrated are used for each step phase of the motor. When the input signal to diode D1 is LO, the current through the  $1k\Omega$  resistor is sunk to ground through the diode by the LO TTL output. A germanium diode is used to ensure that the base of transistor T1 is turned fully off. When the input signal to the diode is HI, the diode is reverse biased and Tl is switched on, allowing the emitter current to switch current to the base of power transistor T2. This allows current from the 25 VDC power supply to pass through a ballast resistor and the motor coil to ground. Clipping of inductive voltage spikes generated by the motor coils as they turn off is done by Zener diode D2. Potential damage of T2 by these spikes would occur by exceeding the transistor's maximum collector-to-emitter voltage rating if the clipping was not done.

## E. The Controlling Software

The controlling software was written to provide for stand-alone operation of the dilutor after any required data

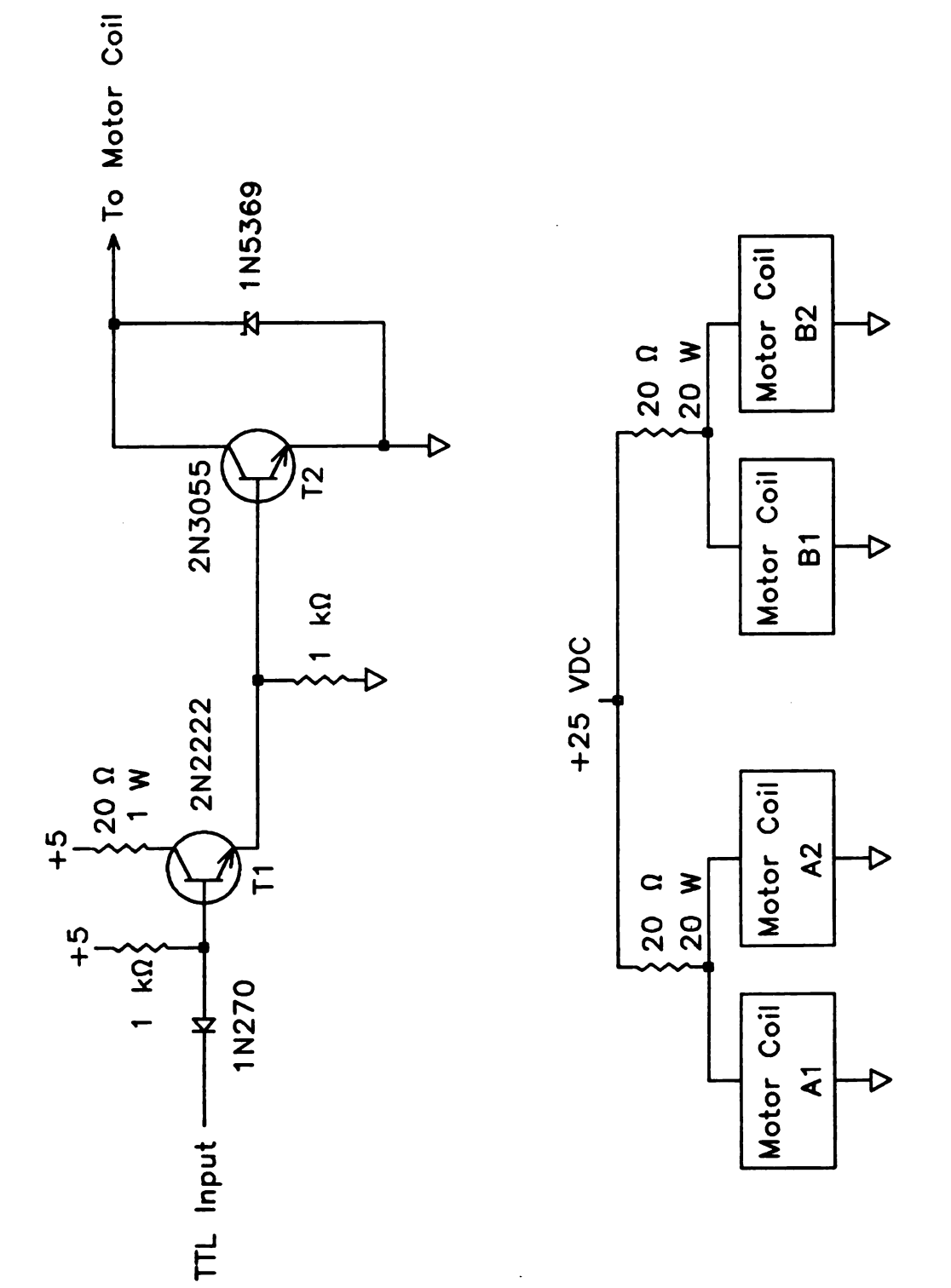


Figure 9. Stepper motor driver circuit.

were received from the minicomputer. The operations available to the operator consist of selection of data input for control from a file stored in the minicomputer or from the console device, use of the data to prepare solutions individually or sequentially, and selection of manual control functions by typing characters on the console corresponding to the operation.

The controlling routine uses a series of subroutines for input and output of data and responses to and from the operator console. All numbers entered from the console are considered to be decimal and are converted to octal prior to Special subroutines were written to handle doubleprecision number storage and retrieval because the stepper motors typically require 19,000 steps to move the plunger from one limit to the other. Storage of these values is critical because the program keeps track of the number of steps the syringe motor has used to deliver or draw up a given volume. This number is used to check if there is sufficient solution remaining in a given syringe for the next dilution, and if not, to refill the syringe and reset the appropriate counter. A resident monitor routine is used to detect error conditions and print out appropriate warnings. The monitor also handles local communication between the microcomputer and the PDP 8/e for data transmission. A software timing subroutine is available to set up delay loops in increments of one second. All of the motor control functions are handled via subroutines that

update the controller device code for the syringe used, and ensure that the six-way valve is in the proper position for reagent or diluent delivery, and that the flow control valves are in the required states for the given operation. A description of the subroutine functions is found in appendix A.

PAL8 assembly language (30) was chosen as the basis for the controlling software package of the reagent preparation system. Programs written in FORTRAN II could run in the microcomputer, but their utility is limited by the large overhead routine needed to run FORTRAN II programs. The overhead utility takes up essentially all available memory space in the microcomputer. Instead, a series of general purpose subroutine modules were developed using the PAL8 language. This method of programming is highly efficient in terms of execution time and memory allocation, but programming is somewhat difficult because every segment of operation from simple character I/O to mathematical operations must be explicitly defined.

The controlling routine resides in octal memory locations 0200 to 5000. Pointers to subroutines, counter registers, delay times for rotation of the stepper motor shafts, various status flag registers, and temporary data storage registers are resident in octal memory locations 0000 to 0177. The data are stored in these locations because the data can be directly accessed from any other memory location. One 4096 word memory module is divided

into 32 decimal pages of 128 decimal words each. Except for page zero, memory locations on pages other than the page of the instruction that is currently fetching or storing the data must be indirectly addressed, requiring two bytes of information. Therefore, accessing data from page zero saves execution time and memory space.

## F. Sequence of Operation for a Dilution Series: User Input

Operation of the automatic reagent preparation system is rather straightforward, provided no malfunctions or error conditions are encountered during use. Error recovery normally consists of restarting the controller program after correction of the error condition. The operational sequence is outlined in Figure 10.

The user initially sets up a link with the minicomputer through the transparent mode of the microcomputer and loads the controller routine into memory by downloading the file SMAKER.BN. The details of this operation are described elsewhere (31). Prior to doing anything from the console device, the user should verify that the controller power supply is on, the air supplies to the valve solenoids and the volumetric flask are on and at the correct pressure, the water for the vacuum aspirator is flowing, the diluent and auxiliary diluent vessels are filled, and the comparator voltages for the meniscus detectors are set to ~0.250 volts below the output of the detectors. The user then types "0200G" in response to the "\$" prompt to start the controller

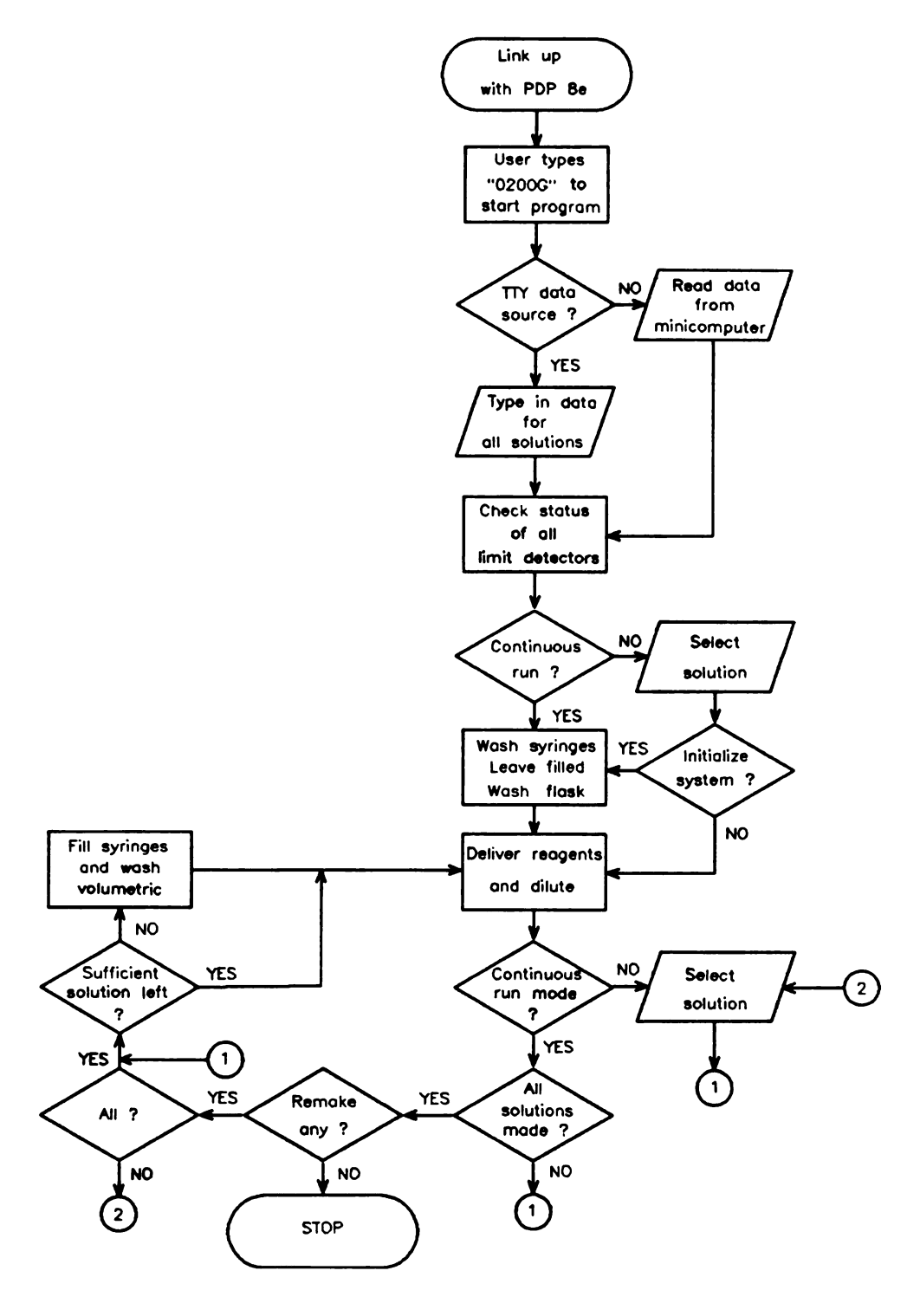


Figure 10. Sequence of operations for automatic reagent preparation.

program. At this point the user selects the source of data as being from the console or from the minicomputer. data source is the minicomputer, the local monitor routine is called to enable reception and storage of data. At this point, the user is in a locally transparent mode to the PDP 8/e and executes the transmission routine that is used to send data to the microcomputer. The user types a CNTRL/R on the console to return to the local data receiving program. The parameters for all of the reagents to be prepared come downline from the minicomputer as the total number of syringe deliveries in the entire dilution series, i.e. the number of pushes per solution times the total number of solutions, followed by the data for all syringe plunger motions. These data consist of three bytes per motion: 1) the position for the six-way rotary valve corresponding to the syringe used for the delivery, 2) low 12-bit byte, and 3) a high 12-bit byte, the combination of which define the number of steps required to deliver that volume increment. Once all of the parameters are acquired, the final two bytes of data contain the number of syringe deliveries to be used in a single dilution and the number of dilutions to be performed.

If the data source is the console, the user enters the number of dilutions to be performed, followed by the number of syringes that will be used in any dilution. The data for each dilution are then entered as the syringe identification number followed by the number of steps the syringe motor

must turn to deliver a given volume. This process is repeated until all of the data are entered. The user has the option of correcting any mistakes upon entry. All of the data for the number of steps required for a given delivery are stored as negative values to facilitate their use in counters.

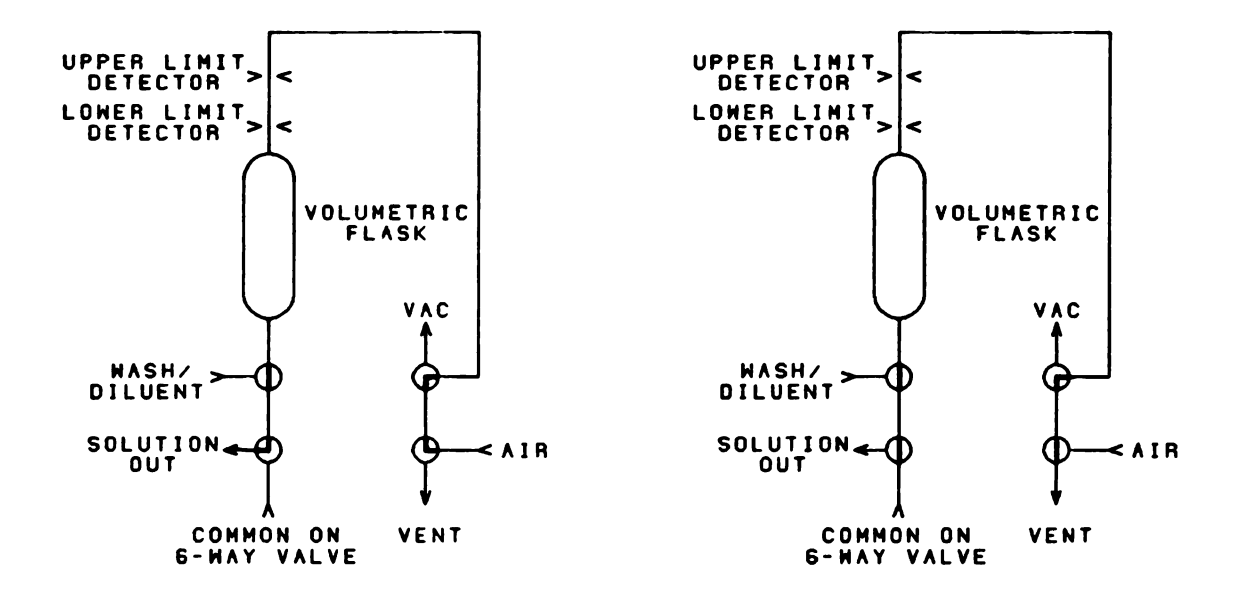
The status of the optical interrupters and the meniscus detectors is checked with appropriate queries typed on the terminal. The position of the six-port valve is read and stored in a register. The program then asks the user which syringes will be used throughout the dilution series and checks the data stored in memory to ensure that the syringes selected in the data table have been selected as active. If there is a discrepancy, an error message is printed and the program restarts itself.

At this point, the user selects whether the solutions will be prepared sequentially or individually from the data stored in memory. Appropriate limit counters are then set and the program then jumps into the manual mode of operation. The user can instruct the system to cycle through a syringe and a volumetric flask washing sequence using the "cycle" command. After doing any operations in this mode, the user supplies a solution receptacle at the outlet line of the dilution vessel and types a CNTRL/R to initiate the dilution process. The microcomputer takes over the control functions at this point and does the dilution. After delivery of the diluted solution, the program ascertains whether or not there

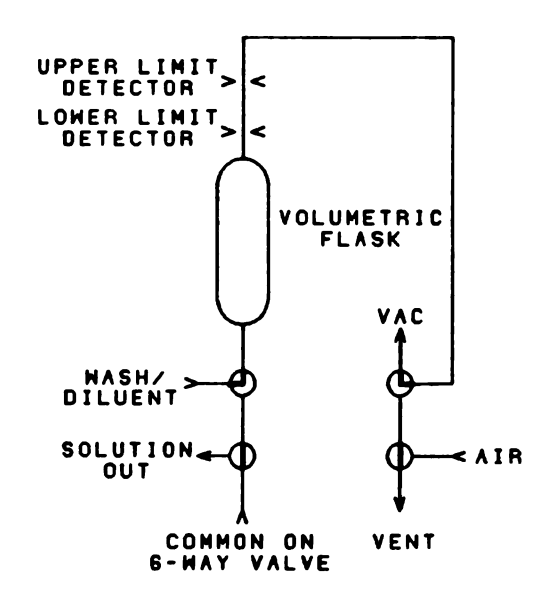
is enough solution left in each of the syringes for the next dilution, fills those requiring reagent, and rinses the volumetric flask. In the continuous dilution mode of operation, the controller continues performing dilutions, volume checking, and washing until all of the data are used up. The user normally has sufficient time after the wash cycle to provide a new solution receptacle. During individual solution preparation, the user is queried by the program for the solution identification number that he wishes to prepare. This is done prior to the reagent volume checking and dilution flask rinsing steps. Upon completion of a day's work, the user should cycle the system through the syringe rinse/fill sequences and the flask wash sequence using distilled water to purge the system of reagents.

## G. Reagent Preparation Sequence: Mechanical Actions

The hardware operations involved in the preparation of a single solution is diagrammed in Figure 11. The six-way valve turns to position 4 with the flow control valves in the delivery position. The valves then switch to dilution step I in Figure 11 to connect the common line of the six-port valve to the volumetric flask and vent the system. Approximately 10 mL of diluent is pressure-injected into the volumetric flask through the common line from the diluent vessel. An appropriate volume of reagent is delivered from each of the syringes through the corresponding



# A> DEFAULT/DELIVERY B> DILUTION I, III



### C) DILUTION II/WASH

Figure 11. Mechanical actions for a reagent preparation sequence.

parts of the rotary valve into the dilution vessel, followed by another 10 mL portion of diluent that is used to flush the reagents into the volumetric flask. The flow control valves then switch to draw up 90% of the diluent through the auxiliary diluent line into the flask by a vacuum (dilution step II in Figure 11c). When the solution meniscus crosses the lower meniscus detector, the flow control valves switch to allow a slower flow of diluent through the six-way valve common line until the solution reaches the upper meniscus detector. Finally, the flow control valves switch to the delivery phase to expel the diluted solution into the receptacle. The default/delivery position in Figure 11a leaves all of the valves in the deactivated state and disconnects them from the six-port valve. The microcomputer then decides whether or not enough reagent is available in each of the active syringes for the preparation of the next solution, if there is one, and fills those that are too low. The six-way valve turns to position 4 and the volumetric flask rinse cycle starts. The washing sequence is performed twice before the next reagent is prepared.

### H. Component Evaluation

The stepper motor-driven syringes and various-sized dilution vessels were tested as stand-alone devices. The reproducibility of positioning and calibration of the syringes was done as well as calibration of the volumetric

flasks.

The positioning reproducibility of the stepper motor was tested first. The motor shaft was coupled to a micrometer, and the distance displaced by the micrometer for 1000 step pulses was measured for six trials. The results showed that the motor displaced the micrometer head an average distance of 2.499 ±0.001 mm. The precision of the figure is limited by reading error of the micrometer vernier scale.

The next step in the component evaluation consisted of determining the number of steps required to move the syringe plungers between the limits of their travel. This test used software counting routines and the limit-of-travel status lines of the interface to establish a step count for the travel limits. After the syringe under test was run to one limit of travel, the program generated step pulses to the motor, and simultaneously checked the status line for that direction of travel; this was followed by incrementing a counter register. The number of step pulses generated by the program was printed out at the limit of travel. plunger was then moved in the opposite direction under the same conditions. The average of 20 trials showed that it took 20,594 ±2 steps for the 50 mL syringe, 18,360 ±1 steps for the 5 mL syringe, and 21,736 ±1 steps for the 1 mL syringe slider to travel from one limit to the other. These results indicate that the mechanical tolerances of the commercial sliders are indeed as good as their specifications and that there is no play in the stepper motor to slider lead screw linkage. It should be noted that only the 5 mL and 1 mL syringes use the commercial dovetail slider, while the 50 mL syringe uses the threaded plunger rod as the driving mechanism.

## 1. Calibration of the Syringes

Each of the syringes was calibrated to determine the number of stepper motor pulses required to deliver a 1 mL volume. In general, the calibration procedure consisted of at least eight delivery trials of a fixed amount of distilled-deionized water (equilibrated to room temperature) into a stoppered, pre-weighed flask. The volume delivered was computed from the measured mass and the density of water at its measured temperature; the volume was corrected to 20 degrees C. The results of the calibration trials are shown in Table 3. The 5 mL and 1 mL syringe calibrations were based upon weighing the amount of water delivered from the entire syringe, while the 50 mL syringe calibration was based on delivery of 10 mL increments. The resolution data presented in Table 3 were determined by using the following formula:

Resolution = 
$$\frac{2x \text{ (error in calibration value)}}{\text{(steps per mL value)}}$$
 (3.1)

The calibration of the syringes was checked periodically over the course of a year and was found to be within the specifications of precision defined in the first calibration

Table 3. Syringe Calibration Data.

SYRINGE CAPACITY	STEPS REQUIRED TO	RESOLUTION	
(mL)	DELIVER 1 mL	(µL)	
50	400 ± 0.2	1.0	
5	3502 ± 0.29	0.17	
1	20698 ± 8	0.77	

series. Practical considerations such as gross temperature and solution density changes will affect the calibration data, but this was not observed in normal use. The data for a more rigorous evaluation of the 5 mL syringe done by the author are presented in another document (15).

#### 2. Dilution Vessel Evaluation

Calibration of dilution flasks was done by delivering distilled-deionized water into the vessel in the same manner as used in the dilution sequence but with no reagents delivered. The weight of the water expelled into a stoppered flask was converted into volume using appropriate density correction factors for the solution temperature. The volume was then corrected to 20 degrees C. The averages of the calculated volumes delivered (eight trials) for each flask are presented in Table 4. Note that the delivery precision is at least an order of magnitude better than that of Class A glassware in all cases. It should be emphasized that as long as the volume of the dilution vessel is known, it is immaterial that the volume of the dilution vessel is not exactly 10 mL, 50 mL, or 100 mL. The calibrated volume figure is supplied as data for calculation of concentrations of solutions by the minicomputer. Also, normal highprecision procedures require calibration of glassware prior to use. Calibration of the dilution vessel requires no more time than the analogous procedure for glassware. the upper meniscus detector is not moved, one can use the

Table 4. Volumetric Flask Delivery Precision.

NOMINAL VOLUME	MEASURED VOLUME
10 mL	10.252 ± 0.001 mL
50 mL	46.916 ± 0.004 mI
100 mL	99.522 ± 0.006 mI

calibrated volume figure for that flask for weeks after the initial calibration.

### 3. Carry-Over of Reagents and Diluted Solution

An experiment suggested by C.J. Patton (37) was used to determine if carry-over of reagents or diluted solution would be a problem in performing dilutions. The worst-case condition of no washing of the system lines was assumed. The experiment involved serial dilutions of  $\sim 0.01$  M 5-nitro-1, 10-phenanthroline ferrous sulfate redox indicator solution delivered from the 5 mL syringe. The other syringes were deactivated, but were also filled with the colored solution as if they were to be used in a dilution Three consecutive dilutions of a 5 µL increments of indicator were followed by three consecutive dilutions of 5 mL increments of indicator, and then by three consecutive dilutions of 5  $\mu$ L increments of indicator. The dilution volume was 100 mL in all cases. The absorbances of the diluted solutions were measured at 510 nm on a Heath single beam spectrophotometer. The first series of 5  $\mu L$  dilutions was used to set the 100%T level. As can be seen in Table 5, the system exhibited very little solution carry-over from the 5  $\mu$ L to the 5 mL dilutions and from the 5 mL to the 5 μL dilutions. Using a wash cycle in between dilutions would ensure minimal carry-over of reagents.

Table 5. Data for Carry-over Experiment.

VOLUME OF DELIVERED	 ABSORBANCE
<b>0.</b> 005	$0.0 \pm 0.007$ $0.0 \pm 0.007$
0.005 5.00	$0.0 \pm 0.007$ $0.491 \pm 0.007$
5.00 5.00	$0.502 \pm 0.007$ $0.501 \pm 0.007$
0.005 0.005 0.005	0.002 ± 0.007 0.001 ± 0.007 0.0 ± 0.007

#### I. System Performance

In order to obtain a rough estimate of the range of dilution and the precision with which the dilution can be made, let us conservatively assume that we can deliver 500  $\mu$ L from the 5 mL syringe with a 0.1% relative precision ( $\sigma(\text{syringe})$ ). This figure is not unreasonable in light of the precision obtained during the calibration of the syringe. An estimate of the precision of dilution  $\sigma(\text{dil})$  may be calculated from:

$$\sigma(\text{dil})^2 = \sigma(\text{flask})^2 + \sigma(\text{syringe})^2$$
 (3.2)

$$\sigma(dil)^2 = (0.0006^2 + 0.001^2)$$
 (3.3)

$$\sigma(dil) = 0.1\% \tag{3.4}$$

where  $\sigma(\text{flask})$  is the relative precision of the dilution to 100 mL. The dilution ratio here would be 1:200, a factor of 2 greater than any system reported in the literature. In practice, as will be shown later, the syringes are capable of reproducibly delivering volumes down to 10  $\mu$ L to provide a theoretical upper limit of dilution of 1:10,000 with a 0.1% precision using a single set of stock solutions. It should be emphasized that the weighing error in the calibration of the syringes appears to be the largest error-producing element in the evaluation of the performance of the system.

# 1. Chemical Complexation Reactions - Mole Ratio Study

The goal of the first study was to use two chemical complexation reactions to evaluate the performance of the

entire system. The first reaction used was a mole-ratio study of the copper(II)-EDTA 1:1 complexation reaction (38). This method involves the preparation of a series of solutions in which the concentration of the metal ion is held constant while the concentration of the ligand is varied. A plot of the absorbance of the solution  $\underline{vs}$ , the mole ratio of the reactants usually gives two straight lines of different slopes. The intersection of the two lines occurs at a mole ratio corresponding to the stoichiometry of the reaction. The stock solutions used in this study were 0.3969  $\underline{M}$  Cu(II) prepared form CuCl<sub>2</sub>°2H<sub>2</sub>0, 0.01984  $\underline{M}$  EDTA prepared from the disodium salt, and a 0.1  $\underline{M}$  acetate buffer adjusted to pH 2.2 with a 10% HCl solution. The buffer was used as the diluent for all of the solutions.

The spectrophotometric measurements were done using a single-beam, molecular absorption spectrophotometer (39) with a high-quality current-to-voltage converter (40) that was interfaced to a custom-built 12-bit analog to digital converter data acquisition system. The absorbances of the prepared solutions were obtained according to the guidelines for high-precision spectrophotometric measurement (41). Absorption measurements were made at 710 nm.

Three series of 20 solutions were prepared, each 4  $\underline{mM}$  in Cu(II) and containing concentrations of EDTA varying from 0.4 to 8.0  $\underline{mM}$ . The Cu(II) solution was delivered from the 1 mL syringe and the EDTA was delivered from the 5 mL syringe, with volumes ranging from 0.2 to 4.0 mL. The resulting plot

of the absorbance of the Cu-EDTA complex  $\underline{vs}$ . the mole ratio of EDTA/Cu(II) is shown in Figure 12. The intersection of the extrapolated linear regions of the plot occurs at a mole ratio of 0.987 $\pm$ 0.044, as is expected for this reaction. The variation of the absorbance of the replicate preparation of a solution at a given mole ratio is negligible compared to the imprecision of the absorbance measurement itself.

# 2. Continuous Variations Study

A more rigorous evaluation of the system performance was done using the iron-1,10-phenanthroline 1:3 complexation reaction in a continuous-variations study (42). This method involves the measurement of the absorbance of solutions containing constant total molar concentrations of metal and ligand. The plot of the absorbance of the complex vs.the mole fraction of one of the reactants gives two lines with different slopes. The intersection of the lines corresponds to a fraction that indicates the stoichiometry of the metal-ligand complexation. The method of continuous variations using a 1:3 complexation reaction is particularly sensitive to any concentration variations in either the metal or ligand solution delivered and is therefore, quite suitable to evaluate the performance of the 1 mL and the 5 mL syringes.

The stock reagents for this study included 0.01500  $\underline{\text{M}}$  Fe(II) solution prepared from ferrous ammonium sulfate, 0.01500  $\underline{\text{M}}$  1,10-phenanthroline solution prepared from the

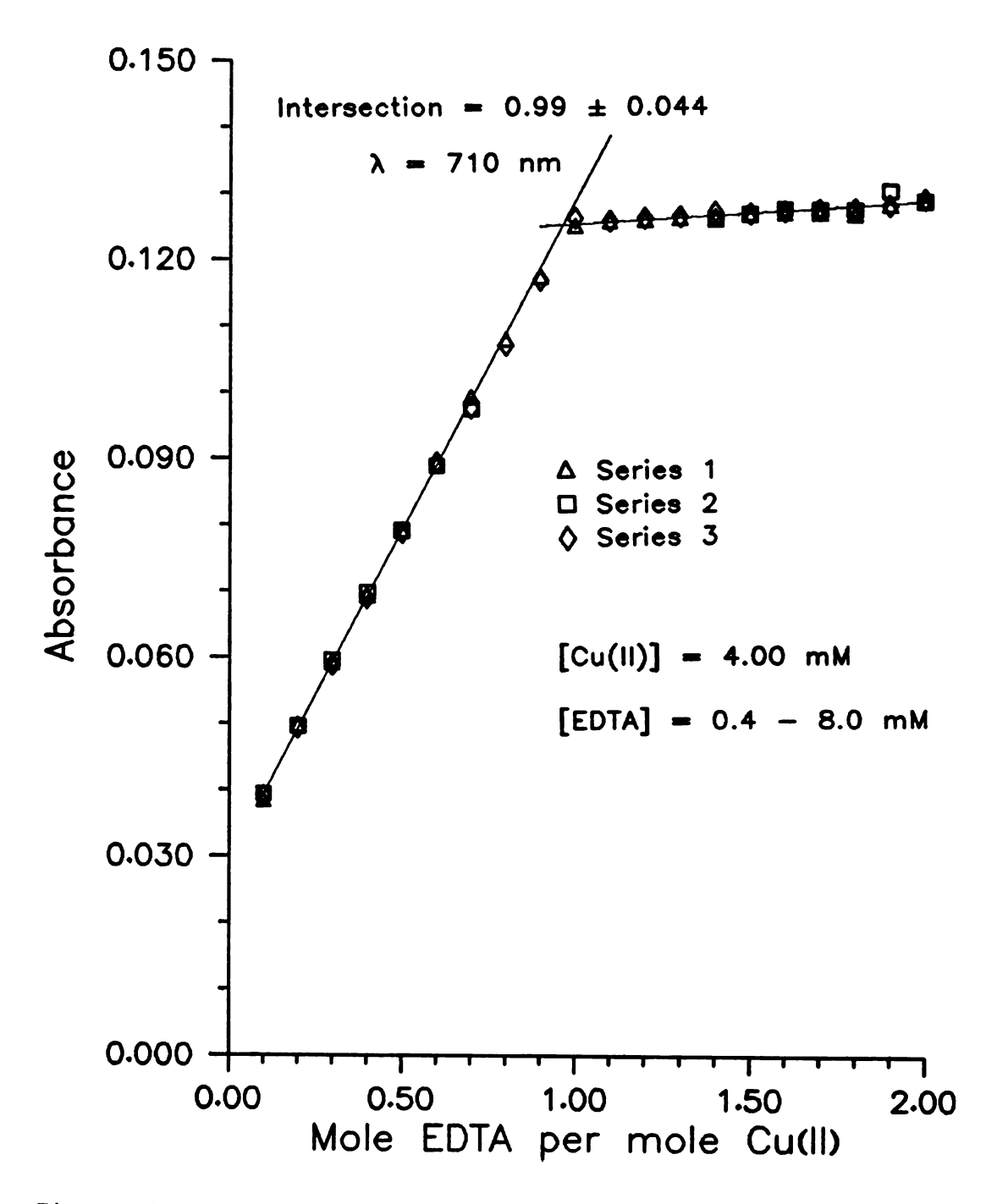


Figure 12. Absorbance vs. mole-ratio EDTA/Cu(II)

monohydrate, and a combination buffer-reducing agent solution that was 0.056 M citric acid, 0.089 M hydroxylamine hydrochloride, and a 0.02 M sodium hydroxide. The sequence of preparation of the solutions consisted of the delivery of 10 mL of buffer-reducing agent from the 50 mL syringe followed by appropriate volumes of iron and 1,10-phenanthroline from the 5 mL and 1 mL syringes, respectively. The absorbance of the resulting solutions was measured at 510 nm using the same equipment and procedures outlined in the previous section.

This particular study was chosen to observe the performance of the 5 mL syringe in delivering small reagent volumes. In the experiment, three series of 14 solutions each were prepared, all containing a constant molar concentration of iron (II) and 1,10-phenanthroline. The concentrations of the two reactants varied from 0.0 to  $150.0\mu M$ . The 5 mL syringe delivered volumes of iron stock solution ranging from 25  $\mu L$  to 900  $\mu L$ . The 1 mL syringe delivered volumes of 1,10-phenanthroline ranging from 100  $\mu L$  to 1000  $\mu L$ .

The results of the plot of absorbance of each of the solutions at varying mole fractions of 1,10-phenanthroline are shown in Figure 13. In this case, the variation of the absorbance of the individual solutions in each of the series was expected to be larger than that of the absorbance measurement because of the small volumes of reagents delivered. The results show that the absorbance of each

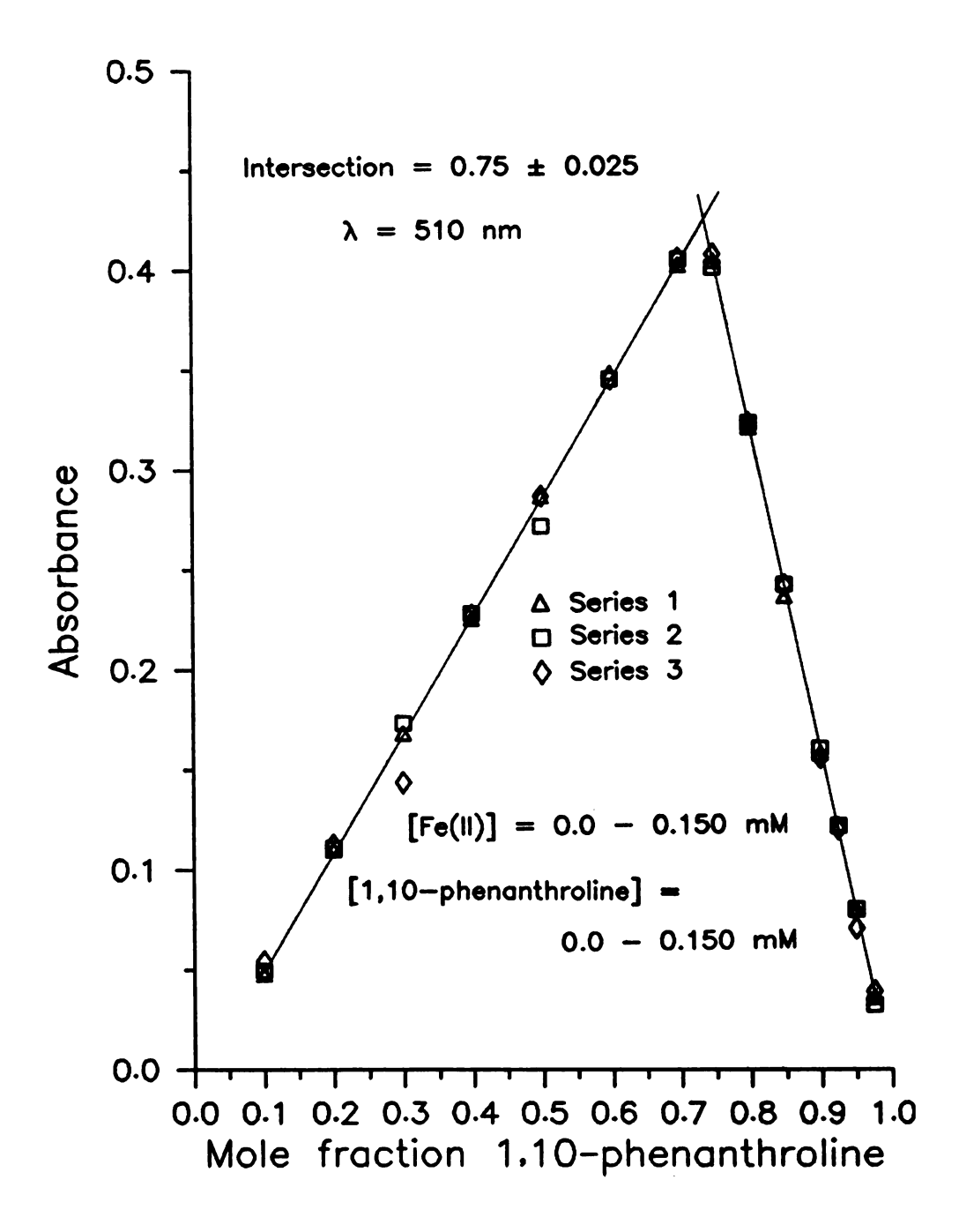


Figure 13. Absorbance vs. mole-fraction 1,10-phenanthroline.

solution at a given mole fraction of 1,10-phenanthroline is the same as or less than the uncertainty involved in the absorbance measurement, particularly in the region of mole fraction of 1,10-phenanthroline of 0.975 to 0.750. This region corresponds to 25 µL to 250 µL of iron delivered. The extrapolated linear portions of the plot intersect at a mole fraction of 1,10-phenanthroline of 0.75, corresponding to a stoichiometry of the iron-1, 10-phenanthroline reaction of 1:3, as is expected. An additional feature of the results of this study is the fact that three orders of magnitude of concentration can be reliably covered using the 5 mL syringe and one concentration of stock reagent. Also, this experiment demonstrates that a dilution factor of 1:4000 can be obtained routinely and reliably.

A simple test was done to see if the 5 mL and 1 mL syringes could be used interchangeably to deliver volumes of up to 1 mL. The same iron 1,10-phenanthroline reaction was used as a basis for evaluation. First, a series of solutions were prepared with the iron stock delivered from the 5 mL syringe and the 1,10-phenanthroline stock from the 1 mL syringe. In the second series, the iron reagent was delivered from the 1 mL syringe and the 1,10-phenanthroline from the 5 mL syringe. The absorbances of the solutions were measured at 510 nm. The plot of absorbance vs. mole fraction of 1,10-phenanthroline is presented in Figure 14. As can be seen from the plot, the two syringes are virtually interchangeable in the delivery of volumes up to 1 mL. The

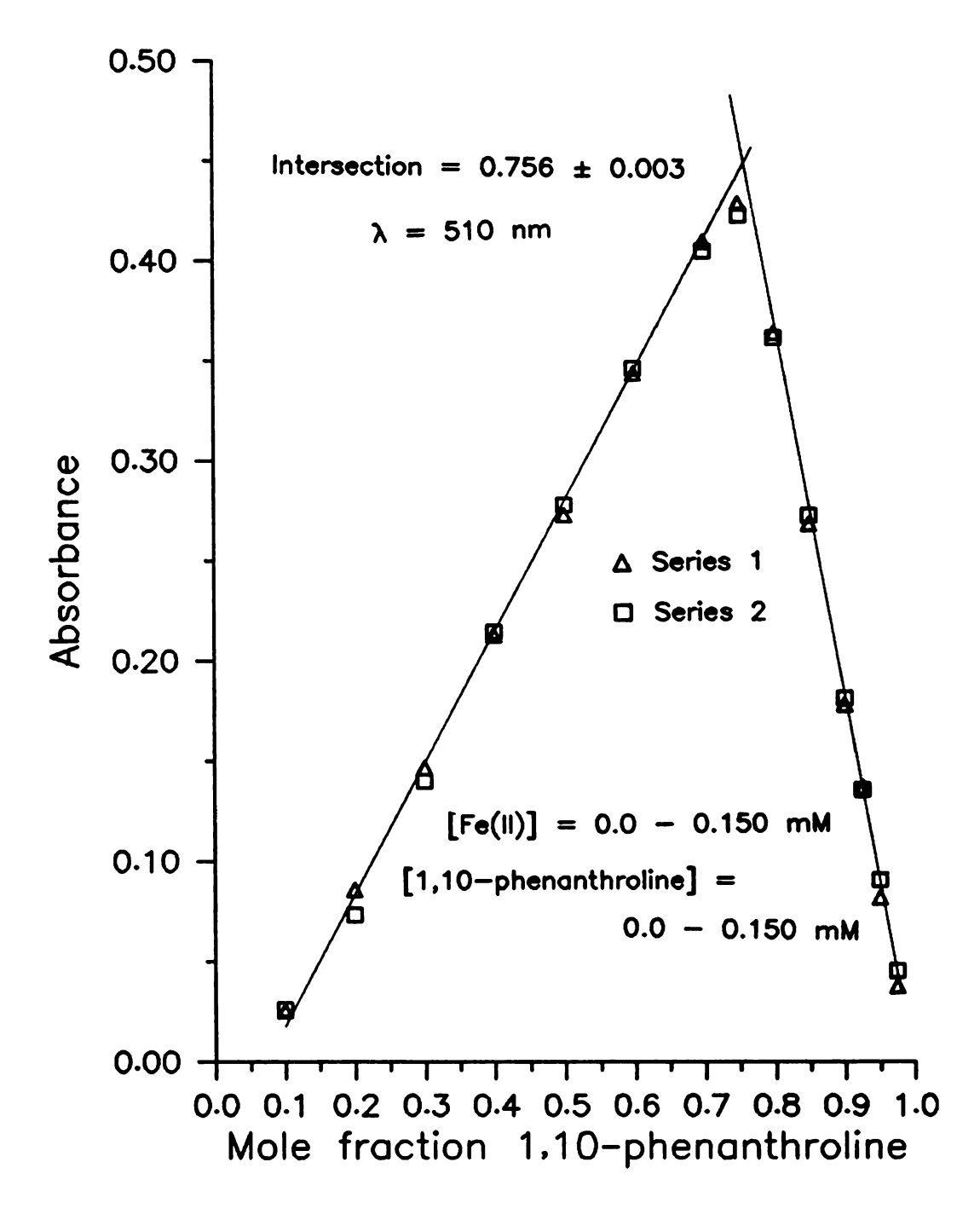


Figure 14. Test of syringe interchangeability using the Fe(II)-1,10-phenanthroline reaction.

slight variation in the measurements is due to imprecision in the absorbance measurement and to differences in the volume resolution between the two syringes.

#### CHAPTER IV

THE EVOLUTION OF AN AUTOMATED STOPPED-FLOW INSTRUMENT

The first building block of a complete automated system was presented in chapter 3. The next logical unit in completing the system is an automated instrument that can be used to encode all of the chemical information of the prepared reagents as digital electronic signals. The approach taken in this chapter is one of fitting the automated method to the existing technique of molecular absorption spectrophotometry used to encode the chemical information.

Equilibrium methods usually require a relatively long time for analysis fo the sample and are inherently prone to interferences that may lead to inaccuracy. All equilibrium methods of measuring solution parameters have their merits. However, equilibrium methods used with slow reactions do not benefit from the increased sample throughput rate of automated methods. Many modern instrument manufacturers have added microprocessors to control the various manual manipulations of modern molecular absorption spectrophotometers, for example, slit adjustment, titration, or light source drift compensation. This has increased the efficiency, precision, and accuracy of the equilibrium absorbance measurement for relatively fast reactions, but in cases where reactions proceed slowly, the analyst must still

wait for the solution to equilibrate after preparation to measure its properties. The time saved in preparing solutions rapidly may be offset by the time required to wait prior to the measurement step.

Along with the electronics revolution in the 1970's, reaction-rate methods have gained widespread acceptance for quantitative analysis. In many cases, rate methods have certain inherent advantages over classical equilibrium methods. Reaction-rate information can be obtained routinely on reactions with half-lives as short as a few milliseconds when the method of stopped-flow mixing of reagents is used. The strongest attributes of the technique in quantitative analysis include rapid availability of information and therefore, large sample throughput for single component determinations, versatility in terms of the wide range of reaction rates that may be conveniently measured, applicability to equilibrium-based methods, and most significantly, the potential for completely automated, rapid mixing of reagents.

As with any method, there are several limitations to be aware of whenever reaction-rate methods are used. For the method to be analytically useful, the reaction in question must occur at a conveniently measureable rate. Reactions with half-lives of less than several milliseconds cannot be measured using conventional stopped flow techniques because of the dead time of the instrument. On the other hand, fluctuations in the detector, source, or temperature of the

system will adversely effect the accuracy of measurement of the rates of slow reactions. Just as in equilibrium methods, the experimental conditions must be carefully controlled in rate methods. Factors such as pH, ionic strength, and temperature effect the results obtained even more so than in stoichiometric methods.

Because reaction-rate methods often measure very small signal changes, the sensitivity of the technique is limited by the signal-to-noise ratio of the measuring system.

Improvements in detection systems, the use of automated reaction-rate measurement instrumentation, and careful selection and control of the experimental parameters can provide circumstances under which the above limitations are minimized.

The intent of the remaining chapters of this thesis is to present the reconstruction and improvement details of the controlling hardware and software of a stopped-flow instrument developed by previous workers in the Crouch group, the completion of a totally automated system that uses the stopped-flow method to analyze solutions prepared with the automated reagent preparation system, and extension of automated stopped-flow measurements to quantitative analysis of several samples.

#### A. General Considerations

In that the purpose of this work is to present the results of using reaction-rate methods for analysis, rather

than present a lengthy review of methods and instrumentation developed by other workers in the past, the reader is referred to two review articles that contain excellent synopses of the development of the stopped-flow technique, its applications, and its automation (11,43).

The automated stopped flow instrument used in the studies presented in this work was originally described by Beckwith (44) and has been used successfully to perform several fundamental reaction-rate studies (45-49). controlling hardware and the software written for the instrument was developed with the technology available at the time, but its operation was somewhat unreliable and required a significant amount of time and manipulation to obtain quantitative results after the measurement occurred. In the interest of completion of a totally automated analysis system, it was decided to reconstruct the controlling and data acquisition electronics as well as write a software package that would provide for more efficient and reliable operation of the stopped-flow instrument. Although an off-line microcomputer would be ideal for the controlling and data-acquisition functions, several constraints prevented its use. The microcomputer requires a real-time clock, an option that was not available at the inception of the project. Although software delay loops can be used to time events, this method does not provide the precision, flexibility, or ease of programming of a real-time clock. Also, the relatively slow cycle time of the processor does

not allow rapid data taking and prohibits any sort of data manipulation in between acquisition of the data points. Finally, a high level programming language must be used to provide for ease of programming, clear interactive communication with the user, and data processing. As mentioned in the previous chapter, FORTRAN II cannot be efficiently utilized with the IM6100 microcomputer systems. Although rudimentary control and data acquisition functions could be implemented using the PAL8 assembly language in the microcomputer, the limitations of difficult programming and limited memory space were considered to prohibit the use of the microcomputer for these functions.

Using the PDP 8/e minicomputer to do all of the control, data acquisition, and data manipulation functions would be advantageous in several ways. All of the programming can be written in the higher level FORTRAN II language, with the individual operation codes for each of the functions embedded within the program. Use of the hardware multiply-divide option in the minicomputer enables rapid averaging of data without having to slow down the data acquisition rate. The large memory space available enables storage and averaging of many data sets, with direct storage on magnetic media.

This chapter serves as a document for modifications to the controlling hardware and construction of an 8-channel data acquisition system. Results utilizing the complete automated analysis system are also presented.

### B. Automated Stopped-Flow System Description

The block diagram of the data acquisition and control system for the stopped-flow instrument is shown in Figure The user controls the operation of the system from a console terminal through the minicomputer. All data and timing signals to and from the PDP 8/e are transferred through a computer interface buffer box (50). Three valves on the stopped-flow instrument control solution uptake, mixing, and waste functions. The stopped flow spectrophotometer consists of a light source (51), a monochromator (52), and the stopped flow instrument. Light passes through a quartz fiber optic through the stopped-flow observation cell and through a quartz rod onto the photocathode of a photomultiplier tube (53). The current generated is converted to voltage by a current-to-voltage converter (40) and routed to a digital voltmeter (DVM) and one channel of the data acquisition system. The digitized analog signals are stored in computer memory until the data acquisition for a single solution is complete. The data then can be displayed on an oscilloscope, whose beam is deflected by the digitized data being played back from memory through a digital-to-analog converter (DAC). After data storage on an appropriate medium, the experimental parameters and data can be printed via a printer.

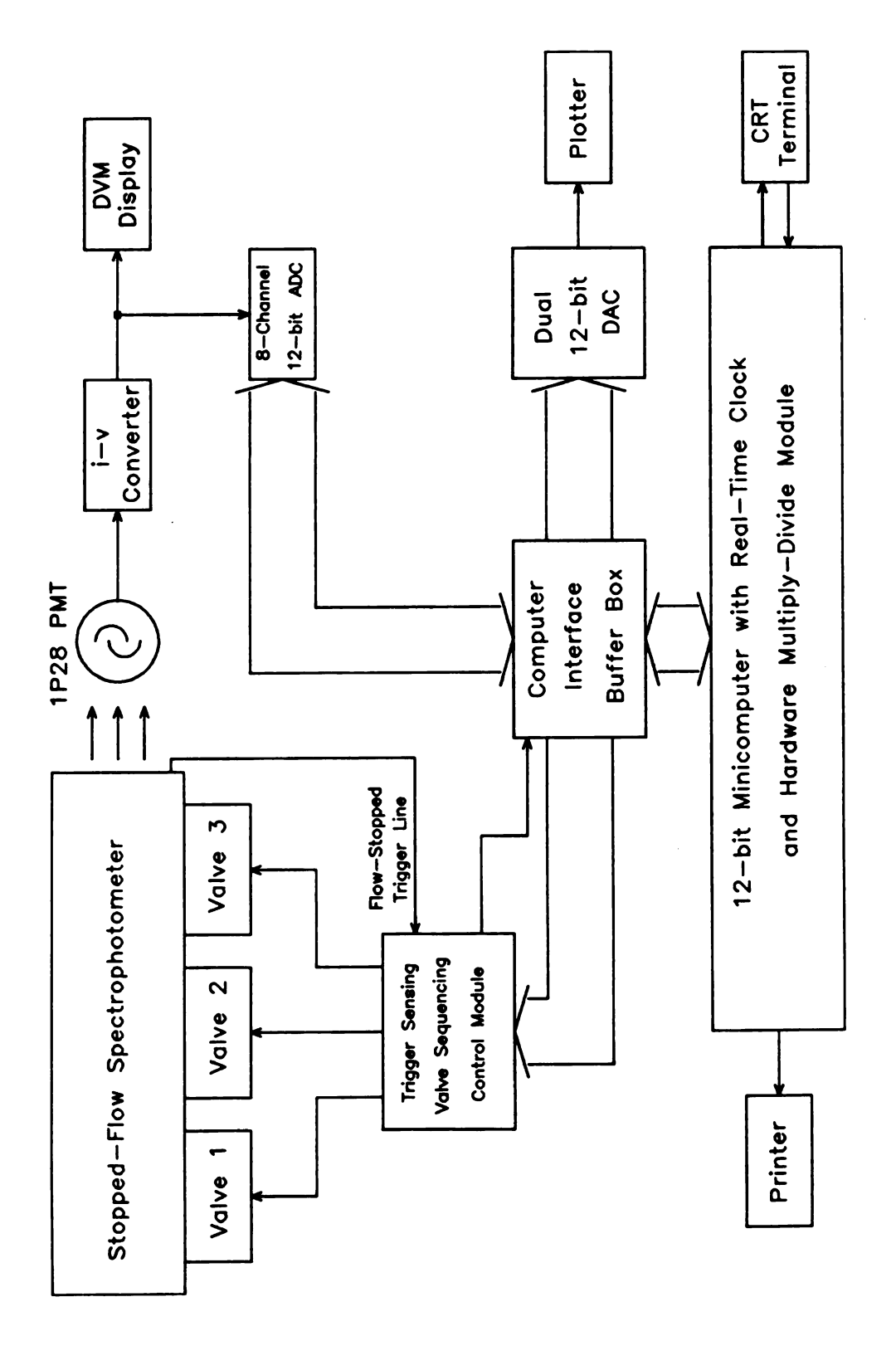


Figure 15. Block diagram of the automated stopped-flow instrument.

#### 1. The Valve Controller Module

The function of the controller module is to provide signals to the pneumatic valve solenoids and to sense the point at which the stop syringe ceases motion. The module has the capability of both manual and computer control of the valves.

The schematic of the circuitry for the controller module is shown in Figure 16. The controller is configured to come up in the remote control mode upon power up and all of the control lines are deactivated by a  $\sim 0.5$  s pulse from monostable in Figure 16. The origin of the control signals, i.e. remote or local, is selected by a two-to-one line multiplexer that is toggled through switch SW4. In the remote mode of operation, the appropriate flip-flops are simply set HI or LO to open or close valves through digital signals generated by the computer. Local control signals are generated from debounced switches SW1-SW3. The output of the particular flip-flop is toggled from its previous state every time the momentary ON switch is depressed. The valve control lines are deactivated whenever the controller is switched into the local mode. The status of the valves is indicated by display LEDs: red for activated, green for deactivated. LO control signals turn the red LEDs off and are inverted to turn the green LEDs on. The signals are inverted again for distribution to zero-crossing, optically isolated solid state relays (34) that switch 120 VAC to the pneumatic valve control solenoids (35), which in turn

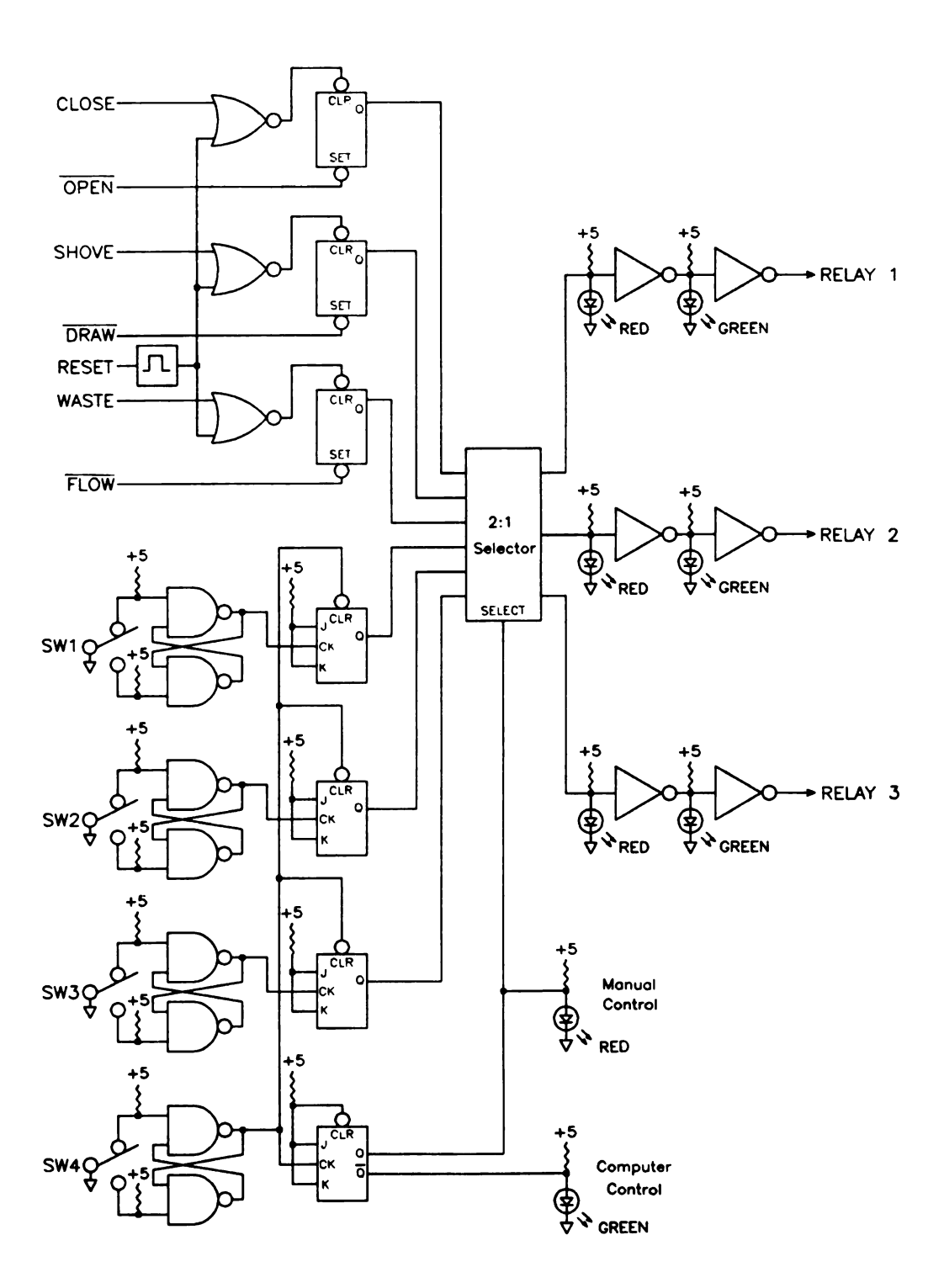


Figure 16. Schematic of the stopped-flow valve controller.

control the position of the valves.

# 2. The Flow-Stopped Status Generator

A circuit designed to provide a trigger signal at the time when the flow of solution through the observation cell has ceased is shown in Figure 17. This circuit is similar to the window detector described in chapter 3 in that an optical interruptor module is used to sense when a bar attached to the stop syringe plunger crosses its light path. The setting of the reference voltage by R1 is not as critical as in the case of the meniscus detectors. The user merely needs to adjust R1 until the front panel indicator LED goes out. The circuit then provides an active LO pulse to the computer interface as a reference point to be used to ascertain "time zero" of the reaction curve.

#### 3. The Computer Interface Module

The decoding of all remote control signals and conditioning of the trigger signal is shown in Figure 18.

Since the exact timing and instruction decoding methods have been well documented elsewhere (54), only the basic principles of instruction decoding and the interface operation will be presented. As with the IM6100 microprocessor, the PDP 8/e recognizes an I/O instruction when bits 0-2 of the instruction are set to an octal 6. The KA8-E positive I/O bus interface generates pulses used to synchronize input and output data with the computer cycle.

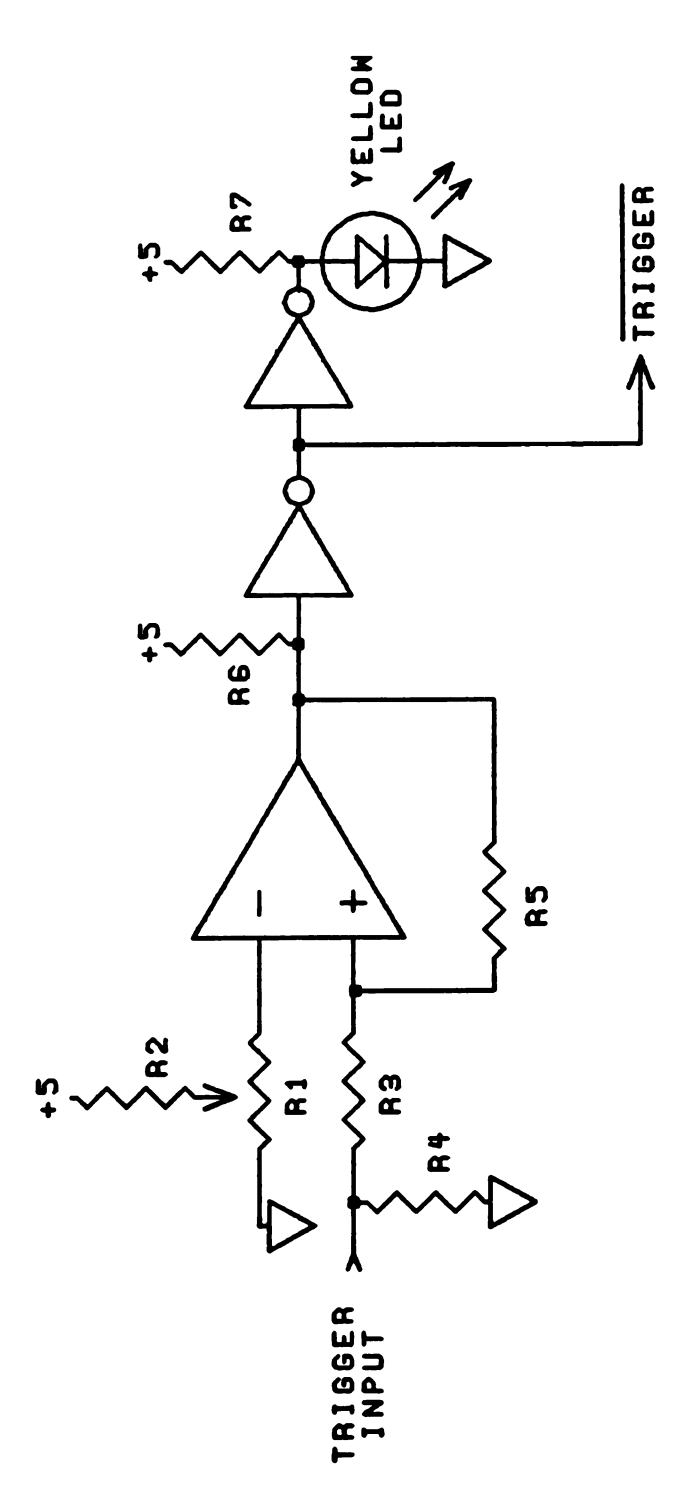


Figure 17. Schematic of the flow-stopped status signal generator.

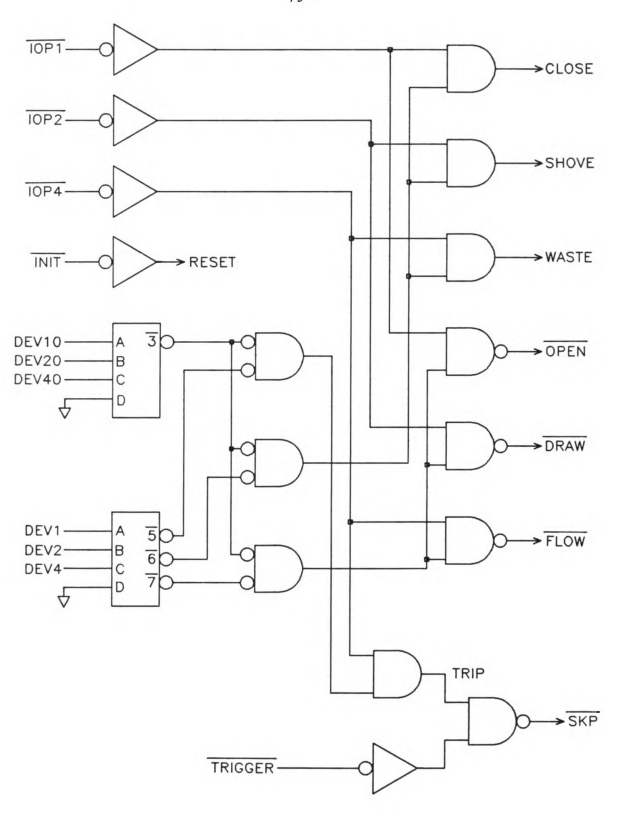


Figure 18. Schematic of the valve controller-to-minicomputer interface.

Three IOP pulses can be generated in sequence: IOP1, IOP2, and IOP4. Bits 9-11 determine which of the IOP pulses will be generated. The IOP pulses are different from the assignment pulses in the microprocessor in that the generation of IOP pulses allows for up to three operations in the external device to be controlled by the minicomputer with a single I/O instruction. Although Digital Equipment Corporation (DEC) has specified their peripherals to respond to IOP pulses in pre-defined ways such as sampling and clearing of flags, sending and receiving data, and loading and clearing of buffers for IOP1, IOP2, and IOP4 respectively, the design of the interface to the external device will ultimately determine what function is to be performed.

The middle six bits of an instruction word are used to identify the device that is to be activated. The familiar octal decoder circuit shown in Figure 18 is used to generate the device code identification pulses via chips. The device select and IOP pulses for a given operation are logically ANDed together to generate the appropriate control signal. In general, any signals involving opening of valves are active LO, while signals that close valves are active HI. This was done to simplify the clearing and setting of the remote control flip-flops in Figure 16. A summary of the operation codes and mnemonics of the software commands for the stopped-flow valve controller appears in Table 6.

The monitoring of the flow-stopped status line is done by the TRIP command. The program executes a status checking

<u>Table 6.</u> Stopped-flow Instrument Controller Software Commands.

MNEMONIC	OPCODE	OPERATION
OPEN	6371	Open valve to draw up reagents.
DRAW	6372	Draw reagents into syringes.
CLOSE	6361	Close valve to prevent draw-up of reagents.
SHOVE	6362	Pressurize reagent syringes.
FLOW	6374	Open valve to allow mixing of reagents.
WASTE	6364	Expel used solution from stop syringe.
TRIP	6354	Skip next instruction on flow-stopped trigger.

loop by continuously jumping back to this instruction until the  $\overline{TRIGGER}$  line is asserted. The status loop is exited by assertion of the  $\overline{SKP}$  line.

# 4. The Data Acquisition System

It was necessary to redesign the data acquisition system to provide the flexibility of monitoring several channels of data simultaneously in future applications of the stopped-flow instrument. The data acquisition system is based upon an 8-channel analog multiplexer (56) with a l  $\mu$ s settling time and a 12-bit hybrid analog-to-digital converter (56) with an 8  $\mu$ s conversion time. The schematic diagram of the system is shown in Figure 19, with the appropriate software commands listed in Table 7.

The LATCH command causes the channel information to be available to a 74174 latch, which in turn selects the proper channel on the multiplexer in Figure 19. The analog signal is the input to a sample-and-hold amplifier (57) that has a 0.5 µs settling time in the "hold" mode. The sample-and-hold stores the analog signal on the rising edge of the pulse generated by the CONVERT instruction. The falling edge of this pulse triggers a monostable multivibrator, which starts the analog-to-digital conversion and simultaneously locks out the CONVERT line from any other spurious pulses, a problem inherent in the positive I/O buffer-driver of our PDP 8/e. The end of conversion (EOC) pulse from the analog-to-digital converter (ADC) sets a flip-flop to provide an

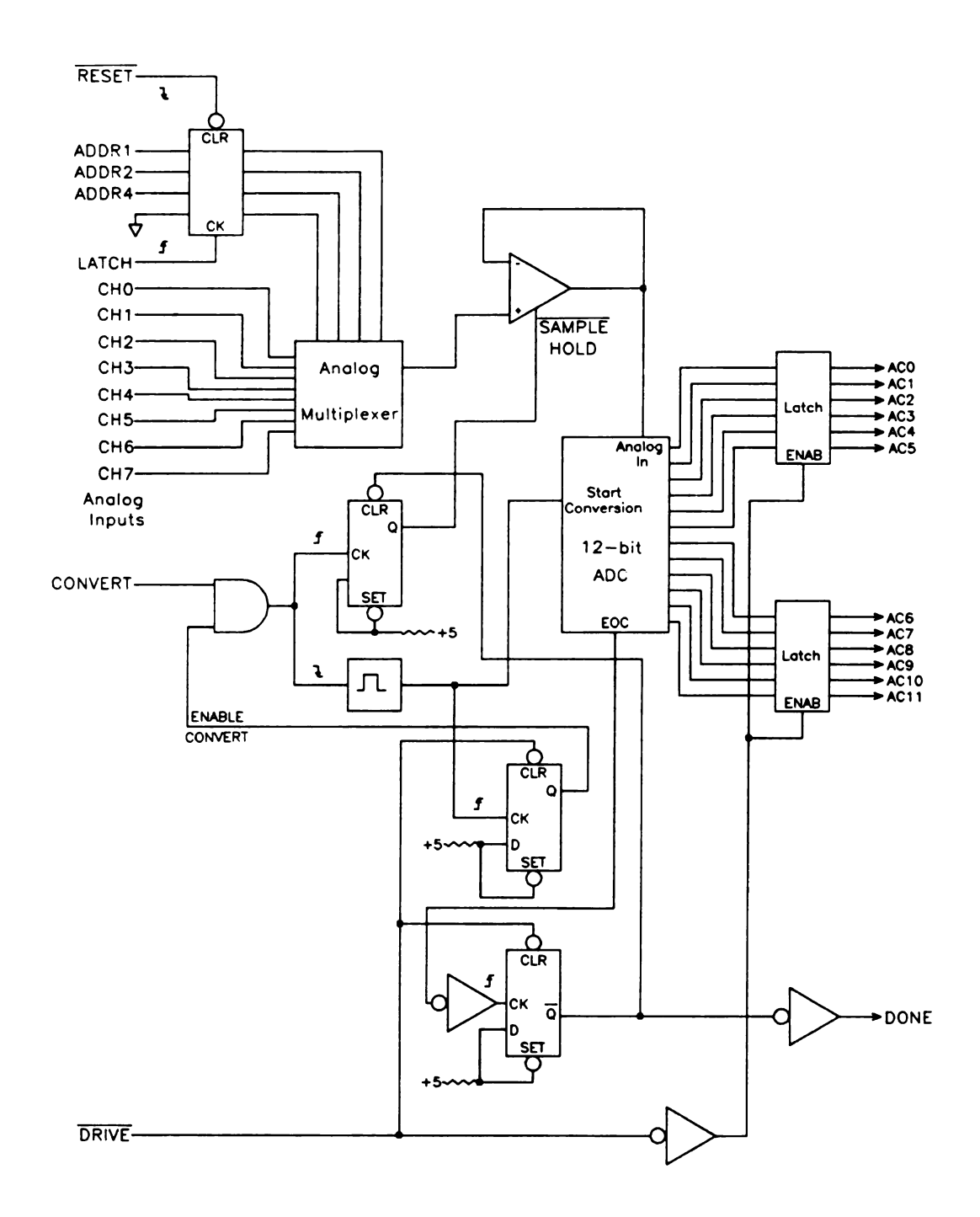


Figure 19. Schematic of 8-channel data acquisition system.

Table 7. Software Commands for Data Acquisition and Display System.

MNEMONIC	OPCODE	OPERATION
LATCH	6521	Latch channel of analog input.
RESET	6522	Reset address decoder to channel 0.
CONVERT	6531	Start A/D conversion; clear accumulator.
DONE	6532	Skip next instruction if conversion is complete.
DRIVE	6534	Send data from A/D to accumulator.
DAC1	6504	Load accumulator into latch of D/A #1.
DAC2	<b>6</b> 514	Load accumulator into latch of D/A #2.

active HI DONE pulse, which is used during the EOC status check operation. When the DONE line is asserted, the next instruction in the status checking loop is skipped. The final instruction of the data acquisition sequence, DRIVE, latches the converted data into two six-bit latches, enables the CONVERT line by clearing the appropriate flip-flop, and clears the EOC flag latch.

Initial evaluation of the data acquisition system indicated that there was no detectable crosstalk of analog information between the channels. However, it appears that the sample-and-hold amplifier requires one conversion cycle to settle on the new data accurately. If multiple channels of the ADC are to be used, the most efficient mode of operation would entail throwing out the first conversion after switching channels. Since a single conversion cycle is on the order of 10  $\mu s$ , this would not be a great inconvenience in terms of lost data or decreased acquisition time.

# C. Operational Software Description

The software originally developed for the stopped flow analyzer required execution of three separate programs to run the stopped-flow instrument and acquire data, to store the data, and to plot and analyze the stored data. Quite frequently, data were lost because the user had not correctly typed in the name of the data storage program. The object of rewriting the software was to provide a general purpose

routine to perform all of the above functions, with the exception of data analysis, which the user could write to fit his specific needs. The task was made simpler by the availability of an extended FORTRAN II programming language (58) that allows use of logical relationships, which were only available through DEC's FORTRAN IV language at the time. It is very inconvenient to write assembly code instructions in FORTRAN IV because they have to be coded in a manner specific to the language and may not reside within the body of the main program. FORTRAN II allows direct insertion of machine code operations within the flow of the program by prefixing the instruction with an "S" to indicate the operation as such.

The controlling software package consists of a main program with 11 subroutines, whose functions are listed in Table 8. The program flow is tailored so that any user may work with the stopped-flow instrument by reading the instructions and prompts printed out on the console during program execution. Figure 20 shows the flow of the operations during a typical stopped-flow analysis. The user first initializes the system by turning on the appropriate power supplies and plugging in the paddles for the valve controller module, data acquisition, and data display interfaces. When the program is started, a checklist page of instructions is typed on the terminal followed by a list of available options. There is sufficient checking of software flags in the program to ensure that the parameters are set

- Table 8. Functions of Stopped-Flow Controller Software Modules.
- MAIN All bells and whistles for user interaction. Routine checks flags, inputs operation options, and lists options on terminal.
- GO Controls stopped-flow operation: valve sequencing and data acquisition.
- STORE Averages data from one stopped-flow run to obtain standard deviation for each point. Data are corrected for a blank rate if present and converted to absorbance. Routine stores data on a floppy disk.
- SFPLOT Plots out data from a run or from a file on the oscilloscope.
- INPUT Reads in stored data file and parameters.
- RINSE Rinses stopped-flow reagent syringes three times.
- FILL Fills the stopped-flow reagent syringes.
- WAIT(n) Executes wait loop for "n" seconds.
- BELL Rings the TTY bell.
- ERASE Erases the terminal screen.
- CKSTRT Start real-time clock running.
- CSTOP Halt real-time clock.

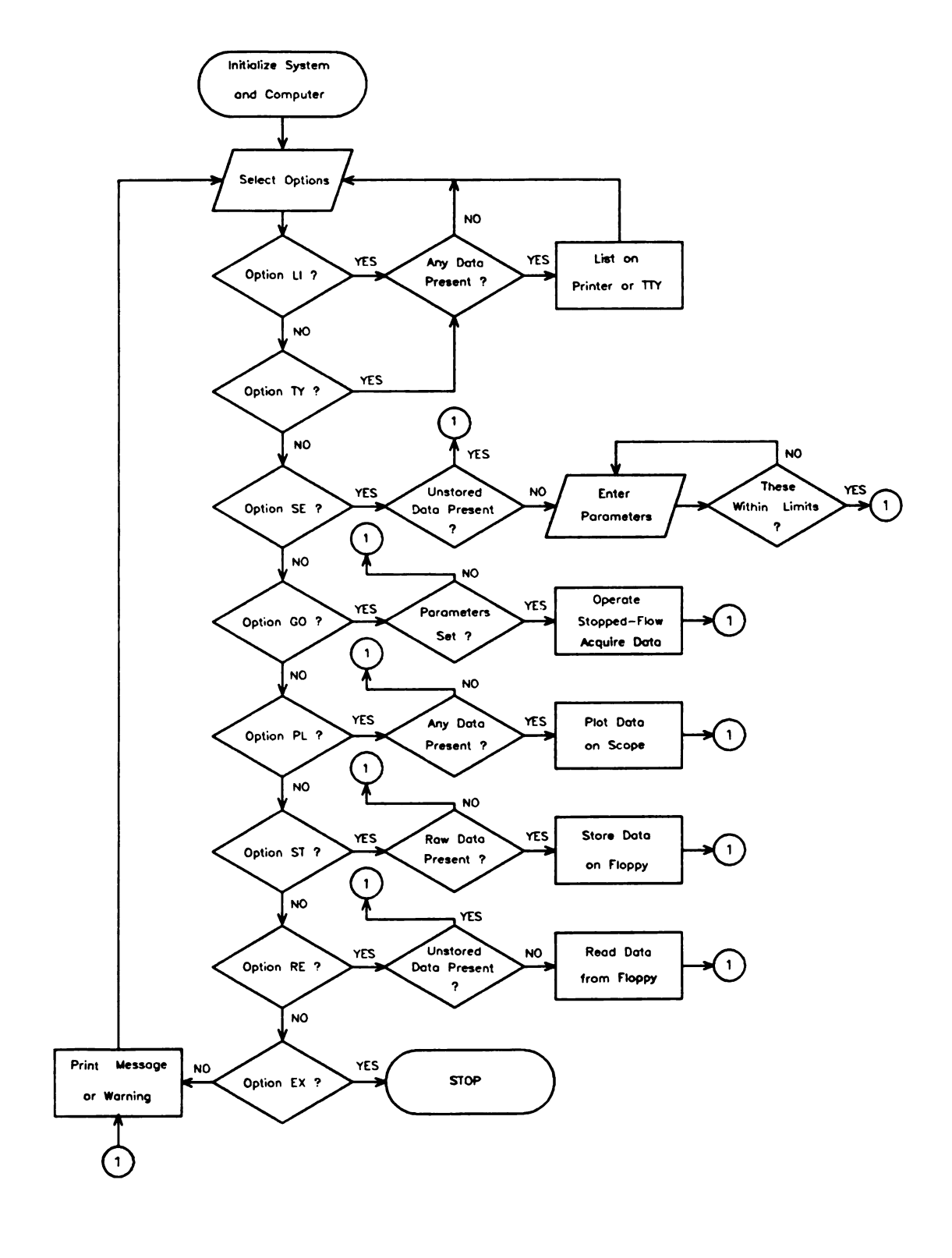


Figure 20. Sequence of operations for a typical stopped-flow analysis.

before an analysis, or that the data have been stored after a run, before a potentially data-destructive option is chosen. In normal operation, the user first sets the data acquisition parameters. These consist of the data acquisition rate in milliseconds, the number of analog points to be averaged to form one data point per time interval, the time interval between data points in units of one data point time interval, the delay time before data acquisition starts after the stop syringe crosses the flow-stopped detector, the number of data points to be taken per push, the number of data pushes per syringe filling, and the number of syringe fillings per analysis. The appropriate limits for these parameters are printed out along with the request for the parameters. The data input subroutine checks the input parameters to see if they are within the limits defined. Once the parameters are set, the user calls for the operation and data acquisition subroutine. The user then has the option of doing a blank run to ascertain the 100% transmittance level if necessary. The dark current of the PMT is recorded by the program. The user is requested to close the light source shutter and to strike any console key to initiate acquisition of the dark current level. The program then tells the user to open the shutter and to check that everything is set to do the analysis. After this point, the program takes over to do all of the automatic valve sequencing and data acquisition. The syringes are rinsed if the option was selected, and the valves are

sequenced through the data acquisition routine. The dark current is subtracted from each data point as it is acquired. Once all of the data have been collected, the user has the option of plotting out the raw data on an oscilloscope. If this option is selected, the computer sequentially sends out the data just taken to the digital-to-analog converter (DAC) connected to one channel of the oscilloscope. data are plotted out continuously until a key is struck on the console. The user then initiates data storage by typing the appropriate option code followed by the file identifica-The data storage routine averages all of the pushes, corrects for any blank absorption of the solutions, and stores the time-correlated absorbance data with the appropriate standard deviation values for each point. first line of the data file contains the data acquisition and control parameters so that these conditions may be duplicated in future experiments. After the data are stored, the user may ask for a plot of the scaled, averaged absorbance data on the oscilloscope. If the parameters for the remaining solutions in the analysis are the same, the operator may directly enter into the control and data acquisition routine, since the parameters are still resident in memory. Finally, the user has the option of reading in an existing data file to reset parameters or to display or print data. Once all of the required data are stored for a given experiment, the user then chains the data file to his own data analysis routine. This permits individuals to write

custom routines to handle their specific applications, which may consist of obtaining initial rates from the data, fitting rate equations to the data, and so on.

#### D. Stopped-Flow Instrument Characteristics

The observation cell path length and dead time of the stopped-flow instrument were measured to re-establish these specifications. Standard test reactions and calibration solutions were used to determine these characteristics.

#### 1. Observation Cell Path Length

Three solutions containing accurately known concentrations of potassium dichromate in 0.005  $\underline{\text{M}}$   $\text{H}_2\text{SO}_4$  were used to determine the path length of the stopped-flow instrument observation cell. The absorptivity of the dichromate was determined by measuring the absorbance of the solutions at 350 nm on a Cary-17 UV-visible spectrophotometer with a 4-1/2 digit absorbance readout. All solutions were corrected for any blank absorbance and their absorbances were measured in a 1.003 cm quartz cell. The average absorptivity of 10.77  $\pm$  0.01 L g $^{-1}$ cm $^{-1}$  is in good agreement with the accepted value of 10.70 L g $^{-1}$ cm $^{-1}$  (59). The same solutions were injected into the observation cell of the stopped-flow. The path length was determined from triplicate absorbance measurements of each solution to be 1.84±0.01 cm.

#### 2. Stopped-Flow Dead Time

A 0.001  $\underline{M}$  Fe(III) solution in 0.05  $\underline{M}$  HNO $_3$  was mixed with a 0.005  $\underline{M}$  KSCN solution 0.05  $\underline{M}$  in HNO $_3$  in the stopped flow. The course of the reaction was followed spectrophotometrically at 450 nm, and the data were acquired at a rate of one point per millisecond. Data acquisition was initiated immediately after the stop syringe plunger crossed the detector light path. The dead time was determined from a plot of the data on the oscilloscope; the acquisition routine counted the number of data points on the level initial portion of the reaction curve. The dead time was found to be 8  $\pm 1$  ms.

# E. Evaluation of the Performance of the Automated Reagent Preparation System Using Reaction-Rate Methods of Analysis

Up to this point, the functional characteristics of the modules that make up an automated reaction-rate measurement system have been presented. It has been shown how reagents are automatically prepared, then manually transported to desired locations for mixing and measurement with a convenient transducer to encode the chemical information as electrical signals. The rate data are electronically manipulated to prepare them for display or for use in quantitative measurements. This section consists of the results of studies of two well-characterized reactions to determine how effective the automated reagent preparation system is in maintaining optimum accuracy and precision in

reaction-rate measurements using the stopped-flow instrument.

## 1. Iron-thiocyante Kinetics Study

The purpose of this experiment was to generate a series of initial reaction rate  $\underline{vs}$ , reactant concentration curves to determine if maintenance of constant ionic strength is critical for reactions involving charged species in solutions prepared by classical manual methods and by automated methods. The reaction chosen for this study is the familiar iron(III)-thiocyanate reaction, with operational conditions and procedures similar to those reported by other workers (44, 60-62). Both methods of preparation were used to make the iron and the thiocyanate solutions. The iron solutions contained a constant amount of perchloric acid, while the thiocyante solutions contained amounts of sodium perchlorate that were varied to adjust the ionic strength of the mixture of iron and thiocyante solutions in the stopped-flow observation cell to 0.4  $\underline{M}$ .

a. Reagents - The stock solutions used in the automatic preparation mode consisted of 0.09997  $\underline{M}$  Fe(III) prepared from Fe(NO<sub>3</sub>)<sub>3</sub>·9H<sub>2</sub>0, 0.02519  $\underline{M}$  NaSCN, 1.003  $\underline{M}$  NaClO<sub>4</sub>, and perchloric acid that was standardized at 1.094  $\underline{M}$ . All working solutions were diluted to 47.005 mL and stored in polypropylene bottles.

The stock solutions used to prepare solutions manually were 0.4063  $\underline{M}$  Fe(III), 0.1017  $\underline{M}$  NaSCN, 0.4902  $\underline{M}$  NaClO $_4$  , and

perchloric acid standardized to 0.781  $\underline{M}$ . All working solutions were diluted to 50.00 mL and stored in polypropylene bottles.

b. <u>Procedures</u> - All of the Fe(III)-SCN reaction-rate measurements were done at 450 nm with a data acquisition rate of a point per millisecond. The rate data for eight separate measurements of a given concentration of iron and thiocyanate were averaged into one set of rate data. The rate measurements were done by first measuring the rate of reaction of solutions with constant iron concentration and varying thiocyanate concentration, followed by measuring the rate of reaction of solutions with constant thiocyanate concentration and varying iron concentration. This was done in order to establish conditions for first-order kinetics.

All of the required volumes of reagents to be used in the dilutions were calculated by the minicomputer once the values of the stock solution concentrations and the dilution volume were established. All of the parameters were shipped to the microcomputer for automatic preparation of the reagents, with manual provision of solution receptacles. The parameters for dilution using the numbers from the manual mode stock reagents were calculated by the same program. All of the solutions were prepared using the appropriate pipets, burets, and volumetric flasks. The rate data for all measurements done with the stopped-flow instrument

were analyzed by a weighted linear least-squares curve fitting routine to obtain the slopes of the reaction curves. Conditions for all of the studies were selected so that the requirements for pseudo-first order in concentration kinetics could be observed, i.e. the change in rate with initial reactant concentration for the reagents used is unity.

c. Results of Initial Rate Measurements - The plots of the rate of reaction  $\underline{vs}$ . reactant concentration for solutions prepared manually are shown in Figures 21 and 22. As can be seen in the figures, the rate data vary linearly with concentration. Log-log treatments of the data gave a slope of 1.056  $\pm 0.011$  for solutions at constant iron concentration and a slope of 0.995  $\pm 0.007$  for solutions at constant thiocyanate concentration, thus verifying the assumed pseudo-first order in concentration of thiocyanate kinetics conditions.

The plots of the rate data for solutions prepared automatically are shown in Figures 23 and 24. Log-log plots of the data gave a slope of  $0.9794 \pm 0.0006$  for the solutions with constant iron concentration and a slope of  $0.997 \pm 0.008$  for the solutions with constant thiocyanate concentration, again verifying pseudo-first order in iron concentration conditions.

One feature is obvious when the plots of the data obtained by both methods are compared: the measurement of

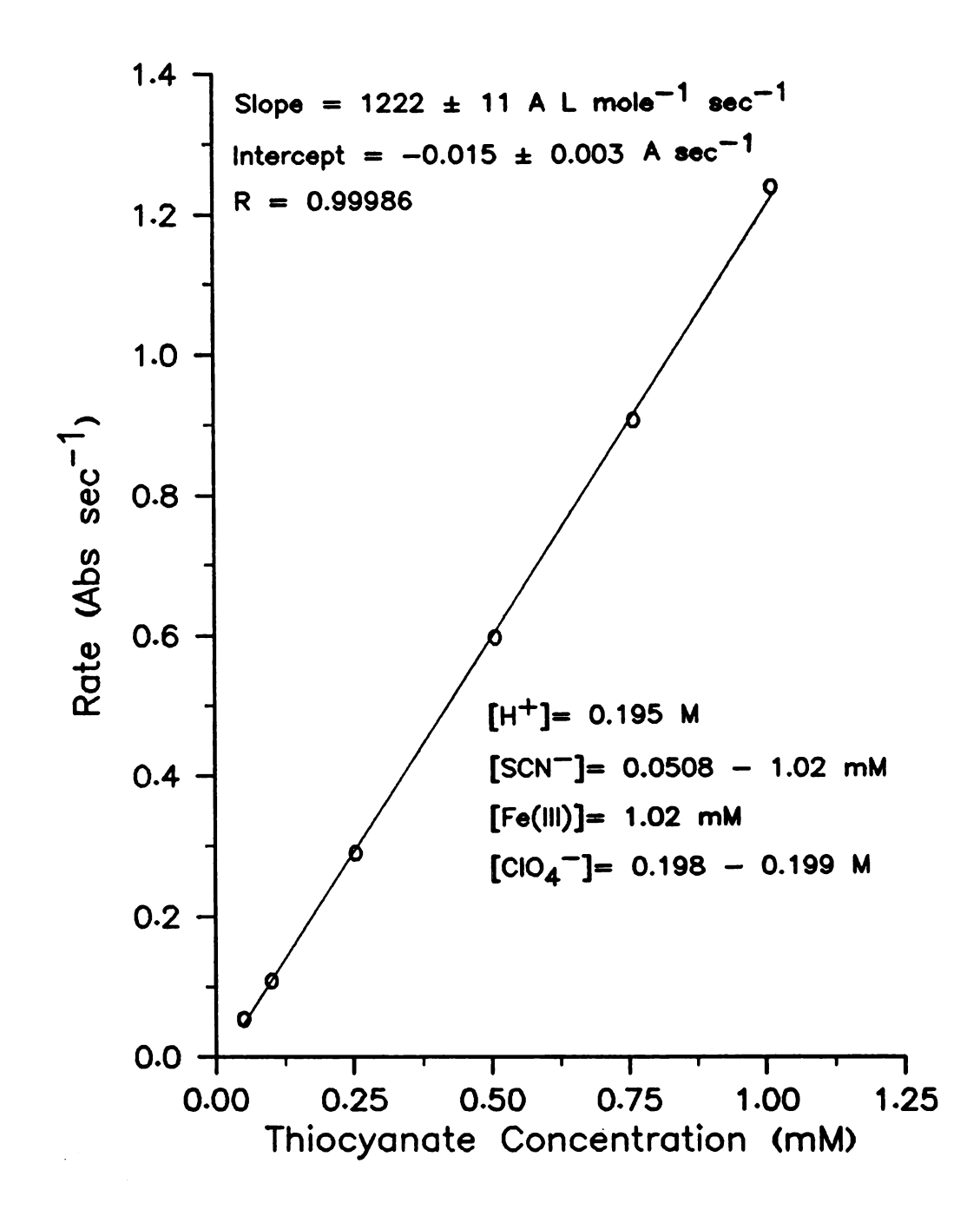


Figure 21. Initial rate vs. thiocyanate concentration. Solutions prepared manually.

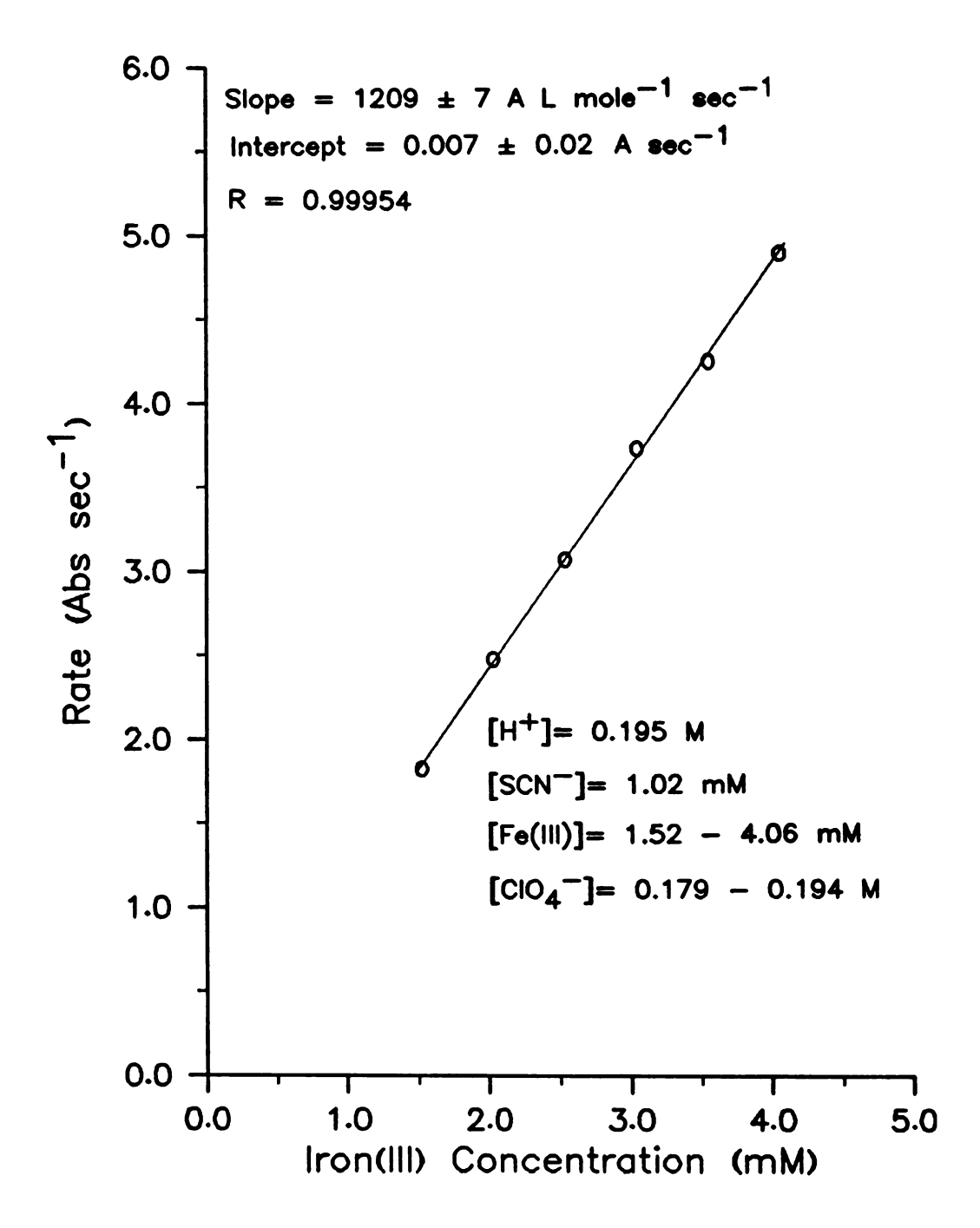


Figure 22. Initial rate  $\underline{vs}$ . Fe(III) concentration. Solutions prepared manually.

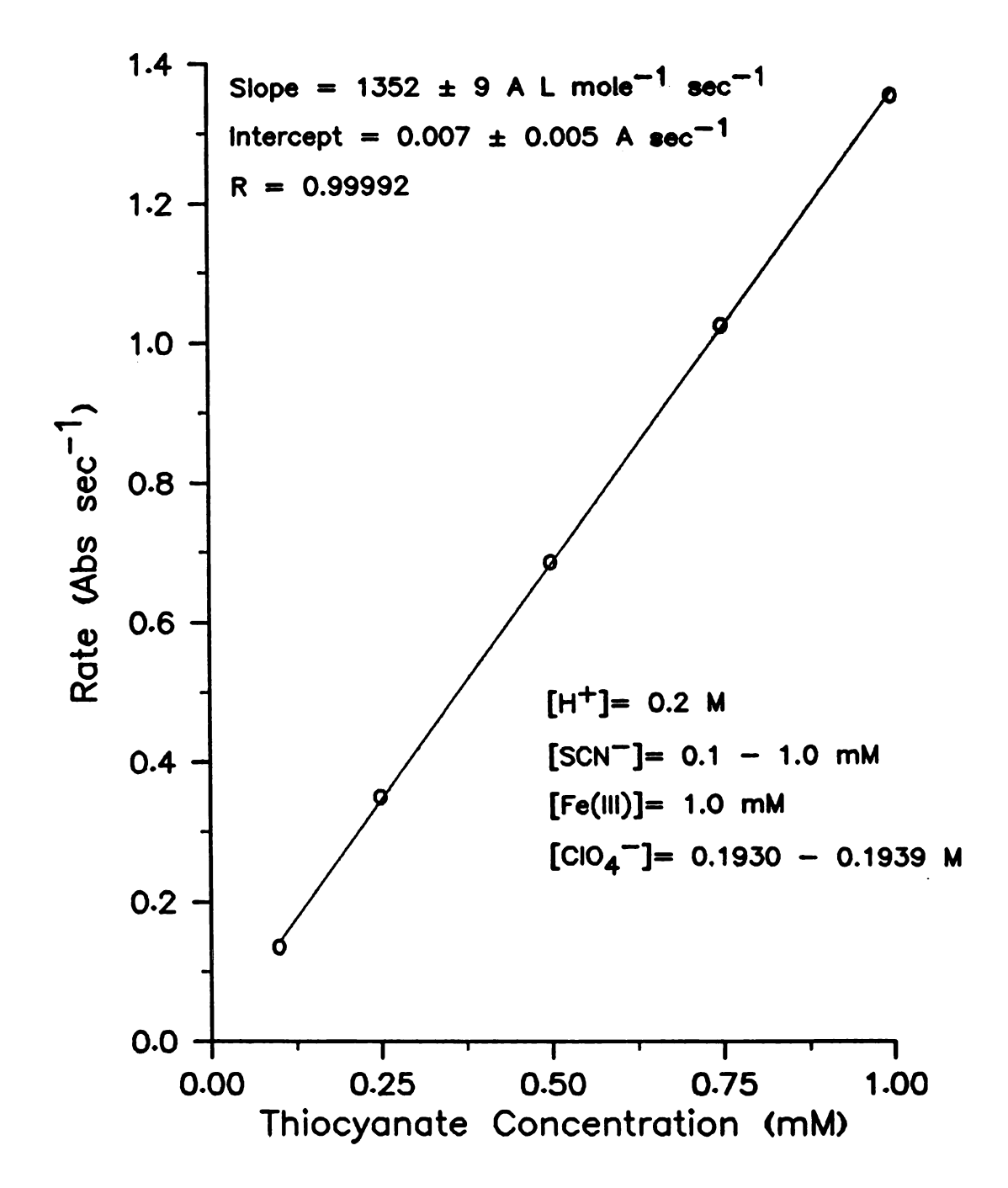


Figure 23. Initial rate vs. thiocyanate concentration. Solutions prepared automatically.

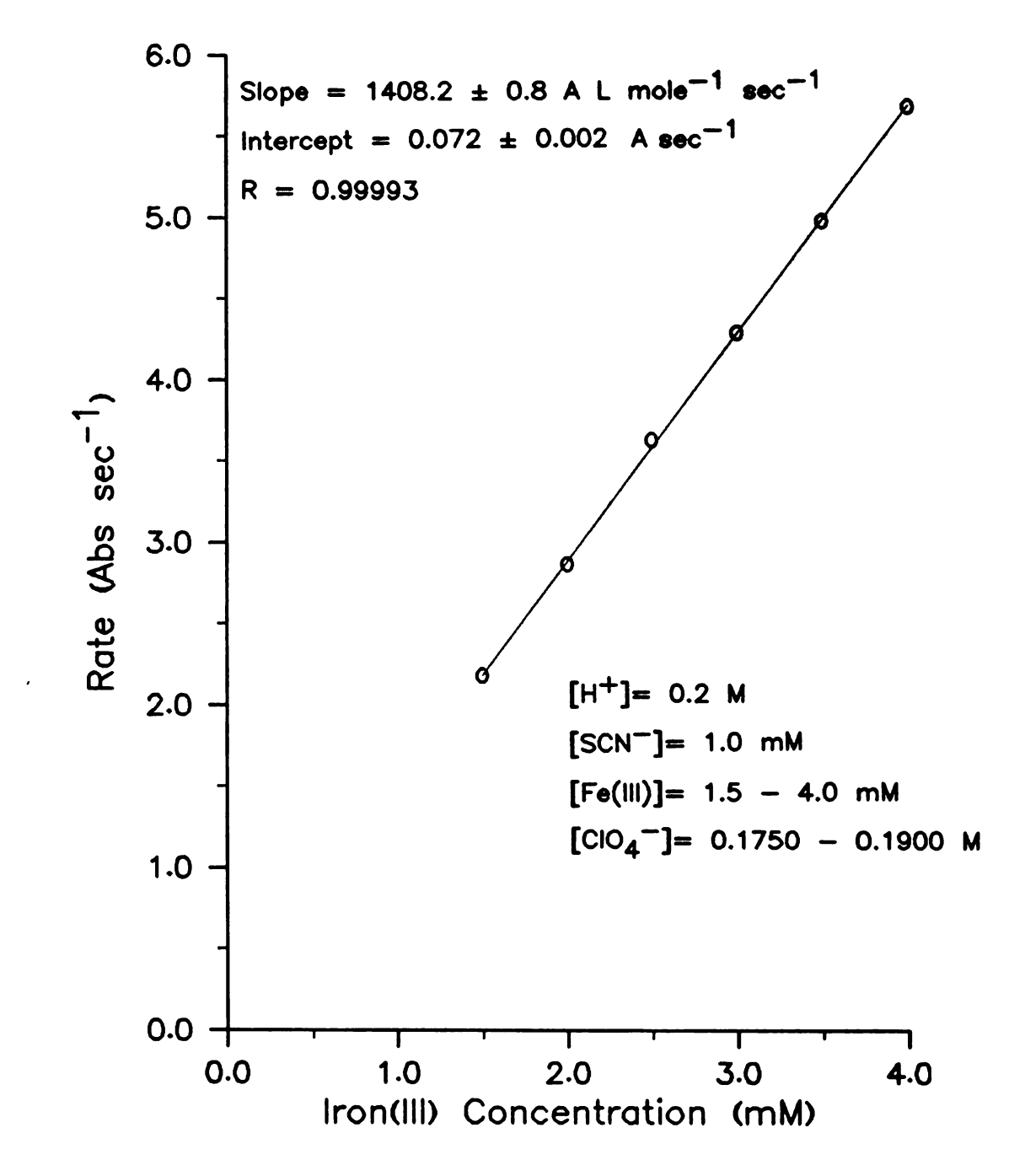


Figure 24. Initial rate vs. Fe(III) concentration. Solutions prepared automatically.

the rate of reaction appears to be the most error-prone measurement in the experiment. Any errors introduced by the preparation of the solutions do not immediately show up in the plots. In conclusion, the apparent advantages in preparing the solutions automatically are that the user can let the system do all of the work for him, rather than manipulate all of the solutions and glassware himself, and that gross errors due to mishandling of solutions are minimized. The time involved for the preparation of solutions was approximately the same for either method.

## 2. Phospho-Molybdate Reaction

Another experiment was devised to ascertain if the uncertainty of replicate preparation of solutions manually or automatically would show up in reaction rate studies. The reaction of phosphate with molybdenum (VI) in a strongly acid medium to yield 12-molybdophosphoric acid (12-MPA) was used in this study. The reagent preparation and solution analysis was similar to that described by Beckwith and Crouch (44) and Javier et al. (62). The phosphate and molybdate rapidly react to yield rate data that are proportional to the phosphate concentration for ∿100 ms after mixing. The formation of 12-MPA is monitored at 400 nm.

a. Reagents - Stock solutions for use in this study include 2490 ppm P prepared from dried  ${
m KH_2PO_4}$  and 0.1647  $\underline{{
m M}}$ 

Mo (VI) prepared from Na<sub>2</sub>MoO<sub>4</sub>  $^{\circ}$ 2H<sub>2</sub>O in  $^{\circ}$ 0.1  $\underline{M}$  nitric acid. Dilute phosphate solutions were prepared both manually and automatically in the range of 1-25 ppm P, with three replicate solutions for each concentration. The average time involved to prepare solutions was about 2 minutes per solution for aliquoting and dilution.

b. Results - The rate data spanned 100 ms after the flowstopped trigger was asserted, with a one data point per millisecond data acquisition rate. Eight pushes per solution were averaged into one data set. The plot of the rate data obtained for each solution prepared manually is shown in Figure 25 and for each solution prepared automatically is shown in Figure 26. The results indicate that the variation of the solution phosphorous concentration for a given set of measurements is negligible compared to the uncertainty in the measurement of the rates of reaction for that series of solutions. The data shown in Table 9 were obtained under differing conditions, i.e. no attempt was made to control the temperature of the reaction mixture. data indicate that the rate measurement varies by as much as 2% at low phosphate concentrations, with an average relative standard deviation of  $\sim 1\%$ . Therefore, it would be safe to assume that the rate measurements are the error-determining process in the entire automated system of solution preparation and analysis, and the best precision one can expect is on the order of 0.5% RSD.

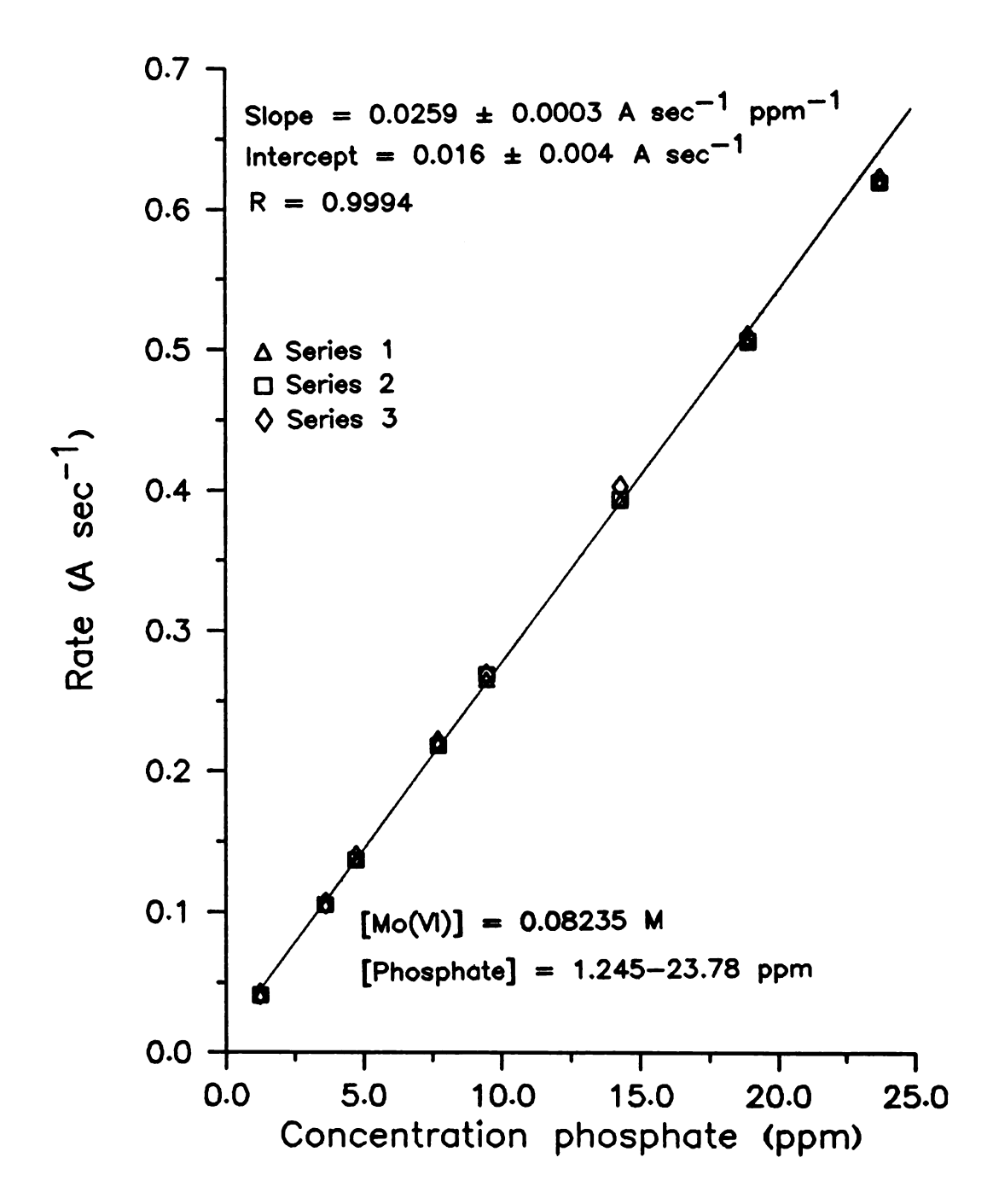


Figure 25. Initial rate vs. phosphate concentration. Solutions prepared manually.

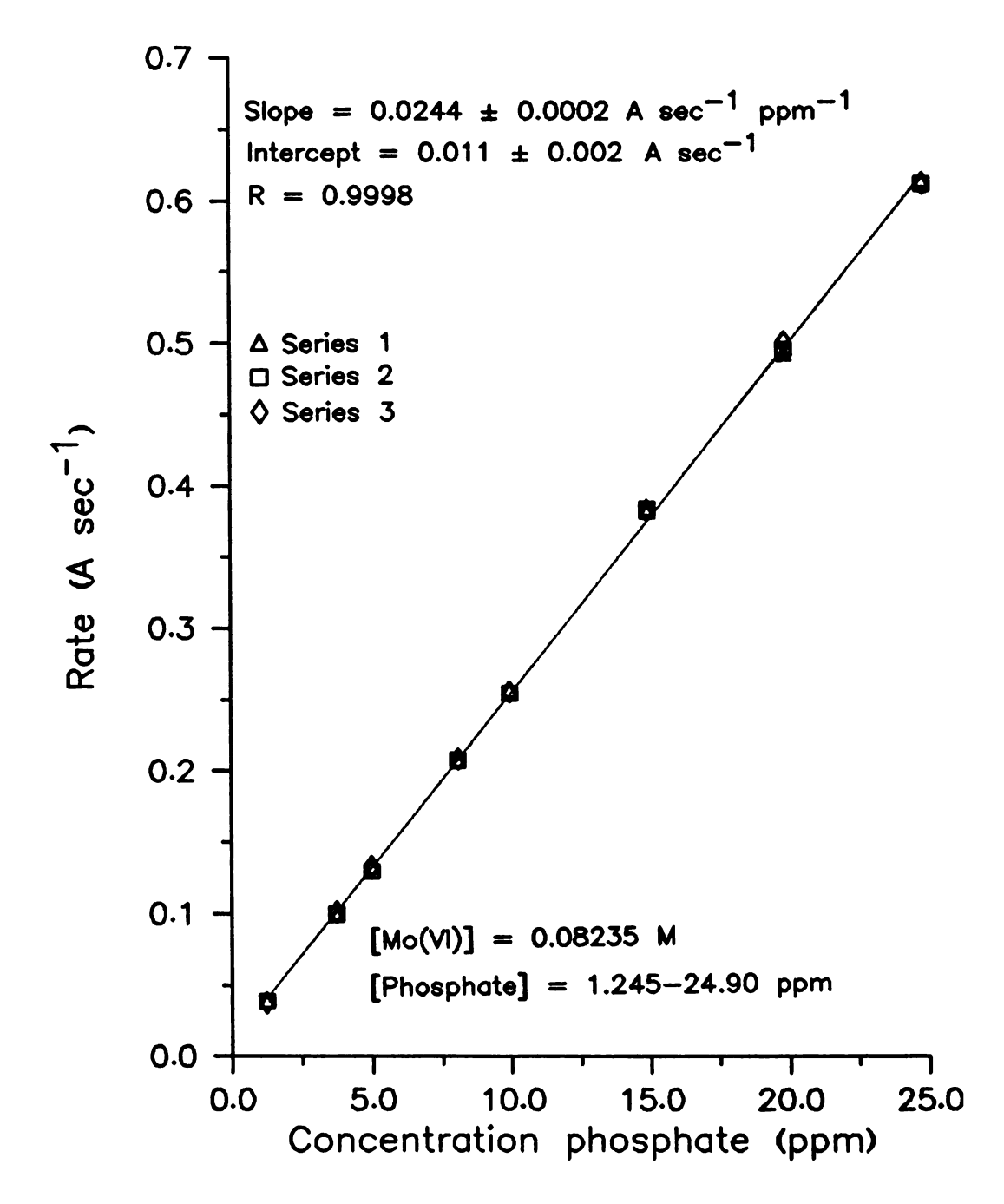


Figure 26. Initial rate <u>vs.</u> phosphate concentration. Solutions prepared automatically.

<u>Table 9</u>. Phospho-molybdate Reaction Kinetics Study Data.

# A. Solutions prepared manually -

Phosphate Conc. (ppm)	Rate (A $L^{-1}$ sec <sup>-1</sup> )	%RSD
1.245	$0.0410 \pm 0.0004$	0.98
3.611	0.1056 ± 0.0008	0.80
4.731	$0.1377 \pm 0.0015$	1.1
7.719	$0.2198 \pm 0.0015$	0.69
9.462	$0.2678 \pm 0.0020$	0.74
14.318	$0.3970 \pm 0.0053$	1.3
18.924	$0.5082 \pm 0.0019$	0.38
23.780	$0.6215 \pm 0.0013$	0.21

# B. Solutions prepared automatically -

Phosphate Conc. (ppm)	Rate (A $L^{-1}$ sec <sup>-1</sup> )	%RSD
1.245	0.0385 ± 0.0008	2.0
3.735	$0.1003 \pm 0.0009$	0.93
4.980	$0.1319 \pm 0.0019$	1.4
8.093	$0.2081 \pm 0.0005$	0.24
9.960	$0.2558 \pm 0.0014$	0.55
14.940	$0.3830 \pm 0.0009$	0.22
19.920	$0.4967 \pm 0.0042$	0.85
24.900	$0.6131 \pm 0.0012$	0.20

#### CHAPTER V

# ANALYTICAL APPLICATIONS OF THE AUTOMATED STOPPED-FLOW INSTRUMENT

The characterization of a complete automated reaction rate measurement system has been presented in previous chapters. The final test of the utility of such a system is its use in "real" laboratory problems. The results of two reaction-rate analyses utilizing the automated system as well as the characterization of the luminol-hypochlorite chemiluminescence reaction for determining ammonia are presented in this chapter.

#### A. Phosphate in Blood Serum

The determination of electrolytes in serum is one of the more important functions of the clinical laboratory.

Abnormal phosphorous levels in serum may indicate severe disorders such as rickets, renal failure, or hypo-and hyperparathyroidism. The rapid and accurate determination of phosphorous levels in serum would assist in the overall effectiveness of clinical analyses.

The reaction of phosphate and Mo(VI) in acid solution to form the 12-molybdophosphate heteropolyanion (12-MPA) was used in this study. The acid concentration of the Mo(VI) solution was adjusted to pH 1 so that the rate law

$$\frac{d[12-MPA]}{dt} = k[H_3PO_4][Mo(VI)]$$
 (5.1)

would be followed. The formation of 12-MPA preferentially over other molybdenum complexes was ensured by keeping the concentration of Mo(VI) in at least 100-fold excess of the phosphate concentration. With excess Mo(VI) and excess acid the rate of reaction is pseudo-first order with respect to phosphate concentration over at least a 10-fold concentration range (44). The rate of formation of 12-MPA was monitored at 400 nm, where absorption due to unreacted Mo(VI) species is negligibly small.

The purpose of this study was to evaluate the performance of the stopped-flow instrument in determining serum phosphorous levels accurately and to establish the number of samples that could be analyzed per hour; a figure of merit for automated analyzers.

#### 1. Reagents

The solutions prepared automatically for the phosphate study presented in the previous chapter were used as calibration standards for this study. A Monitrol I (63) chemistry control blood serum sample was prepared for use by adding 5 mL of distilled water. Two, 2.5-mL portions were treated by adding 10 mL of 9% trichloroacetic acid, followed by centrifugation. The supernatant liquid of each sample was drawn off and diluted to 25 mL. These solutions were then used in the analysis. Measurements of the rate of

reaction for standards and samples were begun 10 ms after the flow-stopped signal was received by the computer. The data taking rate was one point per millisecond for 100 ms after the initial data point; eight pushes were averaged into one data set.

# 2. Results

The mean value of the phosphate concentration in the blood serum sample (expressed as mg P/dL) as determined by the Centrifichem System 400 analysis, which uses a similar reaction of  $PO_4^{-3}$  and Mo(VI), was 2.8 mg/dL with a standard deviation of 0.40 mg/dL. The expected range using this method for a normal blood serum sample is 2.5-4.5 mg/dL. The average value found in the stopped-flow analysis of the two samples was 2.9  $\pm$ 0.2 mg P/dL. The relatively large deviation in the result is due in part to not using the entire reaction curve of the samples for fitting to a line because a significant lag period in the reaction was observed during the first 30-40 ms of the rate curve. The average phosphorous value found in the blood serum sample does fall within the assayed value.

The analysis rate for P in serum by the stopped-flow reaction-rate measurement method was determined to be approximately 50 samples per hour. This figure includes the time for rinsing, reagent draw-up and measurement of the rate data for eight pushes, as well as the time involved to calculate initial slopes. The fact that each data set

requires  $\sim 2.5$  mL of serum for a single analysis makes this particular instrument somewhat impractical for use in a clinical environment. Reduction of the syringe volumes would increase the usefulness of the apparatus.

# B. Determination of Ascorbic Acid by Initial Rates

Ascorbic acid is routinely determined in clinical samples by titration with the redox indicator 2,6-dichlorophenolindophenol (DCPI) in acid solution. The reaction is shown in Figure 27. Ascorbic acid is oxidized to dehydroascorbic acid while the DCPI is reduced to its leuco compound. The ascorbic acid-DCPI reaction goes to completion rapidly, with the solution turning from pink to colorless at the equivalence point in titrations in acidic media. Although the titration is widely used, it has some In the light of current automated techniques, drawbacks. the manual titration method is very time-consuming. concentration of DCPI must be checked frequently against standard quantities of ascorbic acid and adjusted according to the concentration of vitamin C in the sample. The endpoint in the titration is unstable and difficult to detect visually.

Alternative rapid, semi-automated and automated methods that use the stopped-flow technique for the determination of ascorbic acid have been developed by Karayannis (64,65) and Malmstadt et al. (66). The method of Karayannis involves using a commercial stopped-flow instrument for mixing of

Figure 27. Reaction of ascorbic acid with DCPI indicator solution.

reagents. A storage oscilloscope displays the time course of the reaction; the scope display is then photographed with a Polaroid camera. The slopes of the initial linear portion of the reaction-rate curves are measured manually. The method was successfully applied to the determination of standard ascorbic acid samples over a 10-fold concentration range with a typical precision of 1.5% RSD.

An automated stopped-flow/unsegmented solution-storage analyzer was shown to be useful in several dedicated chemical analyses (66). The system was applied to the determination of ascorbic acid using DCPI indicator over a 10-fold concentration range. A precision of 0.5% RSD was obtained and the sample throughput rate was ~200 samples per hour.

The present study employed the stopped-flow technique under first-order conditions with respect to the ascorbic acid concentration to determine if some of the experimental constraints seen by previous workers could be eliminated and if the analysis concentration range could be extended. All measurements were made using the stopped-flow instrument. The rate of disappearance of DCPI was monitored at 520 nm.

#### 1. Reagents

A 0.0722 mM DCPI working solution was prepared from 2.03 mM stock DCPI. Both working and stock solutions were made up in 210 mg/L sodium bicarbonate. A 9.902 mM ascorbic acid stock solution was prepared from reagent grade L-ascorbic acid in 0.05 M oxalic acid. Vitamin C tablets (two each of

Meijer's and Muir's commercial brands) were ground up and dissolved in  $\sim\!200$  mL of distilled water. The solutions were then successively filtered through decreasing pore size filters to remove particulates. The filtrate was diluted to 1 L for all four samples. The solutions were diluted 1:10 for analysis. All reagents were prepared manually in distilled water.

#### 2. Results

A series of standard ascorbic acid solutions ranging in concentration from 0.050 mM to 1.0 mM was first run in the stopped flow. Data acquisition was started 8 ms after the flow-stopped trigger signal, with a data taking rate of one point per millisecond thereafter. Eight pushes were averaged per data file. The vitamin C solutions were then analyzed in a similar manner. The resultant plot of rate vs. ascorbic acid concentration is shown in Figure 28. The plot shows non-linearity at ascorbic acid concentrations exceeding 0.50 mM. The linear part of the working curve in Figure 28 extends for less than an order of magnitude of concentration and has a slope of  $-1.21 \times 10^4$  A L/(sec mole) with an intercept of -0.22 A/s and a correlation coefficient of -0.9987. The high relative standard deviations of the rate data shown in Table 10 are indicative of the limitations of trying to measure the rate of a very fast reaction using the stopped-flow instrument. Only the first 50 ms of data were sufficiently linear for regression purposes.

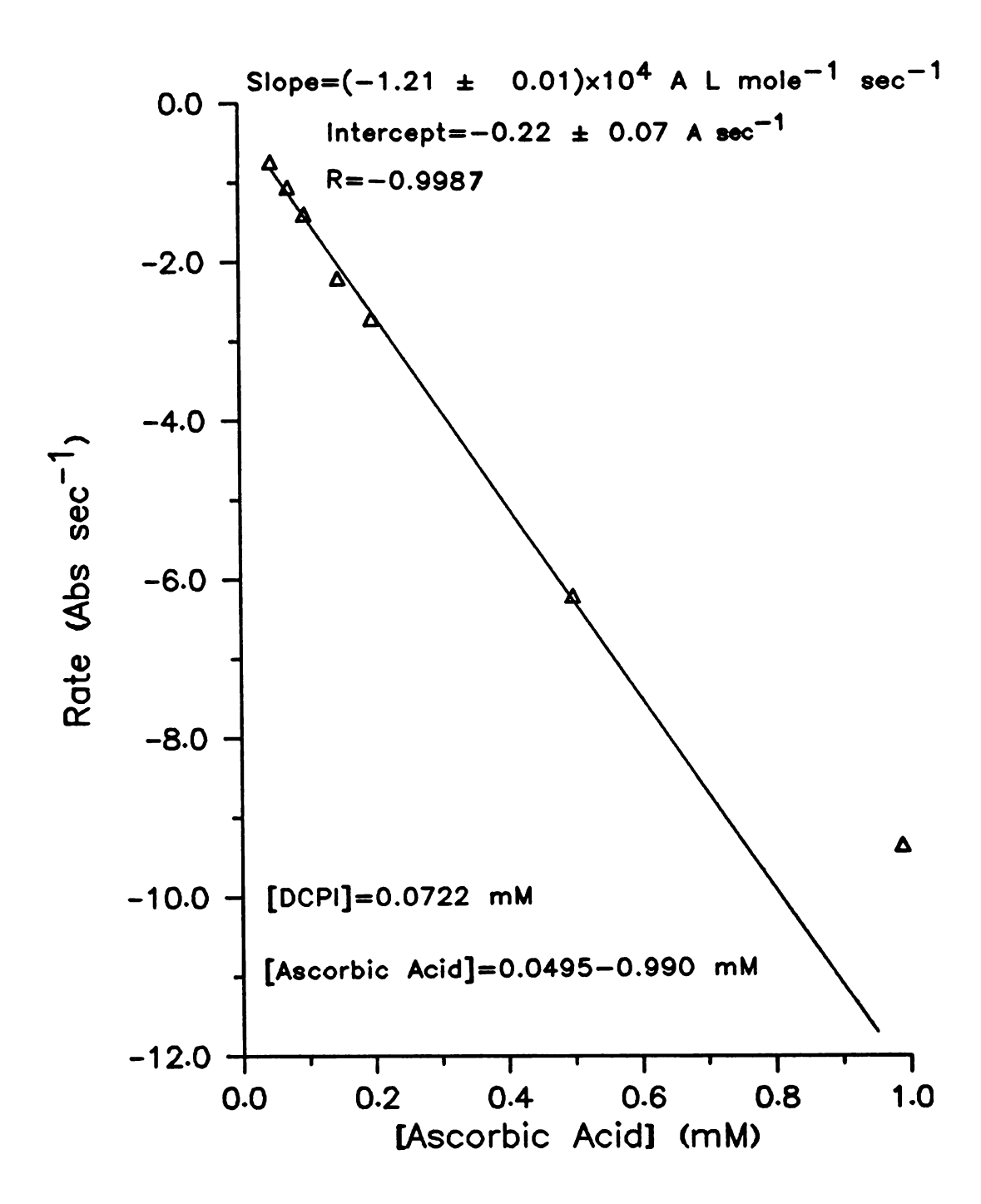


Figure 28. Initial rate vs. ascorbic acid concentration.

Table 10. Results of Initial Rate Measurements of the Reaction of Ascorbic Acid with DCPI.

[ASCORBIC ACID] (mN)	RATE $(A sec^{-1})$	%RSD
0.0495	-0.736 ± 0.059	8.0
0.0753	$-1.06 \pm 0.06$	5.7
0.100	$-1.39 \pm 0.05$	3.6
0.151	$-2.21 \pm 0.1$	4.5
0.200	$-2.7 \pm 0.14$	5.2
0.500	$-6.2 \pm 0.2$	3.2
0.990	$-9.4 \pm 0.4$	4.3

commercial vitamin C tablets were assayed at average values of  $460 \pm 10$  mg and  $590 \pm 10$  mg for the Meijer's and Muir's brand respectively. These values are lower than the reported levels of 500 mg and 600 mg of ascorbic acid for each. Some loss of analyte was expected in the grinding and filtration of the samples.

A follow-up study covering a slightly larger concentration range of ascorbic acid was done to ascertain the available linear working range for a given set of standards. The concentration range of ascorbic acid was extended down to 0.005 mM, a factor of 10 lower than that in the previous study. The working ascorbic acid solutions were prepared from the stock solution prepared earlier and covered a concentration range of 0.005 mM to 0.5 mM. The DCPI working solution was 0.0812 mM. The standards were analyzed in the same manner as previously described. The rate data obtained are shown in Table 11, with the corresponding rate-concentration plot in Figure 29. For the most part, the rate data are linear with respect to concentration up to 0.1 mM ascorbic acid for a 40-fold concentration range, an improvement over the results of Karayannis (65). The measurement of the rate of the reaction at high ascorbic acid concentrations relative to the DCPI concentration is the limiting process in this study, because the reaction is almost complete within the dead time of the stopped-flow instrument, a condition that is far from practical for low-error measurements of reaction rates. Also, the method

Table 11. Extended Concentration Range of Ascorbic Acid Study.

[ASCORBIC ACID] (mM)	INITIAL RATE (A sec <sup>-1</sup> )	%RSD
0.0102	-0.125 ± 0.008	6.4
0.0154	$-0.175 \pm 0.011$	6.3
0.0205	$-0.238 \pm 0.009$	3 . 8
0.0307	$-0.398 \pm 0.019$	4.9
0.0410	$-0.50 \pm 0.02$	4.0
0.0614	$-0.72 \pm 0.02$	2.8
0.0819	$-0.97 \pm 0.03$	3.0
0.102	$-1.18 \pm 0.02$	1.7
0.123	$-1.37 \pm 0.02$	1.5
0.143	$-1.66 \pm 0.05$	3.0
0.164	$-1.92 \pm 0.08$	4.2
0.184	$-2.22 \pm 0.07$	3.2
0.205	$-2.38 \pm 0.08$	3.4
0,512	-5.24 ± 0.15	2.9
1.02	$-8.9 \pm 0.2$	2.3

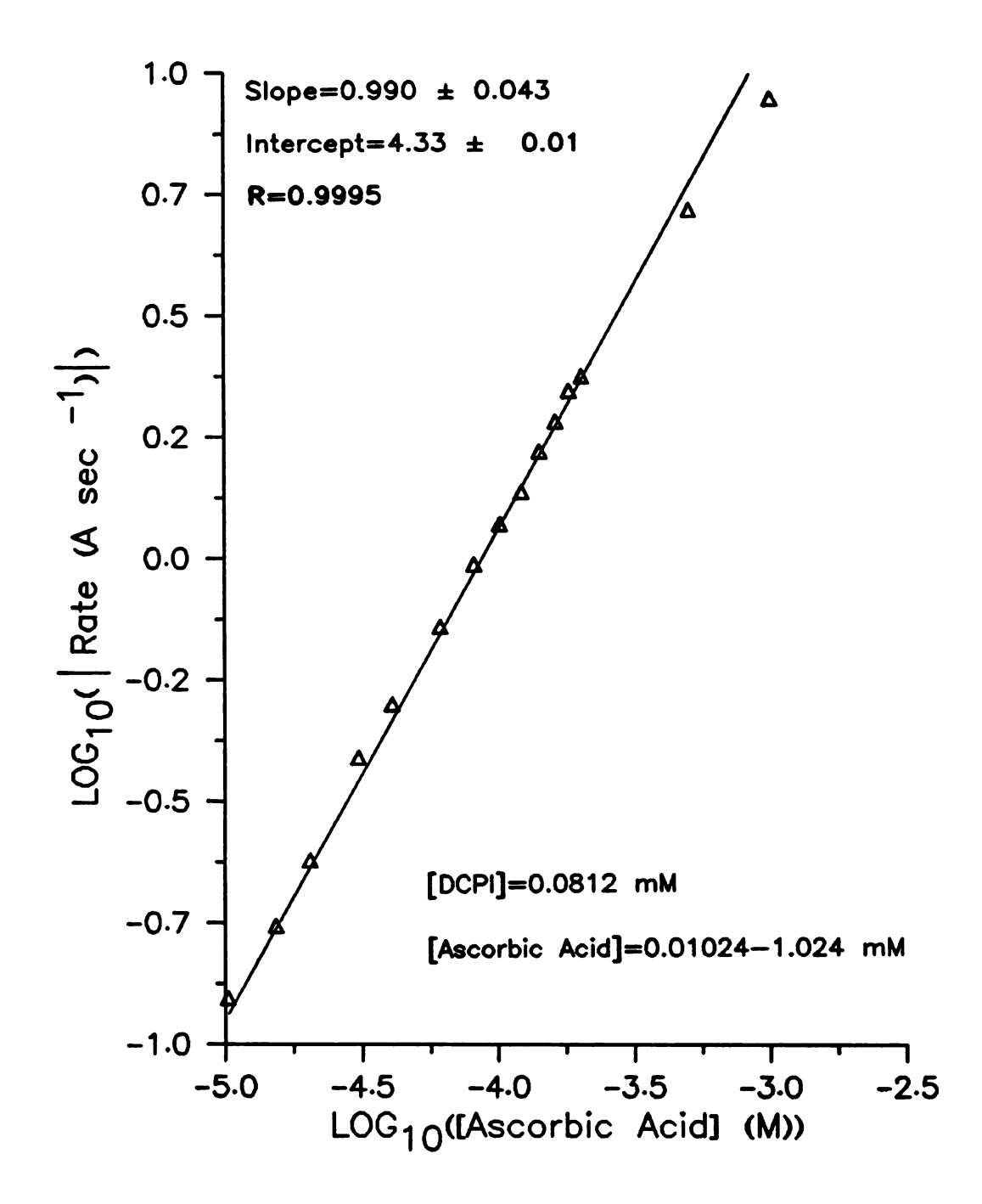


Figure 29. Initial rate <u>vs.</u> ascorbic acid concentration. Extended range of ascorbic acid concentration study.

is limited somewhat by a sample throughput rate of 50 per hour.

# C. Characterization of the Luminol-hypochlorite Chemiluminescence Reaction

One of the more interesting and analytically useful reaction types is a chemiluminescence (CL) reaction. Chemiluminescence occurs whenever a molecule emits a photon as a result of a chemical reaction in which one of the intermediates or end-products is produced in an excited electronic state. Methods based on chemiluminescence are extremely sensitive because the chemiluminescence radiation is produced in a very low background environment. Thus the low light levels obtained from CL can be measured without great difficulty. The instrumentation used for detection of CL signals consists of a sample cell, a photoelectric detector, and a readout device. Errors due to light source drift or stray light through a wavelength dispersion device are not encountered, since these units are not used in the instrumental scheme. The only major requirement in the instrumentation used is that the sample cell must have provision for rapid and complete mixing of the reagents. Sample and reagent introduction into the cell may be done continuously or discretely. In continuous-flow systems, a steady-state signal is obtained, while in discrete systems, a peak response is obtained. In most cases, the detector response is linear over several orders of magnitude of

reactant concentration.

Use of CL reaction types is advantageous for several reasons. The instrumental requirements are minimal. The reaction generating CL is specific in that only one form of the analyte may cause CL. The background signal levels from the reaction mixture are often very low. Finally, the CL signal is linear with analyte concentration over several orders of magnitude.

There are some disadvantages in using CL for specific cases. Non-analyte species that react with the CL species will contribute to the CL signal. The analyte must be present in the proper form in order to react with the CL species. The specificity of the CL reaction prevents use of the technique for general applications.

Many publications (67-71) have dealt with using luminol (5-amino-2,3-dihydro-1,4-phthalazinedione) for analytical purposes since its luminescent properties were discovered by Albrecht in 1928 (72). These publications are summarized in part by Gorus and Schram (73). To obtain chemiluminescence from luminol in aqueous solution, a base and a strong oxidant must be included, often with a catalyst or cooxidant for maximum efficiency.

Several authors have used luminol in the determination of hypochlorite. C.J. Patton (37) has suggested using the luminol-hypochlorite reaction as a means of indirectly determining ammonia, since it is well known that ammonia reacts stoichiometrically with hypochlorite to form

monochloramine. Normally, one could use the UV absorption band of monochloramine for quantitative studies. Use of the luminescence reaction to ascertain the levels of hypochlorite remaining after reaction with ammonia would be advantageous in that two possible sources of error, i.e. a light source and a monochromator, could be eliminated in the analysis scheme. This section documents characterization studies of the stability of the luminol-hypochlorite reaction and the luminol-hypochlorite-ammonia reaction at various pH values. Studies used to determine the detection limits for ammonia are also presented.

#### 1. Reaction Mechanisms

The CL reaction pathway of luminol in solution is complicated and not well characterized. Authors (74,75) have proposed mechanisms for the CL reaction under different experimental conditions (pH, ionic strength, method of sample and reagent mixing). The mechanism shown in Figure 30 was proposed by Isacsson et al. (75) to occur in alkaline media. The results of studies summarized henceforth have partially verified the mechanism and will be presented later.

Ammonia and hypochlorite react in alkaline media to form monochloramine as in equation 5.2.

$$NH_3 + OC1 \rightarrow H_2NC1 + OH$$
 (5.2)

The reaction is useful in determining ammonia indirectly using the luminol-hypochlorite reaction. Monochloramine does not react with luminol to give rise to a CL signal.

Figure 30. Proposed mechanism for luminol-hypochlorite CL reaction (Isacsson et al. (75)).

Measurement of the decrease of CL signal of the reaction of a solution containing hypochlorite and ammonia with luminol relative to the CL signal from the reaction of a solution containing the same initial hypochlorite concentration with luminol gives a linear working curve, relating the decrease in light intensity to ammonia concentration. Patton (76) has found that monochloramine goes through further reaction pathways with complex kinetics expressions. The reactions shown in equations 5.3-5.5 illustrate some of the possible species that are formed by the decomposition of monochloramine.

$$H_2NC1 + HOC1 \rightarrow HNC1_2 + H_2O$$
 (5.3)

$$H_2NC1 + HOC1 \rightarrow H_2NOH + 2C1^-$$
 (5.4)

$$H_2NC1 + H_2NOH \rightarrow 0.5N_2O + NH_3 + 1.5H_2O + C1^-$$
 (5.5)

#### 2. General Procedures

The automated stopped-flow instrument described in the previous chapter was used for mixing reactants and observing the chemiluminescence reaction for all of the studies presented. A unique software data acquisition routine was written to determine automatically the point of maximum flash intensity within a 100 ms time window for any specified delay time after the flow-stopped signal. The user has the option of entering the delay time directly from the terminal for those reactions whose time of maximum intensity is known, or of supplying a value to the program that will be used to sequentially increment the delay before

data acquisition (after the flow-stopped trigger for each push). The peak-finding subroutine of the program does a Savitsky-Golay (77) five-point smooth of the data, looks for the maximum value in the data set, and prints out the average peak flash intensity for five points centered about the maximum. If the raw data values are not within 4% of the average value, appropriate warnings are printed. The identification of the maximum data point is printed along with the delay time after the flow-stopped trigger in order to ascertain the time at which the maximum flash intensity occurs. The use of peak flash intensities values determined by this method ensures minimization of error due to poor resolution of the maximum intensity of the reaction due to long data acquisition rates required for reactions occurring at higher pH values and also due to the inability of the data acquisition system to follow the very fast reactions at low pH values.

All solutions used in the studies were prepared in high-purity (MQ) water obtained from the Millipore-MilliQ purification system. Use of MQ water was found to be necessary because initial studies showed that house distilled water contains sufficient impurities to inhibit the CL reaction. All luminol stock solutions were prepared from 3-aminonaphthal hydrazide (78) in  $\sim 0.01 \ \underline{M}$  NaOH. Hypochlorite standards were prepared from Clorox, which was determined by iodine-thiosulfate titration to be  $0.8 \ \underline{M}$ . Ammonia stock solutions were made from reagent-grade ammonium

chloride. Buffers at the required pH values were made according to standard methods (79).

# 3. Working Range for Hypochlorite Solutions

An experiment was done to assess the sensitivity and linear working range of the CL reaction of luminol and hypochlorite. Two sets of solutions were prepared: one contained 0.65  $\underline{m}\underline{M}$  luminol in  $\sim 0.0015\%$  hydrogen peroxide and pH 10.4 borate buffer, and the other contained buffered hypochlorite ranging in concentration from 0.5  $\underline{\mu}\underline{M}$  to 0.1  $\underline{m}\underline{M}$ . The hypochlorite solutions were prepared individually immediately before use. The full-scale sensitivity of the detection-readout system was set using the reaction of the most concentrated hypochlorite solution and luminol. The gain of the current amplifier was increased by a factor of 10 whenever the luminescence signal from the reaction was below 1 V at the lower hypochlorite concentrations. For all cases observed, the peak flash intensity occurred 65 ms to 75 ms after the flow-stopped trigger signal.

a. Results - The values of the average peak flash intensities for each concentration of hypochlorite are presented in Table 12 and are plotted in Figure 31. The data are linear in the range of hypochlorite concentration of 0.5  $\mu$ M to 0.1  $\mu$ M. The resultant data seem to correlate very well with those reported by Isacsson and Wettermark (67). It should be noted that even at the lowest hypochlorite

Table 12. Sensitivity Study Data for Luminol-hypochlorite CL Reaction.

[HYPOCHLORITE] (µM)	PEAK FLASH INTENSITY (V)
100.0	8.91
50.0	3.89
10,0	0.746
5 . 0	0.338
1.0	0.0797
0.5	0.0307

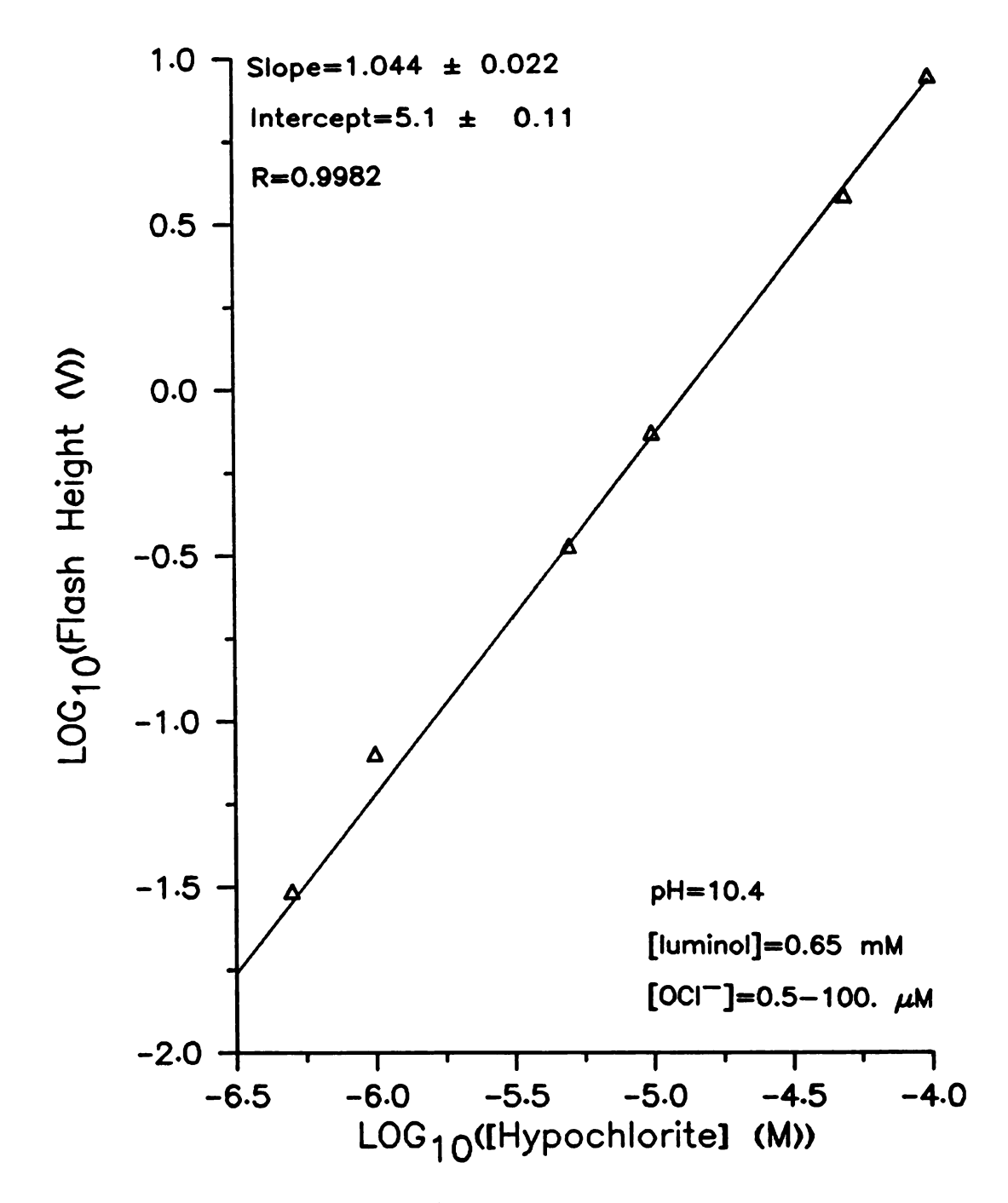


Figure 31. Peak flash intensity of luminol as a function of hypochlorite concentration.

concentration, the signal-to-noise (S/N) ratio is  $\sim 300$ . Obviously, lower concentrations of hypochlorite can be detected, but dilute hypochlorite solutions are known to be unstable (80). Although the rate of the hypochlorite decomposition is pH dependent, later studies by the author verified the results of Chapin (80) in that even in buffered solution, hypochlorite concentrations below 100  $\underline{\text{nM}}$  will tend to decompose rapidly.

If one considers the peak flash intensity to be a measure of the rate of reaction of luminol and hypochlorite, the log-log treatment of the data in Table 12 gives a line with a slope of  $1.044 \pm 0.022$ . This indicates that the reaction generating the CL signal is first order with respect to the hypochlorite concentration.

# 4. Linearity of Calibration Curves

Information about the linearity of calibration curves for ammonia was obtained using the luminol-hypochlorite reaction. Ammonia is known to react with hypochlorite in alkaline media in a 1:1 ratio to form monochloramine, which does not cause chemiluminescence when reacted with luminol. The concept behind the studies presented here is to determine ammonia concentration in a hypochlorite solution by measuring the decrease of the CL signal relative to solutions containing only hypochlorite. This decrease in signal should be proportional to the ammonia concentration, provided no major interferences are present.

Reagents used in the study of the relationship of ammonia concentration to the CL reaction flash intensity included working solutions of 0.65~mM luminol in  $\sim 0.0015\%$  peroxide, 0.01~mM hypochlorite, and ammonia solutions in the concentration range of 0.001 to 0.009~mM. All solutions were buffered with pH 10.4 bicarbonate buffer. Each working solution of hypochlorite and ammonia was prepared just prior to use by adding 1 mL of 1.0~mM hypochlorite and 0.1~mL to 0.9~mL stock ammonia to  $\sim 90~\text{mL}$  of buffered solution in a 100~mL volumetric flask and diluting to the mark. The current amplifier was set at a gain of  $10^7~\text{with a 10 ms}$  rise time on the output. All of the data were collected using the stopped-flow instrument and the peak-finding routine described earlier.

The data presented in Table 13 are plotted in Figure 32. These data indicate a linear relation between the decrease in flash intensity observed with increasing ammonia concentration. The results show that the CL reaction is applicable in detecting ammonia over at least one order of magnitude in concentration range.

# 5. Detection Limits for Ammonia

The purpose of this study was to establish the reliability of observing a very small decrease of the relatively large CL signal when low concentrations of ammonia are present in hypochlorite solutions. The results of studies using hypochlorite and ammonia mixtures

Table 13. Calibration Data for the Determination of Ammonia using the Luminol-hypochlorite CL Reaction.

[NH <sub>3</sub> ] (µM)	PEAK FLASH INTENSITY (V)
0.0	9.18 ± 0.08
1.0	$8.17 \pm 0.06$
3.0	$6.24 \pm 0.07$
5 , 0	$4.57 \pm 0.05$
7,0	$2.73 \pm 0.06$
9.0	$1.25 \pm 0.05$
0.0	$9.12 \pm 0.09$

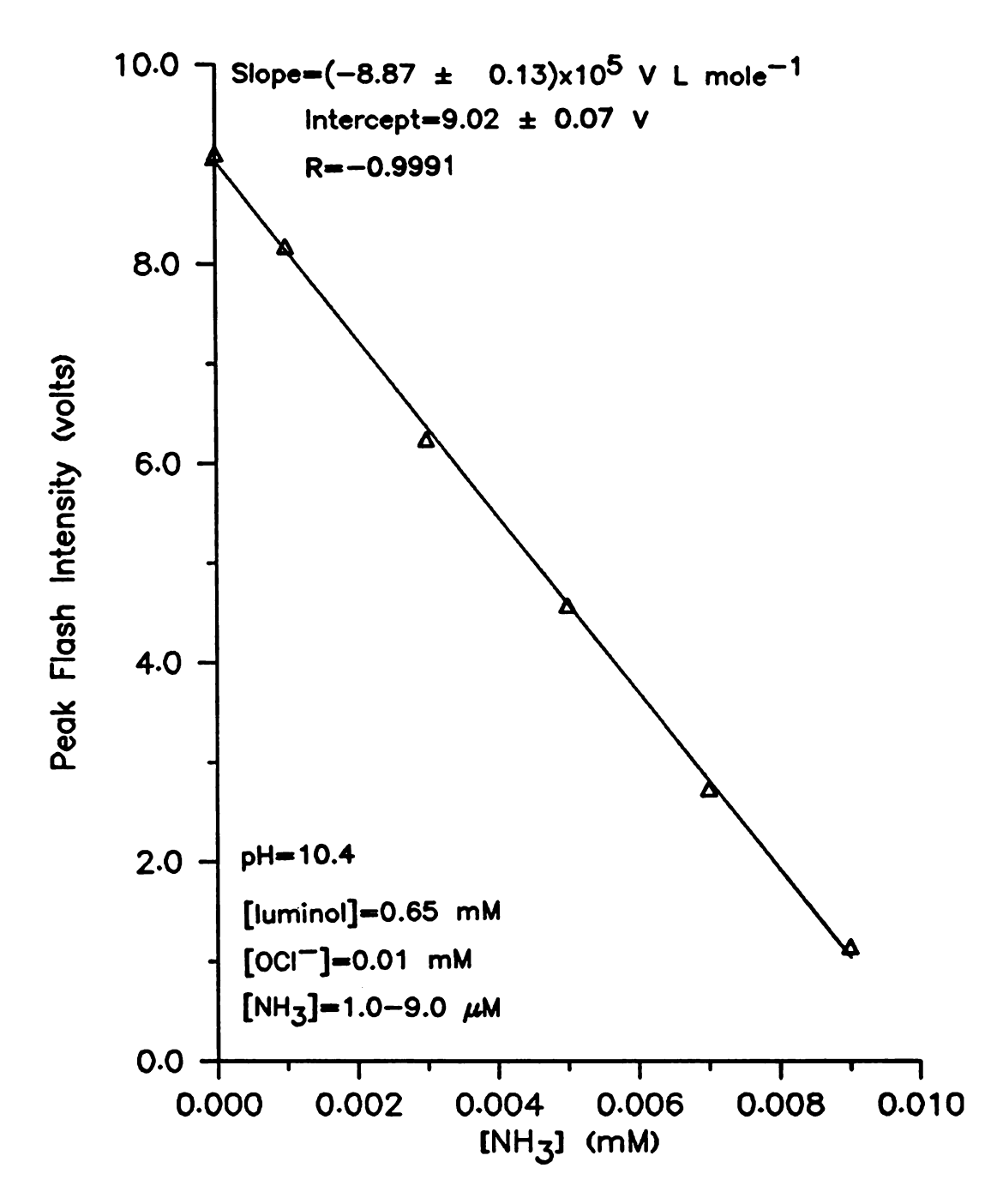


Figure 32. Reduction of CL intensity as a function of  $\mathrm{NH}_3$  concentration.

prepared manually and prepared using the automated reagent preparation device are presented.

The reagents used in this study were freshly prepared and included 0.65  $\underline{\text{mM}}$  luminol in  $\sim 0.0015\%$  peroxide, 0.1  $\underline{\text{mM}}$  and 0.01  $\underline{\text{mM}}$  hypochlorite working solutions. Ammonia concentrations in the hypochlorite solutions varied from 1% to 10% of the hypochlorite concentration. All working solutions were prepared in pH 10.0 borate buffer.

The results of using solutions prepared manually in the detection-limit study are presented in Table 14. was concluded that the preparation of the hypochloriteammonia working solutions was the most error-prone step in the experiment. Therefore, it was decided to use the automated reagent preparation system to determine if this error could be minimized. A series of hypochlorite working solutions at 0.1 mM and 0.01 mM was prepared with ammonia concentrations of 0.0005 mM, 0.001 mM, and 0.005 mM. sequence of preparation involved adding 25 mL of buffer, the appropriate volume of ammonia, and 1 mL or 0.1 mL of 10.0 mM stock hypochlorite solution, followed by dilution to 100 mL. The solutions were used  $\sim 5$  minutes after preparation. As can be seen from the data in Table 15, the reproducibility of the flash intensity at a given concentration of hypochlorite is slightly better than that observed for solutions prepared manually. Apparently, the reproducibility of detecting the flash intensity is the limiting factor in this case because the error involved in preparing the hypochlorite solutions

Table 14. Peak Flash Intensities of Hypochlorite Solutions Containing Ammonia. Solutions Prepared Manually. [OC1 ]=100  $\mu$ M.

[NH <sub>3</sub> ] (µM)	PEAK FLASH INTENSITY (V)
0.0 5.0 1.0 0.5 0.1	8.57 ± 0.03 7.92 ± 0.01 8.72 ± 0.02 8.83 ± 0.03 8.88 ± 0.02 8.94 ± 0.02

Table 15. Peak Flash Intensities of Hypochlorite Solutions Containing Ammonia. Solutions Prepared Automatically. [OC1 ]=100  $\mu M_{\bullet}$ 

[NH <sub>3</sub> ] (µM)	PEAK FLASH INTENSITY (V)
0.0	9.36 ± 0.02
5.0	$8.93 \pm 0.02$
1.0	$9.21 \pm 0.03$
0.0	$9.50 \pm 0.03$

seems to be greater than the ability of the detection system to discriminate small changes in a large luminescence signal. The data in Table 16 represent an attempt to determine what level of ammonia can be reliably determined, assuming a 1% decrease in the CL intensity between hypochlorite solutions and hypochlorite plus ammonia solutions. It was found that approximately 1% to 5% decreases in flash intensity can be reliably detected for amplification of the photomultiplier signal of up to 10<sup>10</sup>, assuming one can reproducibly prepare the hypochlorite standards. Approximately 2 nM of ammonia in 1.0 mM of hypochlorite could be detected at this amplification factor, but use of this concentration of hypochlorite is not recommended because degradation of the CL signal occurs within ∿15 minutes of solution preparation due to decomposition of hypochlorite.

# 6. Stability of Hypochlorite Solutions

The concern over the stability of the hypochlorite and hypochlorite-ammonia working solutions was the basis for the final study of the CL reaction. Patton (76) had found that monochloramine decomposition to ammonia is significant in a five-minute period at pH 8.5, but the decomposition rate is lower at higher pH values. This decomposition would interfere with the luminol-hypochlorite CL reaction in that the ammonia generated by the decomposition would react with hypochlorite. The decomposition-recombination reaction involves rather complicated kinetics that are discussed

Table 16. Data for Detection Limits for Ammonia.[OC1 ]=10  $\mu$ M. Solutions Prepared Automatically.

[NH <sub>3</sub> ] (µM)	PEAK FLASH	INTENSITY	(V)
0.0 1.0 0.5 0.1	9.32 ± 8.19 ± 8.73 ± 9.20 ± 9.52 ±	0.06 0.05 0.07	

elsewhere (76). The purposes of this study were to ascertain if the hypochlorite solutions and the hypochlorite-ammonia mixtures are stable for a reasonable length of time after preparation and to determine optimum pH values for the ammonia assay.

The impetus for an extensive study of the stability of hypochlorite solutions came about as a result of the observation of the decay with time of the CL signal for hypochlorite and hypochlorite-ammonia solutions at pH 10.4, a value at which ammonia solutions were expected to be stable. The plots shown in Figures 33 and 34 are representative of the time decay of the CL signal with time. The object of the study described herein was to determine if the decay of the CL signal was due to decomposition of luminol, hypochlorite, or ammonia and if the time of analysis after the preparation of the reagents was critical in obtaining a reproducible CL signal.

Various buffer solutions in the pH range of 9.5 to

12.4 in 0.5 pH unit increments were used in both studies.

Duplicate phosphate and bicarbonate buffers at pH 11.0 were prepared to determine if phosphate has any effect upon the CL reaction. All buffers were prepared within a few hours prior to use. The general procedure involved modifying the peak-finding routine in order to let the instrument take data at specified time intervals over an hour without operator intervention. Data acquisition consisted of filling the drive syringes of the stopped flow, averaging five

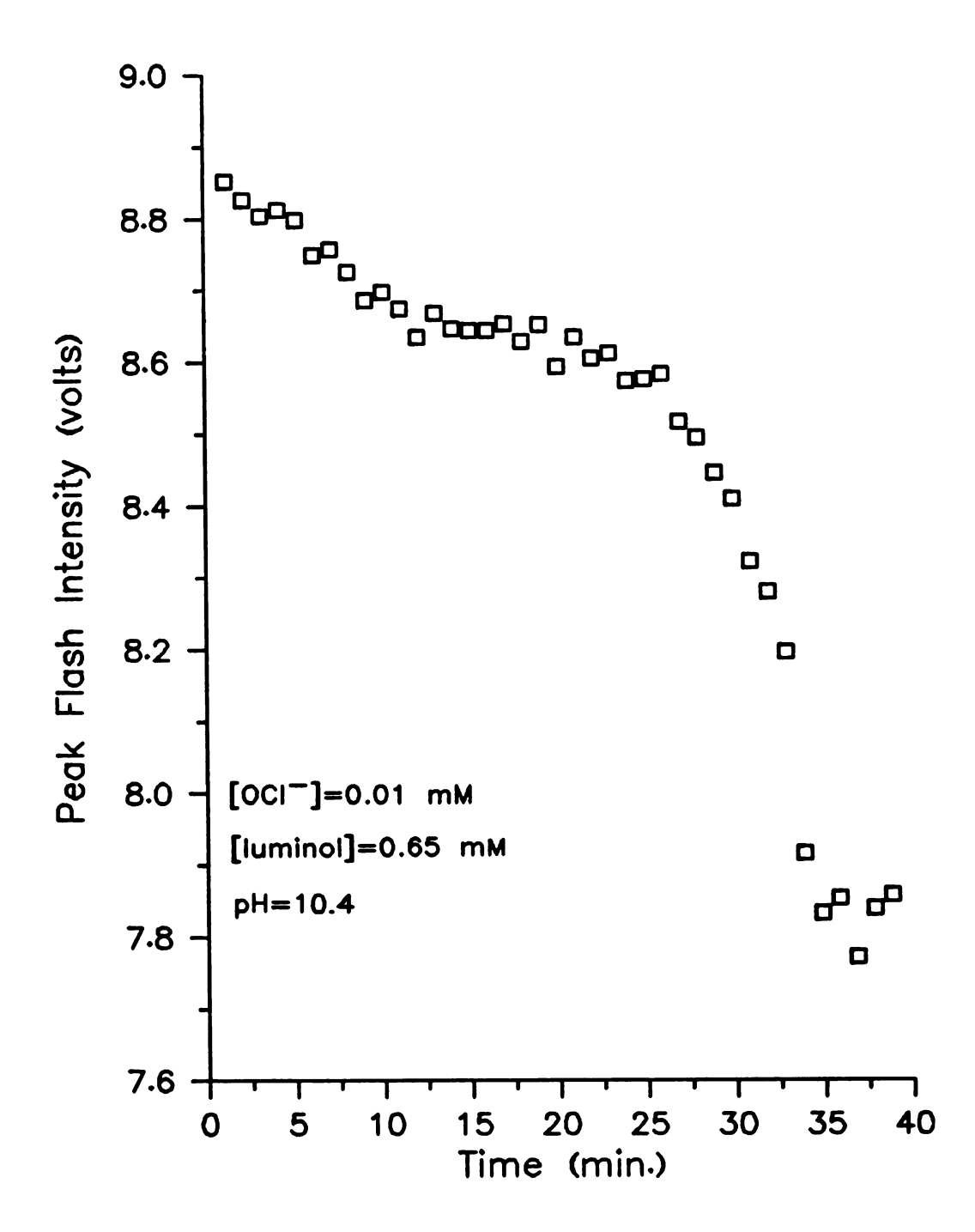


Figure 33. Peak flash intensity of CL reaction of luminol and hypochlorite as a function of time.

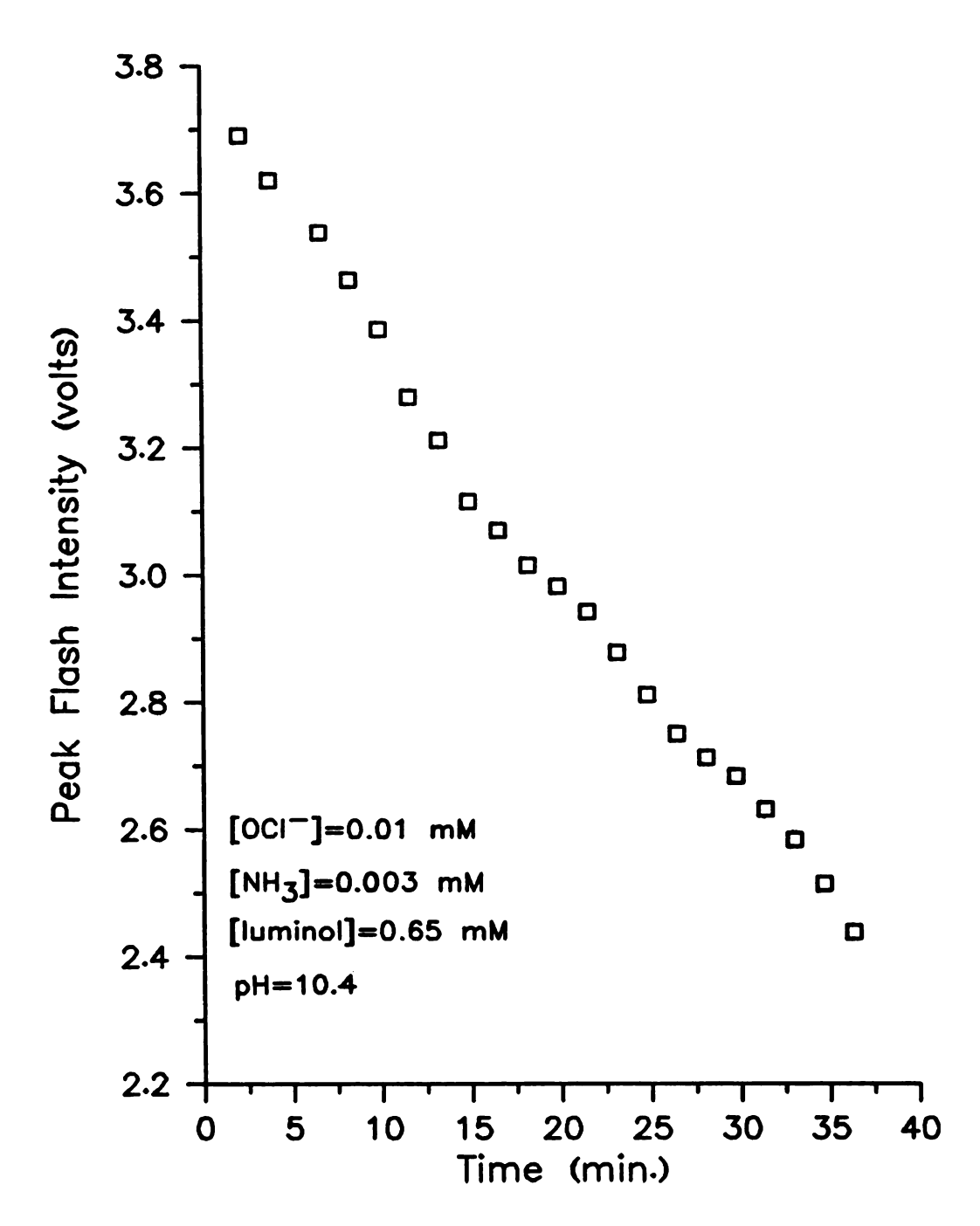


Figure 34. Peak flash intensity  $\underline{vs}$ . time. Hypochlorite solution contains 3  $\mu M$  ammonia.

pushes, printing out the time and the calculated peak flash intensity, and waiting for a specified delay time, after which the entire data taking process was repeated. Solution handling occurred only at the beginning and end of the experiment at a given pH. Fresh luminol and hypochlorite and hypochlorite-ammonia working solutions were prepared at each pH. "Time zero" was taken at the point at which the hypochlorite or the ammonia was added to the buffered solution in the volumetric flask. The solutions were then diluted to the mark and were provided to the stopped-flow for analysis along with the luminol.

a. Hypochlorite Stability Study - The working concentration of hypochlorite used at all of the pH studies was 0.01 The luminol working solution was 0.65 mM in ~0.0015% mM. peroxide and contained 25 mL of the buffer at the pH value used in the individual study. One data acquisition cycle occurred every 2 minutes. At the completion of the acquisition sequence, the peak profile was recorded. Also, the peak flash intensity for a freshly prepared hypochlorite solution was acquired to ascertain if the luminol was decomposing with time. The profiles at various pH values are shown in Figures 35-37. As can be seen from the data in Table 17 and Figure 38, the hypochlorite solutions can be assumed to be stable from 10 to 70 minutes after preparation. This alleviates any worry about decomposition of hypochlorite at a concentration of 0.01 mM. Certainly, one can expect

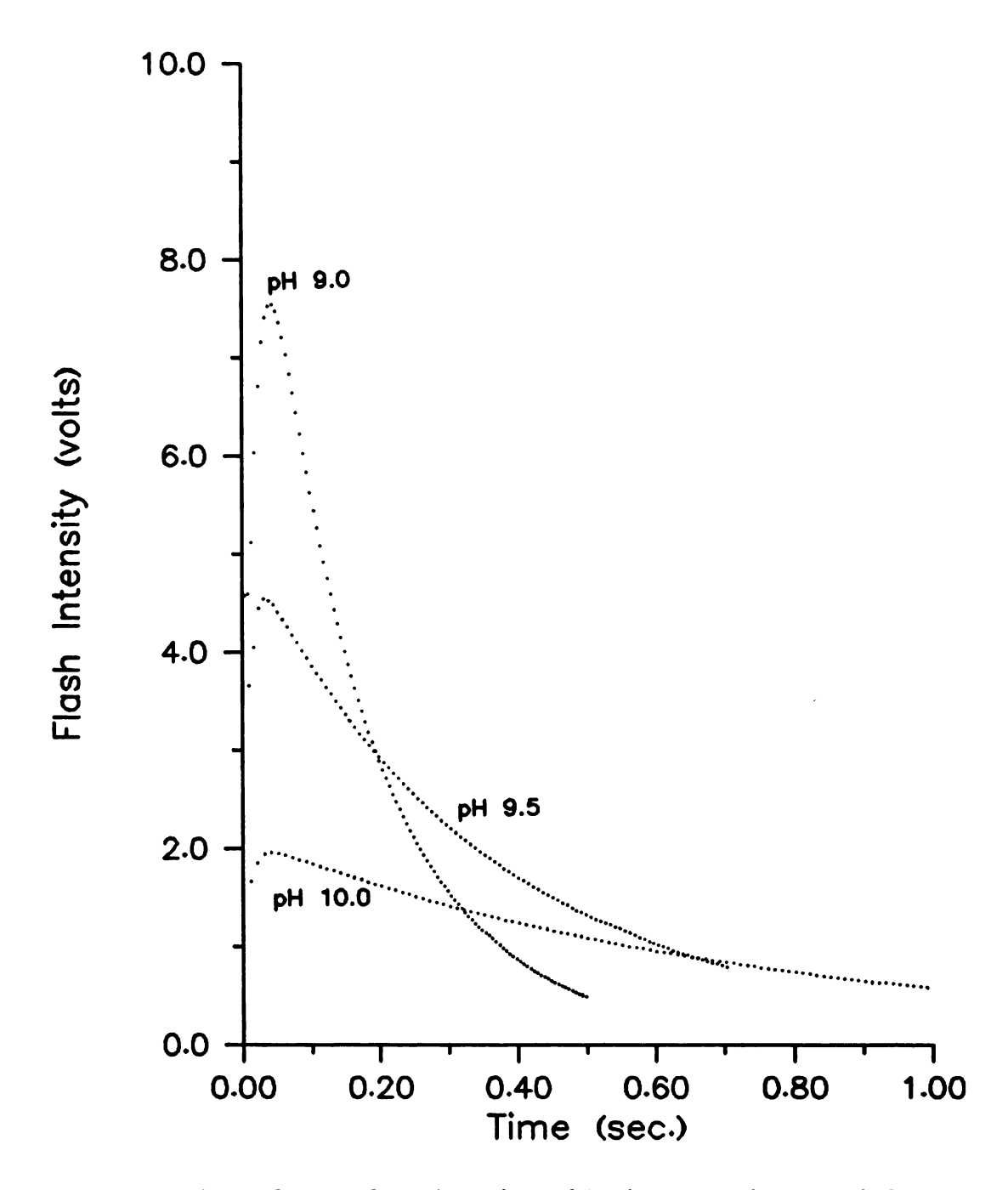


Figure 35. Peak profiles of luminol-hypochlorite reaction. pH=9.0, 9.5, and 10.0.

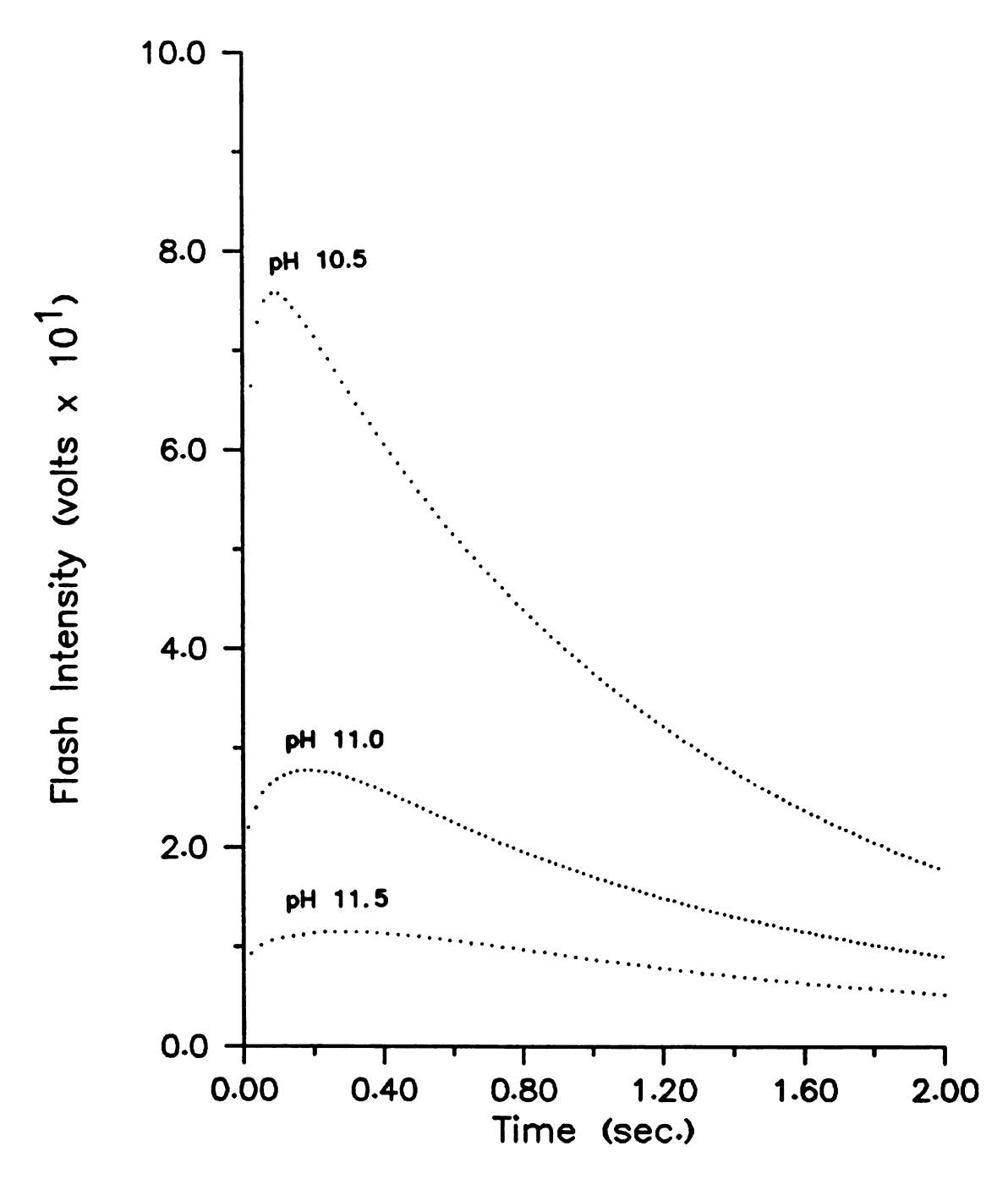


Figure 36. Peak profiles of luminol-hypochlorite reaction. pH = 10.5, 11.0, and 11.5.

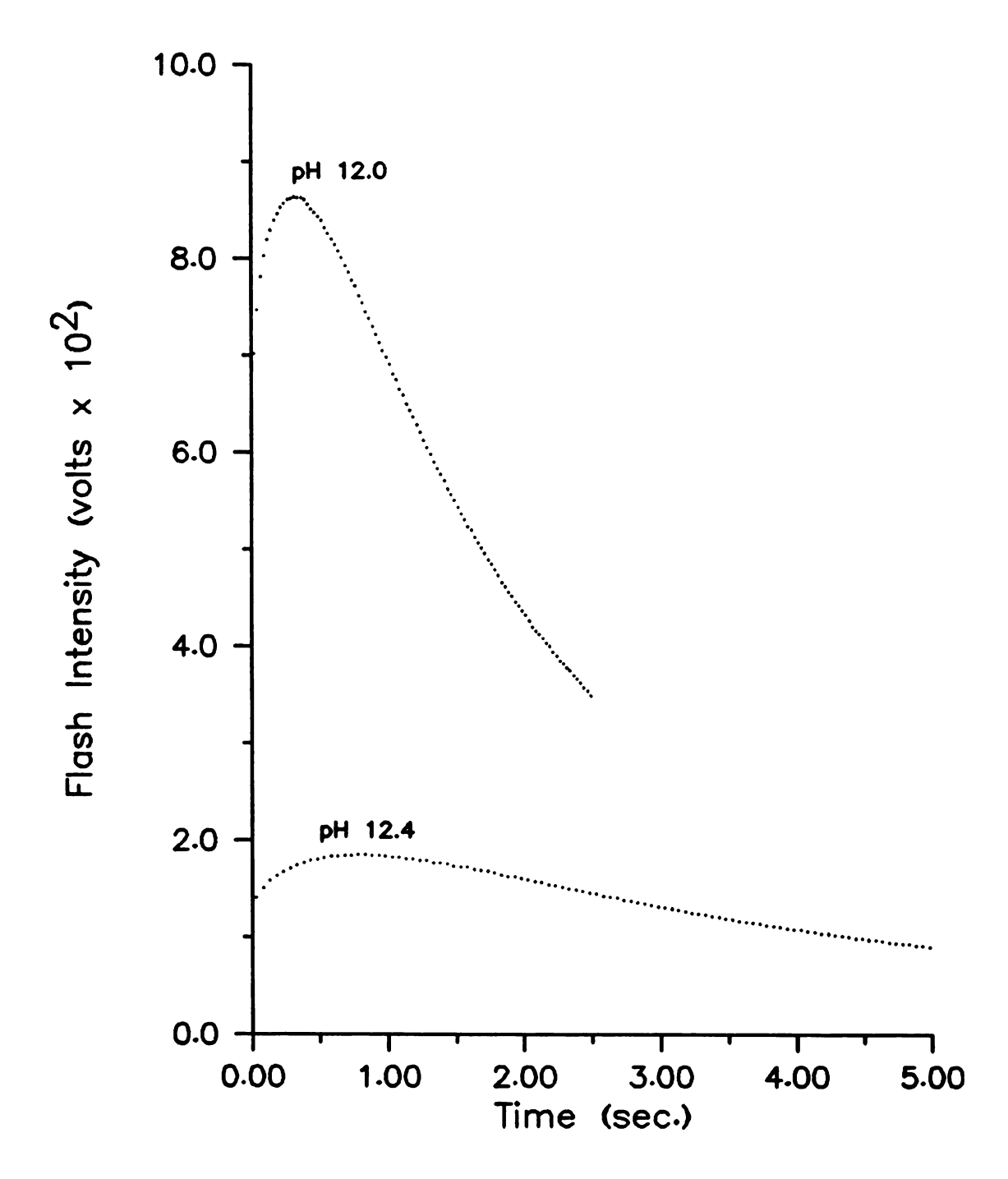


Figure 37. Peak profiles of luminol-hypochlorite reaction. pH = 12.0, 12.4.

 $\frac{\text{Table 17.}}{\text{Addition 17}}$  Peak Flash Intensities of Luminol-hypochlorite CL Reaction as a Function of pH.

рН	AVERAGE PEAK	FLAS	SH INTENSITY	(V)
0.0	7 70		0.05	
9.0	7.78		0.05	
9.5	4.64	± (	0.02	
10.0	2.003	± (	0.008	
10.5	0.734	± (	0.012	
11.0	0.212	± (	0.003	
11.5	0.0804	± (	0.001	
12.0	0.0520	± (	0.0008	
12.4	0.0102	5 ± (	0.00004	
11.0 (phos. buffe	er) 0.293	± (	0.008	

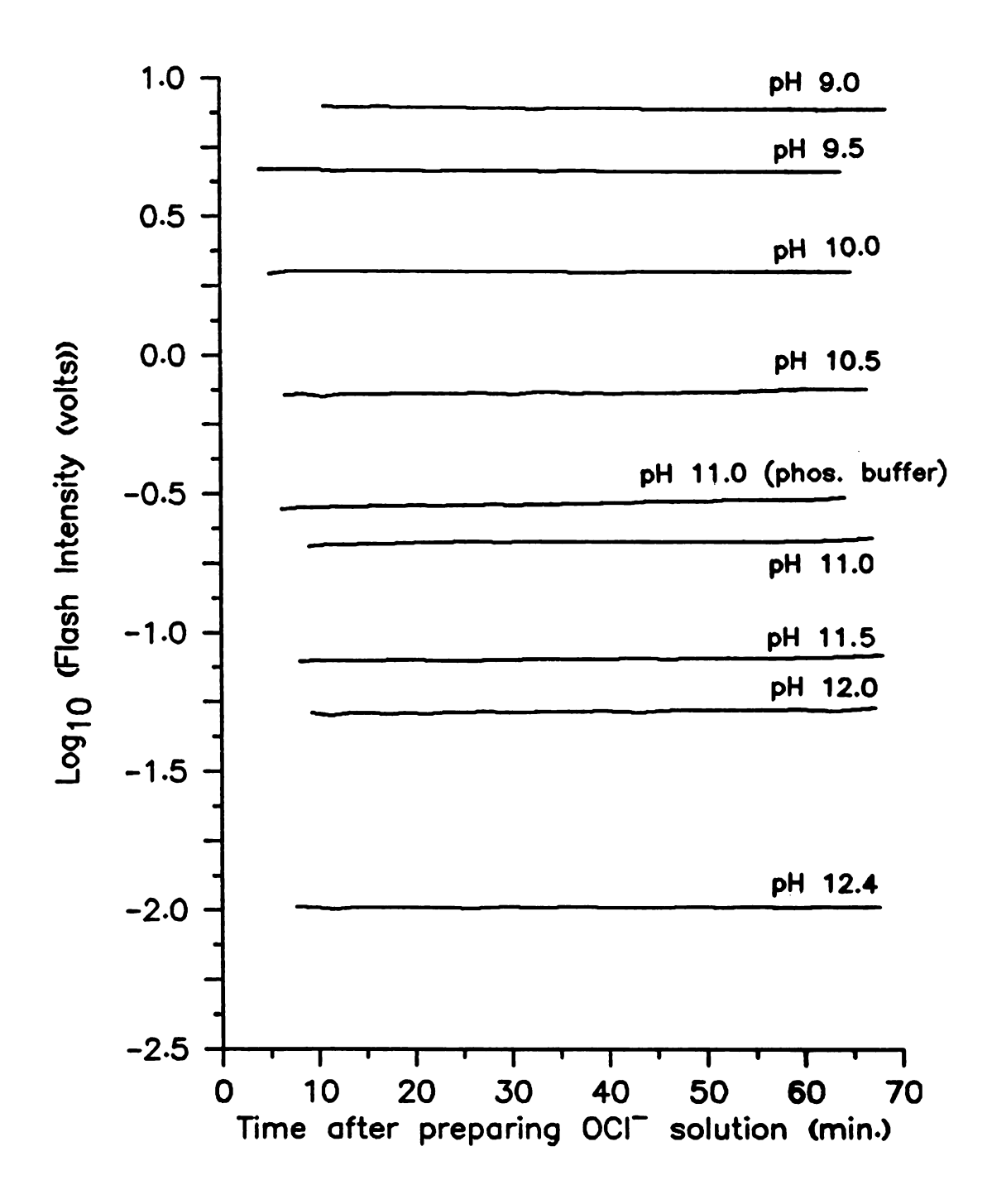


Figure 38. Stability of the peak flash intensity of hypochlorite-luminol solutions with time.

some decomposition at this concentration, but the data show that if it were present, it would be negligible compared to the reproducibility of the measurement of the flash intensity and of the solution preparation. Also, in all cases, the flash intensity of the freshly prepared hypochlorite solution was within a few tenths of a millivolt of the flash intensity of the hypochlorite solution used in the study, indicating minimal luminol decomposition. The variation in the flash intensity may have been due to inaccurate reagent preparation of the hypochlorite solutions, as was observed in the ammonia detection limit study.

It was also observed that the phosphate buffer enhanced the peak flash intensity of the CL reaction. It would be misleading to state that the phosphate played a part in this without closer study of the reaction using replicate preparations of solutions at pH 11.0 with both the phosphate and bicarbonate buffers. Since the CL reaction intensity is highly dependent upon pH, one might expect a change in the intensity if the buffer pH value differs by a few tenth's of a unit in different solutions.

One feature of the peak profile plots shown in Figures 35-37 is that the rate of the CL reaction definitely decreases with time, providing a larger plateau region for determining peak intensity. In general, it can be concluded that for simple hypochlorite determinations, one can use any one of the alkaline pH values, keeping in mind the tradeoffs of higher S/N at lower pH values against improved

stability of the CL signal at higher pH values.

A plot of the effect of pH on the CL signal is shown in Figure 39 using the data in Table 17. The data plotted are the average CL signal for all of the data collected over the time period of the stability study for a given pH value. Again, the data agree well with the results obtained by Isacsson and Wettermark (67).

Theories Concerning Reaction Species - An approximation of species present in solution may be made via logarithmic concentration diagrams that relate the concentrations of the species to pH. The logarithmic concentration diagram of luminol, hydrogen peroxide, and hypochlorous acid and their conjugate bases presented in Figure 40 is useful in making basic assumptions as to what species are involved in the reaction that generates chemiluminescence. The reactions pertaining to the data plotted in Figure 40 are

$$H_2L \rightarrow H^+ + HL^- \qquad K=1.8 \times 10^{-7}$$
 (5.6)

$$HL^{-} \rightarrow H^{+} + L^{-}$$
  $K=6.3 \times 10^{-15}$  (5.7)

$$H_2O_2 \rightarrow H^+ + HO_2^- \qquad K=2.4 \times 10^{-12}$$
 (5.8)

$$HC10 \rightarrow H^{+} + C10^{-} K=2.9 \times 10^{-8}$$
 (5.9)

The neutral luminol molecule is represented by  $H_2L$ . The concentrations of luminol, hydrogen peroxide, and hypochlorous acid are 0.65  $\underline{m}\underline{M}$ , 0.54  $\underline{m}\underline{M}$ , and 0.1  $\underline{m}\underline{M}$  respectively. Equations used to generate data for the curves are

$$[A^{-}] = \frac{CKa}{(Ka + [H^{+}])}$$
 (5.10)

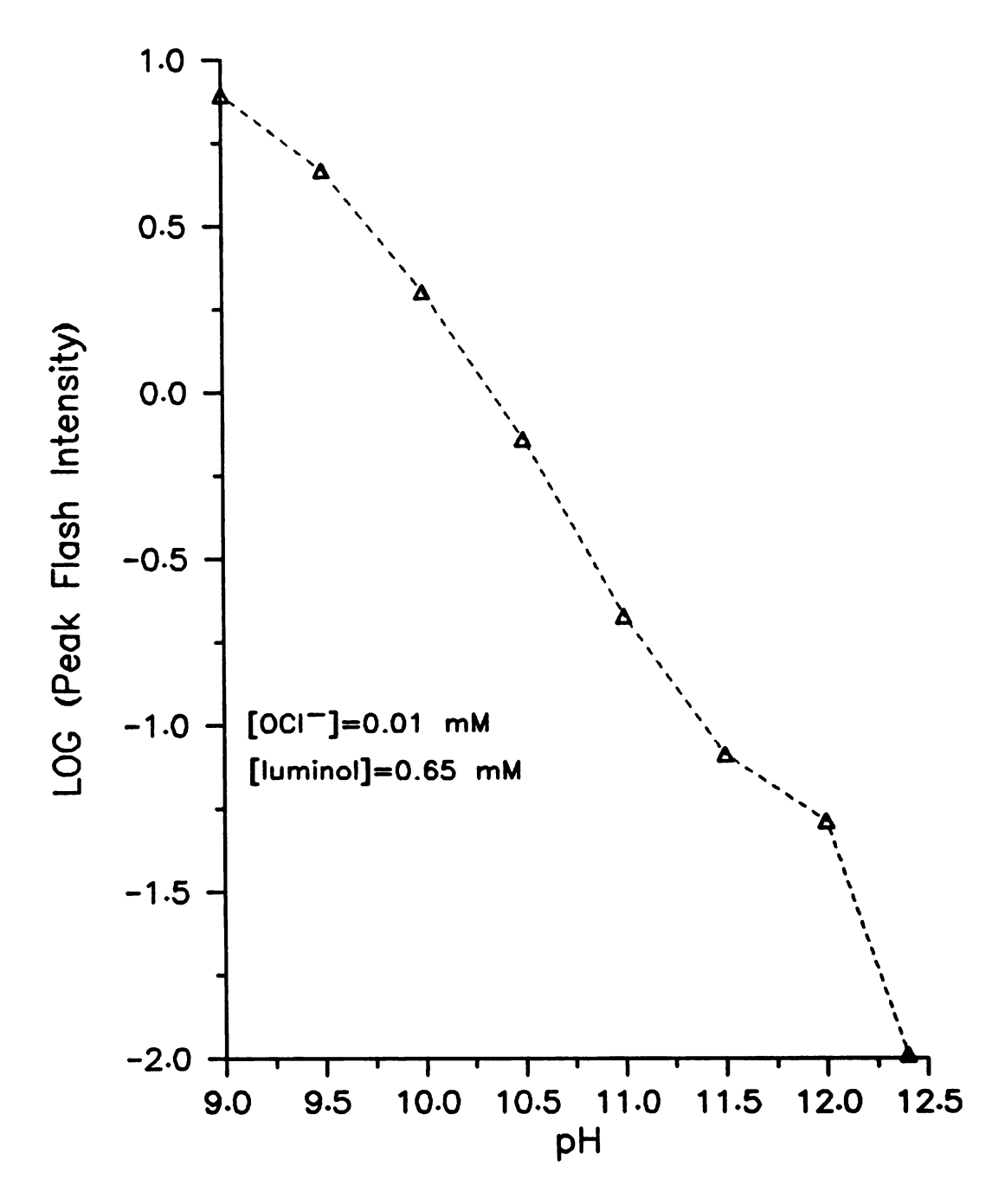


Figure 39. Average peak flash intensity vs. pH.

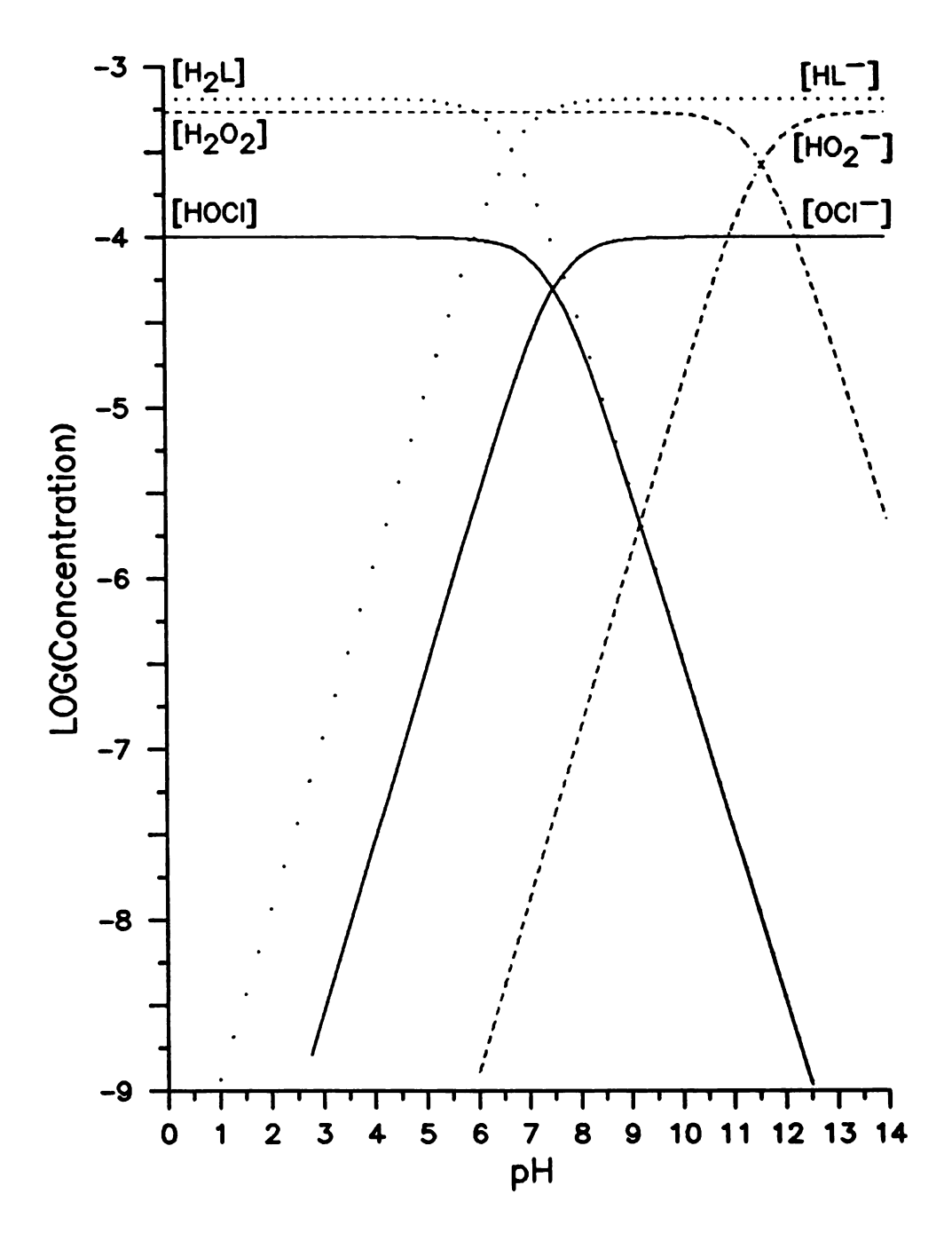


Figure 40. Logarithmic concentration diagram for species present in mixed luminol-hypochlorite solutions.

$$[HA] = \frac{C[H^+]}{(Ka + [H^+])}$$
 (5.11)

where [HA] is the concentration of the acid form of the species present in solution, [A] is the concentration of the conjugate base of the species, C is the initial concentration of the species before dissociation, Ka is the acid dissociation constant, and [H+] is the hydrogen ion concentra-Because the generated data are for approximation purposes, the secondary dissociation constant of luminol and the contributions of other reactions in solution to the concentrations of the above-shown species are assumed to be insignificant. According to the curves in Figure 40, one can make the initial assumption that the decay in the CL intensity observed in Figure 39 is due to either the reaction of the neutral luminol with hypochlorite or to the reaction of the luminol anion with hypochlorous acid. Studies by Isacsson et al.(75) show that peroxide increases the rate of decay of emission for any given hypochlorite concentration in the pH range of 9-12, thus leading to the conclusion that the reacting species leading to chemiluminescence are the luminol anion and hypochlorous acid, as shown in the mechanism presented in Figure 30. this in mind, it is proposed that the aberration seen in the plot of flash intensity vs. pH in Figure 39 is due to the decreasing amounts of hydrogen peroxide available for the oxidation of luminol anion at pH 12. As will be shown in Figure 41, an plot of identical shape was obtained for a

freshly-prepared series of buffer, hypochlorite, and peroxide solutions of similar concentrations to those used in the previous study. It is important to note that at pH values of 9-12 luminol is an anion and might thus react more easily with the neutral hypochlorous acid molecule than with hypochlorite.

However, one cannot rule out the possibility that the CL reaction is due to the initial reaction of hypochlorite and neutral luminol because the relationship of the curves for these species in Figure 40 is similar to that of hypochlorous acid and the luminol anion. The one distinction between the two possible initial reactions that give rise to CL is the pH of the occurrence of the maximum concentration of the limiting reagent. If the CL reaction occurred from the combination of the luminol anion and hypochlorous acid, the concentration of the limiting reagent, hypochlorous acid, would be a maximum at pH 6-7. On the other hand, if CL arose from the reaction of the neutral luminol and hypochlorite, the maximum concentration of hypochlorite would occur at pH 7-8. Further study of the CL reaction using reaction mixtures containing only luminol and hypochlorite at pH 6-12 would serve to establish the exact nature of the species involved in the primary reaction.

b. Stability of Hypochlorite-Ammonia Solutions - The hypochlorite concentration used throughout this study was 0.1  $\underline{mM}$ , with an ammonia concentration of 0.03  $\underline{mM}$ . The

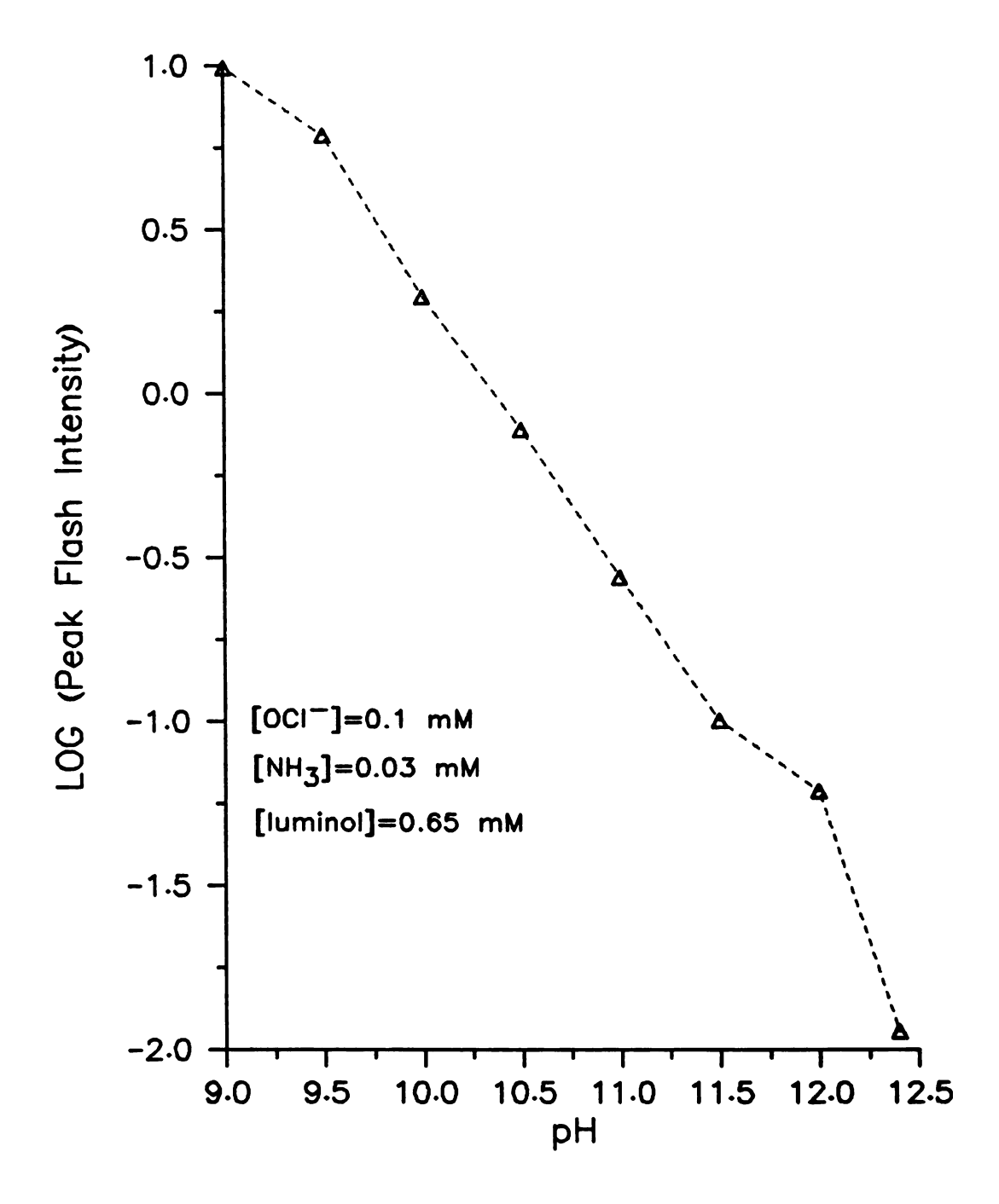


Figure 41. Peak flash intensity as a function of pH for solutions used in the hypochlorite-ammonia mixture stability study.

luminol working solutions were prepared in a similar manner to that described in the previous section. One data acquisition cycle occurred every minute for up to 35 minutes after the first data taking cycle. The procedures involved were the same as described previously. Before and after analysis of the hypochlorite-ammonia mixture, a blank level for the reaction was obtained by preparing a fresh hypochlorite solution and obtaining its peak intensity. This was in essence a two-point reference line used to obtain the relative decrease in the CL signal compared to the CL signal of the hypochlorite-ammonia solution. CL reaction peak profiles were also obtained to determine if there was any difference in the flash profiles of the solutions containing only hypochlorite and those containing hypochlorite and ammonia. The plot of the peak flash intensities of the solutions containing only hypochlorite vs. pH is shown in Figure 41. As was mentioned in the previous section, it appears that the break in the plot is due to the decrease in the amount of hydrogen peroxide available for the oxidation of the azaquinone.

The plots in Figures 42-45 show the CL reaction profiles for the two types of solutions used in this study.

The upper curve of the solid or dotted pair represents the peak profile of the reaction of luminol with buffered solutions containing only hypochlorite, while the lower profiles are of the reaction of luminol with hypochlorite solutions containing ammonia. As can be seen in the

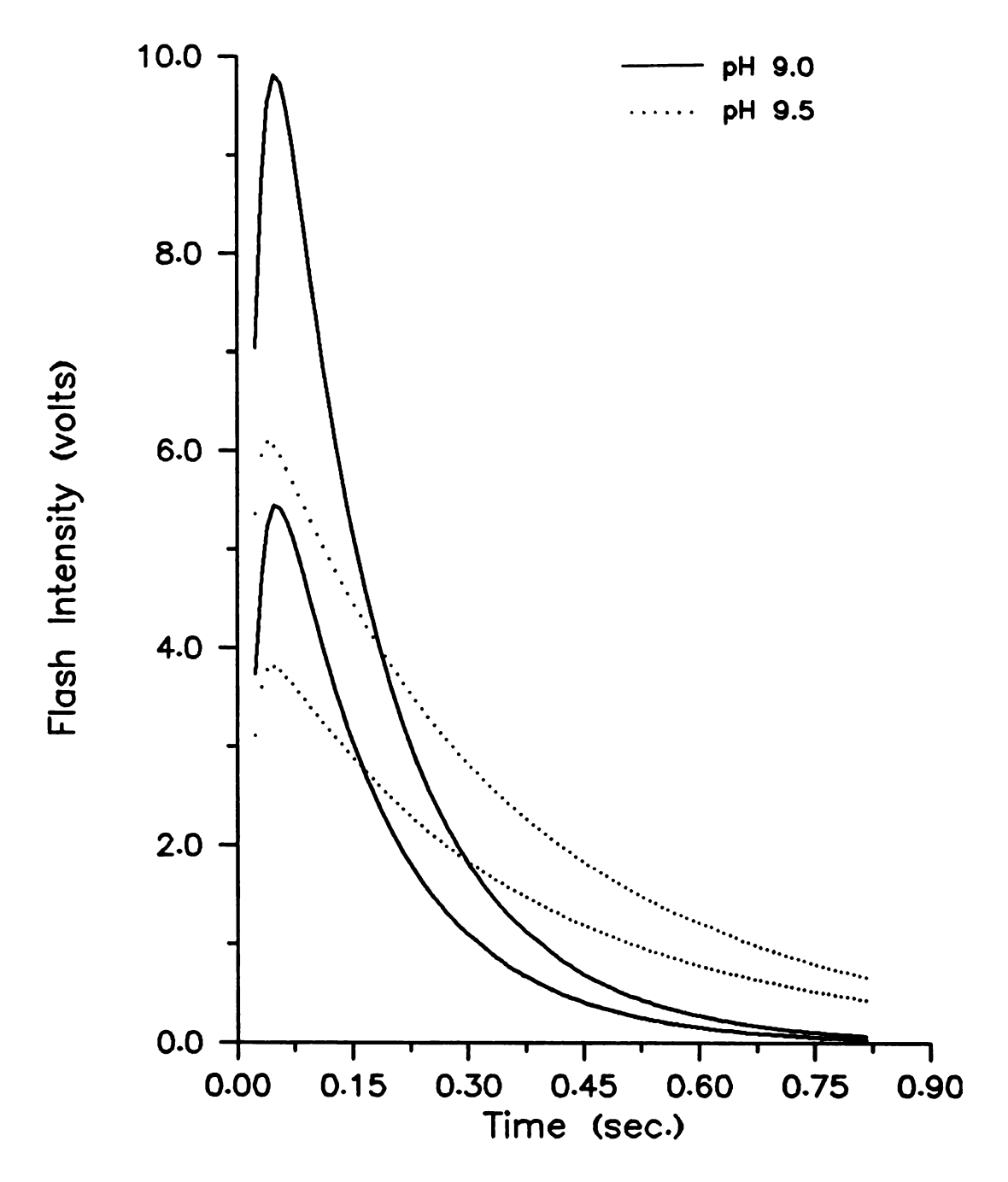


Figure 42. Peak profiles of the CL reaction of luminol solutions and solutions containing hypochlorite (upper curve) and solutions containing hypochlorite and ammonia (lower curve), pH = 9.0, 9.5.

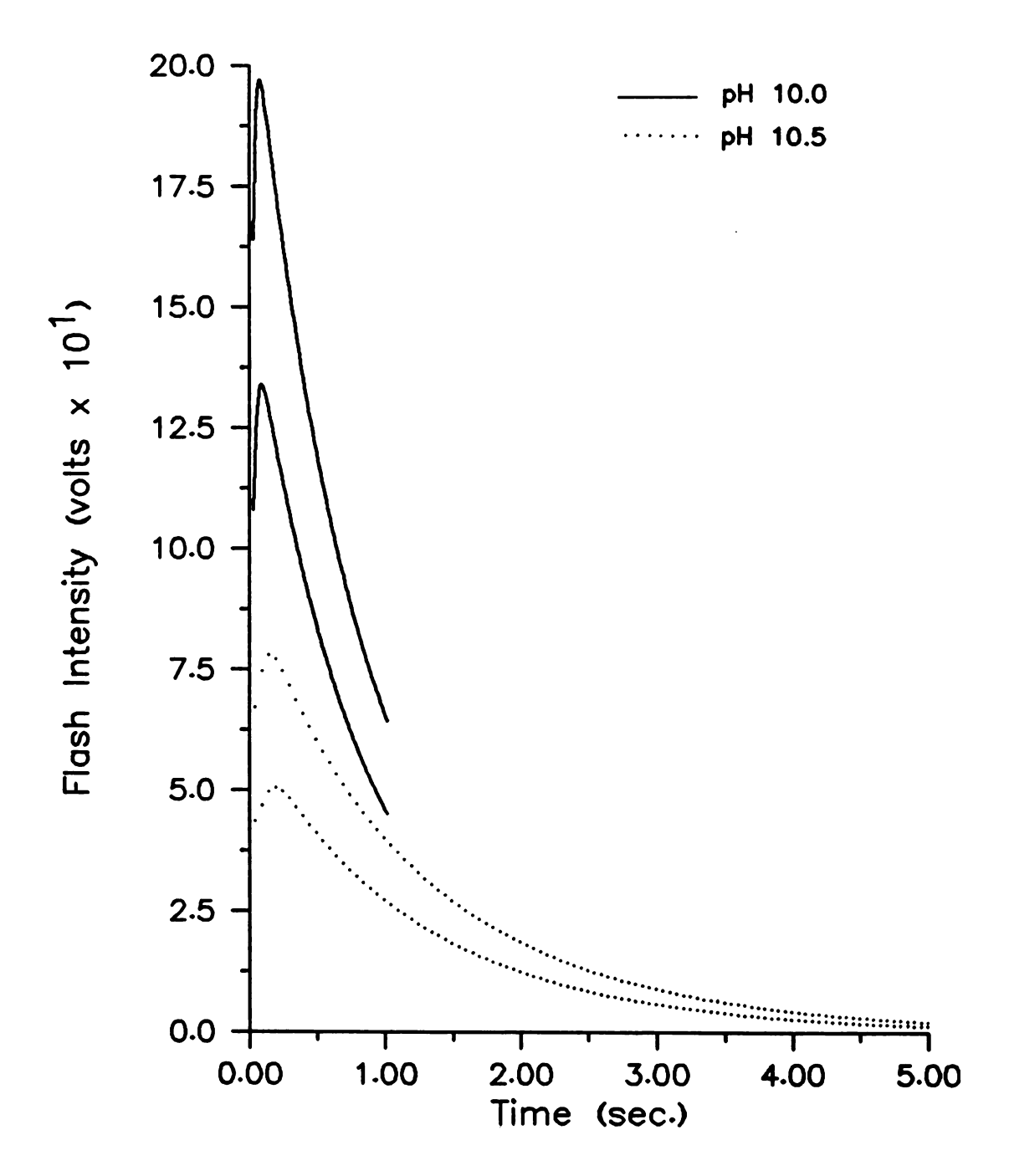


Figure 43. Peak profiles of the CL reaction of luminol solutions and solutions containing hypochlorite (upper curve) and solutions containing hypochlorite and ammonia (lower curve), pH = 10.0, 10.5.

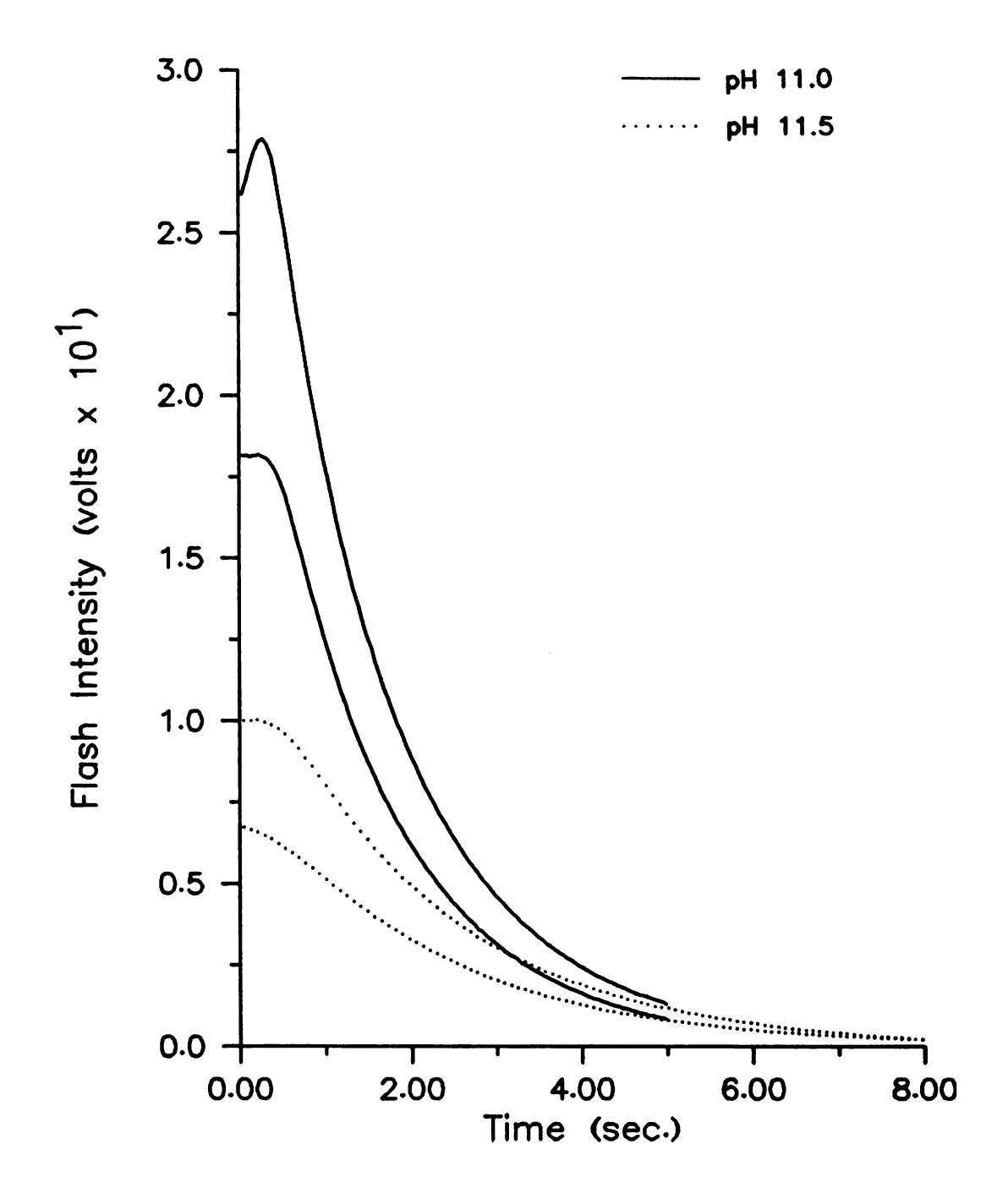


Figure 44. Peak profiles of the CL reaction of luminol solutions and solutions containing hypochlorite (upper curve) and solutions containing hypochlorite and ammonia (lower curve), pH = 11.0, 11.5.

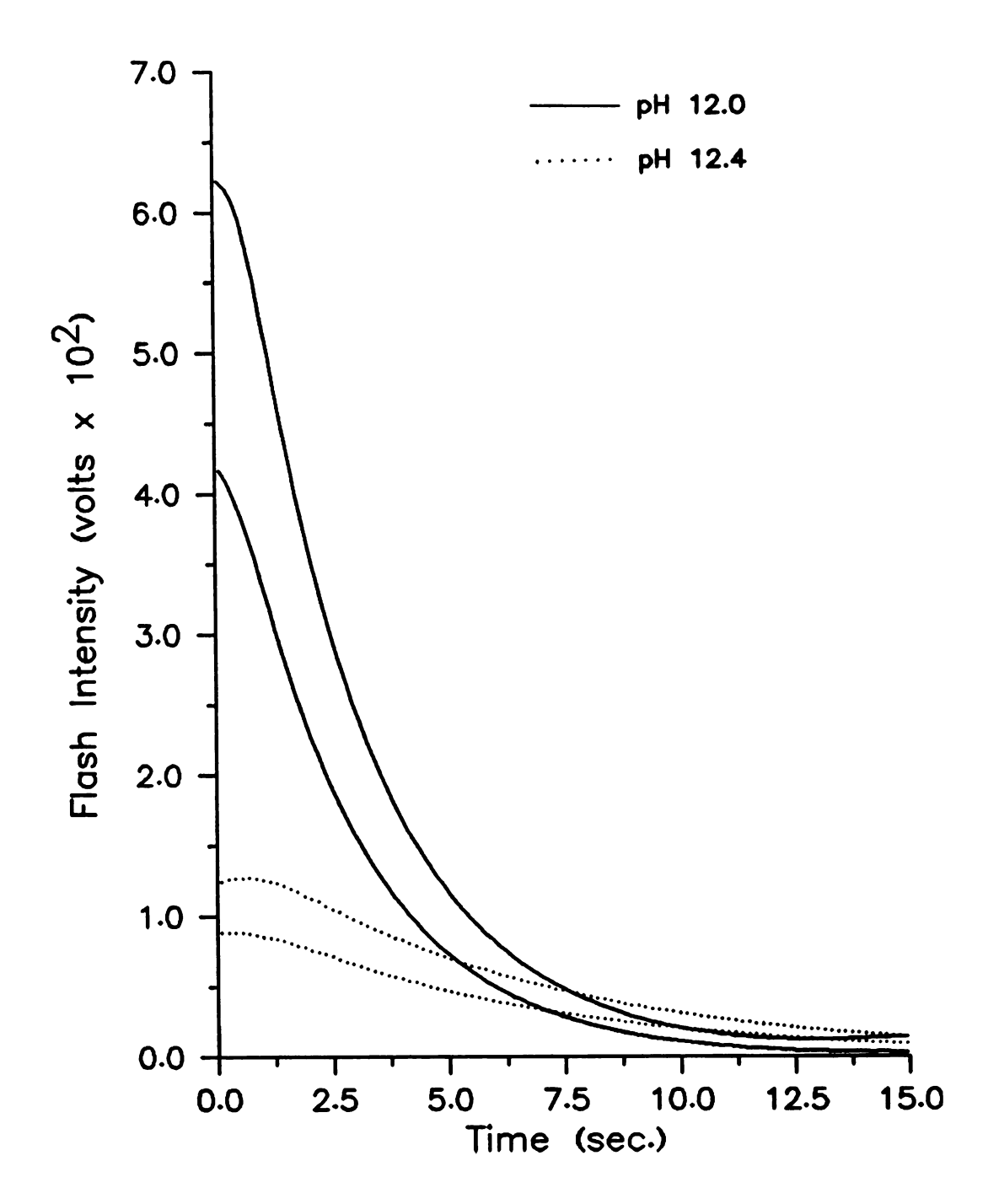


Figure 45. Peak profiles of the CL reaction of luminol solutions and solutions containing hypochlorite (upper curve) and solutions containing hypochlorite and ammonia (lower curve), pH = 12.0, 12.4.

figures, occurrence of the peak of the reaction tends to shift earlier in time for the hypochlorite solutions containing ammonia and in all cases broadens out with increasing pH. The CL reaction slows down considerably at higher pH values, lasting for more than 20 s at pH 12.4.

The results of the stability study of the hypochlorite solutions containing ammonia are plotted in Figures 46-48. As is expected from the studies done by Patton (76), the ammonia-hypochlorite reaction to form monochloramine undergoes rather complex kinetics at low pH values (9,9.5), with the decomposition of monochloramine to ammonia and chloride. It is postulated that the decrease of the peak flash intensity with time observed at pH 9 and 9.5 is due to the removal of hypochlorite from solution by reaction with the ammonia regenerated by the decomposition of monochloramine. In addition, if one looks at the logarithmic concentration diagram in Figure 49, the ammonium and ammonia species are present in significant amounts at pH 9-10. Therefore, we could expect contributions from the ammonia-ammonium ion equilibrium to effect the formation rate of monochloramine in hypochlorite solution. At higher pH values, the solutions are fairly stable with respect to decomposition of monochloramine. The most stable region for determination of ammonia by this reaction method would be pH 10-11.5, giving a reasonable S/N level. In this range, one is assured that most of the ammonia is not in the ionized form and is thus available for reaction with hypochlorite.

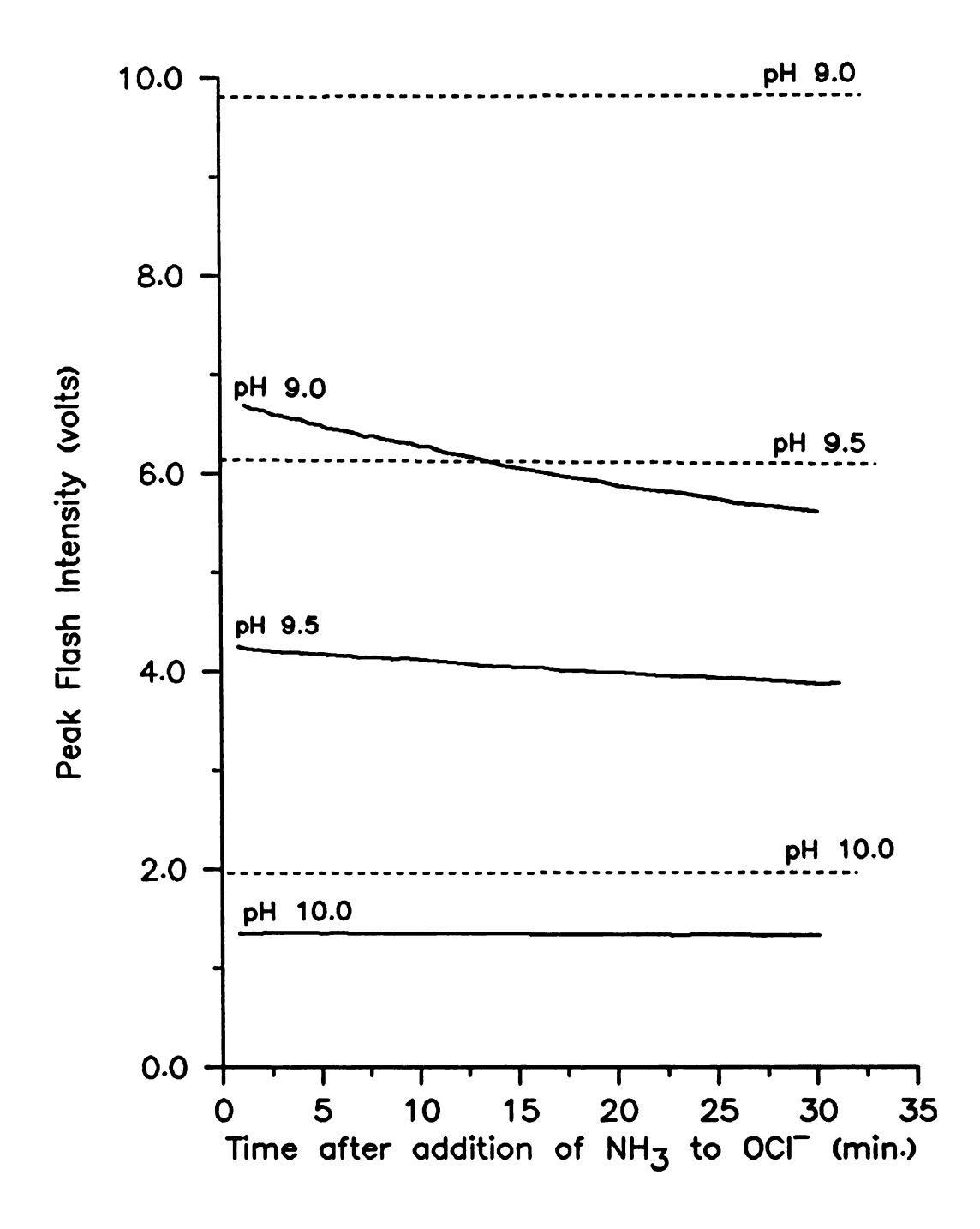


Figure 46. Time-stability of ammonia-hypochlorite solutions at pH 9.0, 9.5, and 10.0.

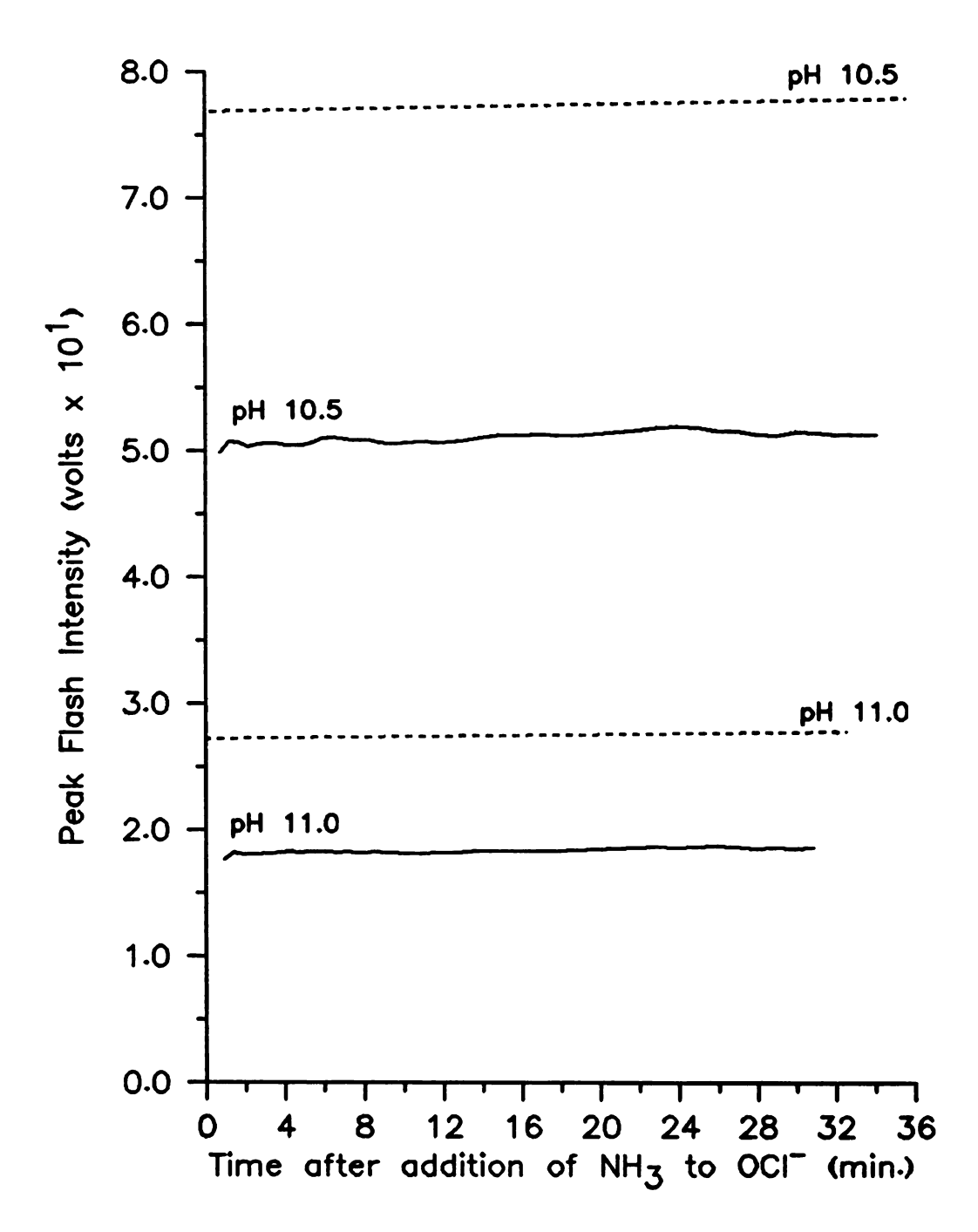


Figure 47. Time stability of ammonia-hypochlorite solutions at pH 10.5 and 11.0.

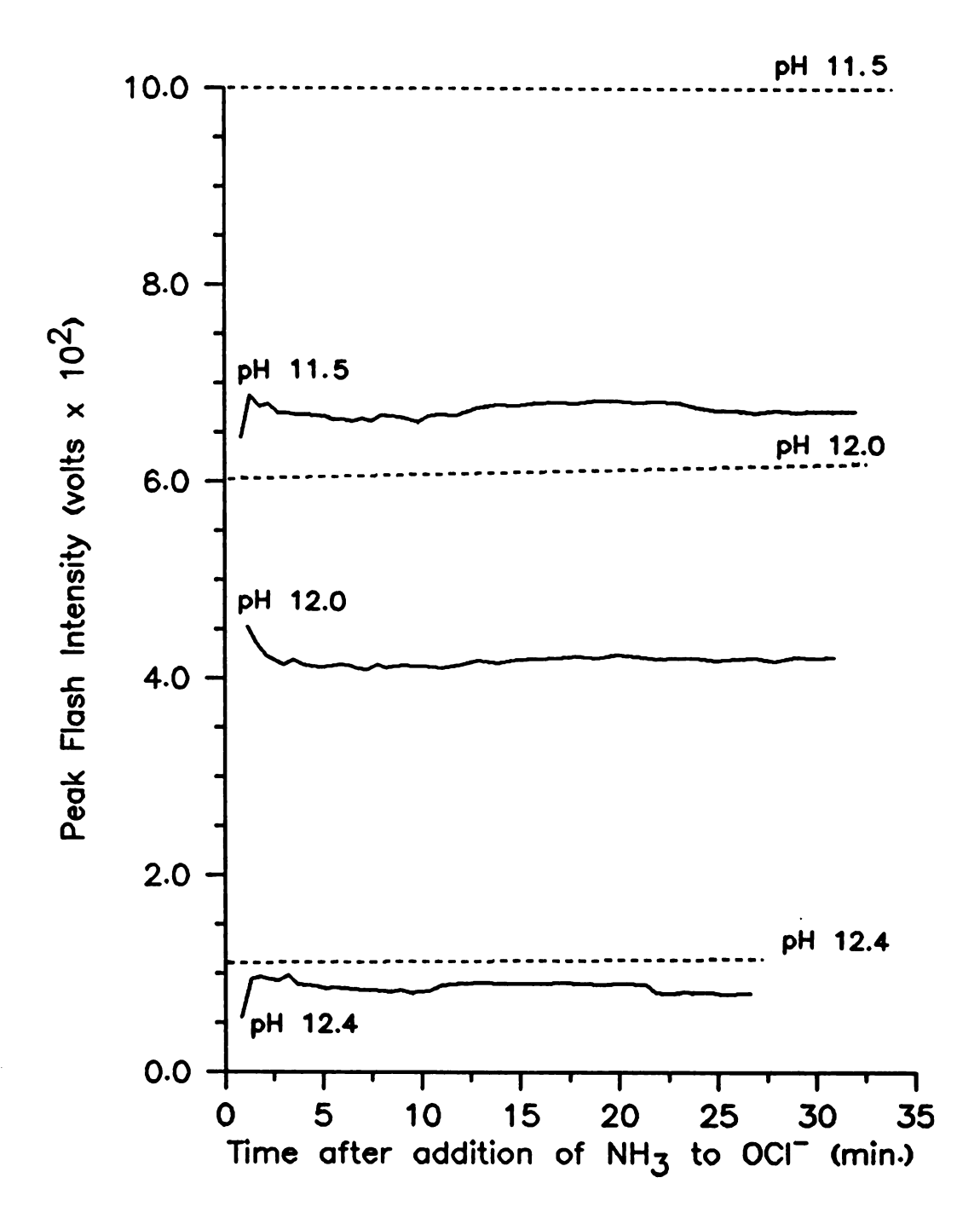


Figure 48. Time stability of ammonia-hypochlorite solutions at pH 11.5, 12.0, and 12.5.

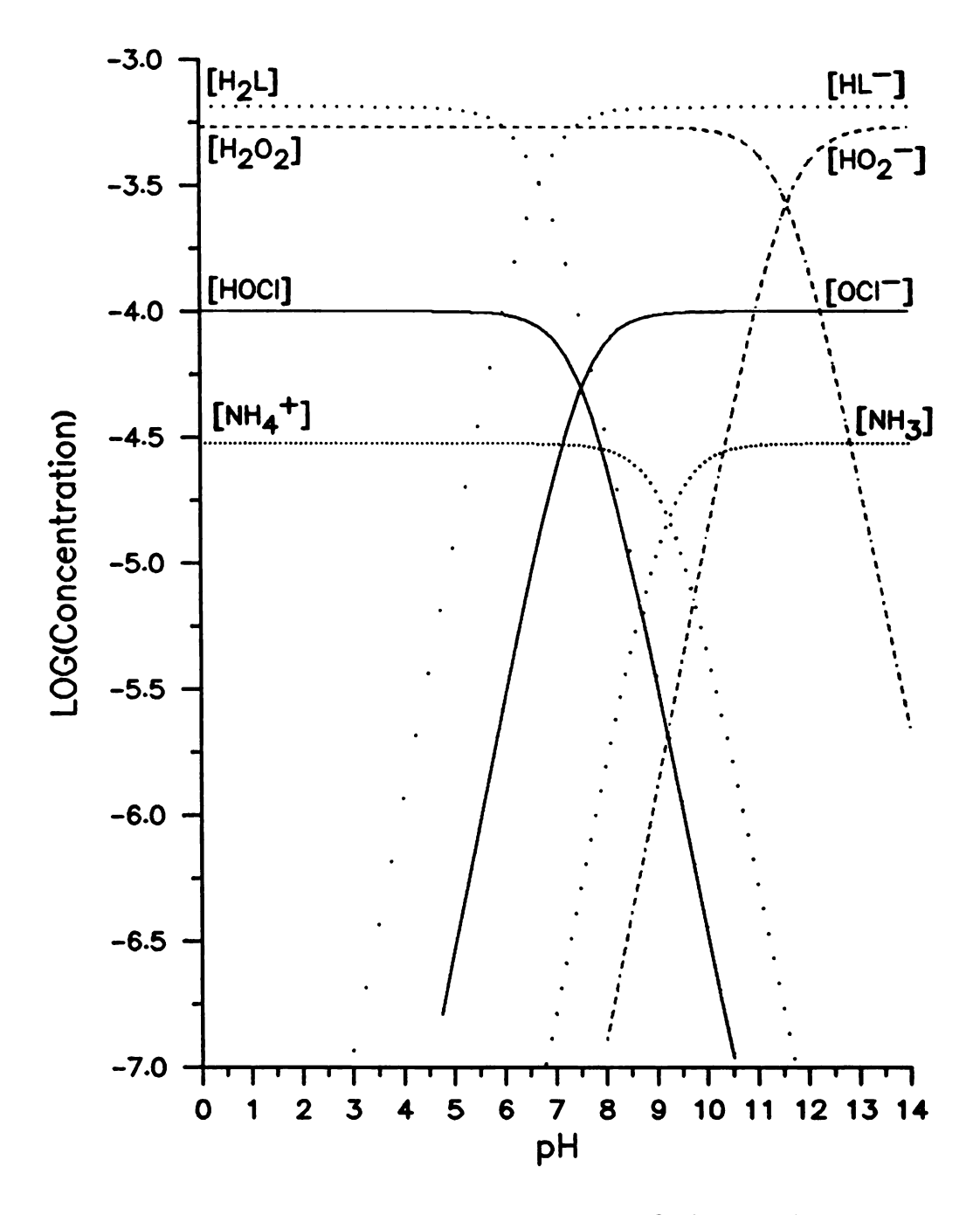


Figure 49. Logarithmic concentration diagram of the species present in luminol-hypochlorite-ammonia mixtures.

## 7. Conclusions

In summary, it has been shown that luminol, hypochlorite, and hypochlorite-ammonia solutions are most stable at pH values greater than 10. The method for indirectly determining ammonia by removing the available hypochlorite for the reaction to generate CL has been shown to be sensitive to low levels of ammonia and is linear for at least a 10-fold concentration range. Hypotheses concerning the species involved in the reaction were presented in an attempt to verify the mechanism proposed by Isacsson et al. (75). Although it has been postulated that the reaction generating the CL signal is that of the luminol anion and hypochlorous acid, the reader should be aware of the fact that there are several complex equilibria occurring when the luminol and hypochlorite reagents are mixed. Further rate studies under controlled conditions of ionic strength and pH would serve to clarify the mechanism leading to chemiluminescence.

### CHAPTER VI

#### CONCLUSIONS AND FUTURE PERSPECTIVES

The projects and results presented in this thesis were part of a learning experience. This final chapter reflects upon mistakes of the past and provides suggestions for the future. Most improvements for the clinical methods used in the various experiments have been discussed earlier in the appropriate sections and will not be repeated here. The intent of this chapter is to discuss various improvements in the hardware concerned with the reagent preparation system and the stopped-flow instrument.

The automated reagent preparation system shows promise for providing a basis for a fully automated - general purpose instrument once several improvements are made. The current electronics technology is constantly improving, providing inexpensive, intelligent, and versatile single-and multi-processor based systems for automation and control of instruments. The first and foremost improvement of the reagent preparation device consists of changing the controlling processor and hardware of the device to one of the newer, more compact systems based upon the Intel 8085 processor. Although the 8085 normally is programmed in assembly language, the availability of compilable languages such as FORTH provides a medium in which most functions can be broken down into rudimentary subroutines. Once these are

tested and implemented, the user would no longer be faced with poring over several pages of machine code to make alterations in the controlling software, but rather would implement the function desired in a line or two of more concise FORTH code. Also, the availability of single-chip, intelligent stepper motor drivers would replace an entire rack of equipment that is presently used for this function. In summary, the 8085-based system would serve as ideal controllers to perform the very basic and uncomplicated functions of mimicing the manual operations of reagent preparation.

As far as the hardware of the reagent preparation system is concerned, future workers might consider using the two unused channels of the six-port valve for additional reagent syringes. This would serve to enhance the ability of the system to prepare very complex solutions, an important feature for fundamental kinetic studies of reactions. Improvements in the rate of reagent preparation may be made by adding another meniscus detector at the bottom of the dilution vessel in order to eliminate arbitrary software delay periods used to guess when the flask is emptied of The author feels that the basic dilution processes are solid and in no need of modification. One can force large volumes of solutions through small orifices at a limited rate; when this is exceeded, the user's results may suffer due to reagent leakage, malfunction of valves, or shattering of the glass syring barrels. Finally, the

addition of a reagent turntable or some other means of transporting prepared solutions to their destination could be an improvement in the efficiency of the preparationanalysis process.

The previously-mentioned use of more compact processors for the reagent preparation system applies even more so to the stopped-flow instrument. Although it is convenient to have controlling programs with many bells and whistles to aid the uninitiated through a kinetics analysis, the program currently in use does not efficiently use the computing power of the 8/e and is wasteful of memory space. In addition, the user must still wait a period of time before hard results can be seen. Some sort of interactive routine to perform real-time analysis of the data is needed. This routine should plot out the data on our high-resolution graphics terminal and make it available for immediate massaging by the user.

The speed of data acquisition and the power of rudimentary data processing in real time are available on the
8/e, but this may have the potential for becoming an expensive
luxury as time goes by. The problems concerning repair and
maintenance of the aging computer make its use costineffective: equivalent money spent on replacement or repair
of memory, interface options, or power supplies could easily
purchase several microprocessor-based controller systems
for the stopped-flow instrument. The valve controller
module and the data acquisition system are easily adaptable

to any new processor: the user merely needs to provide a few controlling signals and data lines. Real-time data acquisition is possible through use of the various single-chip event timers available. Again, a high-level threaded language such as FORTH would facilitate implementation of the control and data acquisition functions.

In conclusion, the potential user has two good tools with which he can do reaction-rate studies. The automated reagent preparation system and the automated stopped-flow instrument have been shown to be applicable to a wide variety of analytical methods, and with some improvements, may someday be available for routine use.

APPENDIX

#### APPENDIX A

This appendix contains a short description of the various subroutines that are used during operation of the automated reagent preparation system. Despite tradition, software listings will not be included; the listings may be found in the Crouch Group Archives if necessary. The following list contains several abbreviations: AC is the 12-bit accumulator of the mini- or microcomputer, CALL is the instruction predefined in the program source code to be a "JMS I O" instruction, and the symbol "↑" signifies typing a control character. The format to be followed consists of the calling sequence, what the character in the AC signifies, and a brief description of what the routine does.

- CALL IDATA AC = pointer to data storage location. Input data from minicomputer.
- CALL ODATA AC = pointer to data storage location. Send data to minicomputer.
- CALL ERROR AC = error code. Print warning message for appropriate code.
- CALL TXOUT AC = pointer to text. Output character string to console. String terminated by a "O".
- CALL TYPE AC = character. Type contents of AC on terminal.
- CALL READ 8-bit character returned in AC. A "+C" chains to resident monitor that is transparent to the microcomputer. ALTMODE chains to manual mode of operation.
- CALL NOUT Outputs contents of AC as ASCII numeric value.
- CALL OCTOUT Outputs contents of AC as an octal number.

- CALL CRLF Outputs carriage return/line feed to terminal.
- CALL DELAY Calling location plus one contains delay time.
  Routine will wait for "n" seconds, while monitoring
  the TTY keyboard.
- CALL MONITR Transparent monitor routine used to enable communication with the minicomputer.
- CALL MANUAL Provides for "manual" control of all diluter functions from the console keyboard.

COMMAND	FUNCTION
WO	open wash valves
WC	close wash valves
0	set lower valves to deliver
D	set lower valves to dilute position
Е	empty syringe; number of steps is
	asked for
F	fill syringe; number of steps is
	asked for
S	step 6-port valve to asked-for position
С	cycle entire system through a wash
↑ R	return to calling routine

- CALL CYCLE Goes through entire wash cycle for the syringes (four rinse/fill cycles) and the volumetric flask (two fill/empty cycles).
- CALL BONG Ring the TTY bell once.
- CALL ROTATE Turn the 6-port valve and keep track of its position.
- CALL MANROT Move syringe (either empty or fill).
- CALL xCODEy "x" = F for fill or P for empty; "y"=1,2 or 3.
  These routines are used to change the device code for
  the empty or fill operations of any of the syringes.
- CALL SCREW General plunger movement handling routine.
  Checks limit-of-travel detectors before energizing the stepper motor.
- CALL STEPS Read in which syringe will be used and the number of step pulses to be supplied to the stepper motor.
- CALL QUERY Read in position desired for 6-port valve from keyboard and move the valve to it.

- CALL SIXCK Check 6-port valve position. Read the position from the display board and check it with the position stored in memory. If no agreement, call monitor with error code 1.
- CALL CMOVE Called from CYCLE subroutine. Moves syringe plunger until limit-of-travel detector is reached.
- CALL DECIN Double-precision decimal number input routine.
  Octal equivalent is stored in two locations on page
  zero.
- CALL DECOUT Double-precision decimal number output routine. Outputs decimal number to the keyboard from the octal equivalent stored on page zero.
- CALL FLAG Simple I/O routine used for YES/NO queries to the keyboard. If AC=O, the reply was YES; if AC \neq 0, the reply was NO.
- CALL SOLTYP Prints solution identification number, syringe number, and the number of steps to be supplied to the stepper motor. Used during reagent preparation.
- CALL VOLRIN Go through two fill/empty volumetric flask cycles.

LIST OF REFERENCES

#### REFERENCES

- (1) H.V. Malmstadt, C.J. Delaney, and E.A. Cordos, Crit. Rev. Anal. Chem., 2, 559 (1972).
- (2) S. Stieg and T.A. Nieman, <u>Anal. Chem.</u>, <u>52</u>, 796 (1980).
- (3) S.N. Deming and H.L. Pardue, <u>Anal. Chem.</u>, <u>43</u>, 192 (1971).
- (4) H.L. Pardue and H.V. Malmstadt, Clin. Chem., 8, 606 (1962).
- (5) A.A. Eggert, G.P. Hicks, and J.E. Davis, <u>Anal. Chem.</u>, <u>43</u>, 736 (1971).
- (6) E.C. Toren, Jr., R.N. Carey, A.E. Sherry, and J.E. Davis, <u>Anal. Chem.</u>, <u>44</u>, 339 (1972).
- (7) K.A. Mueller and M.F. Burke, <u>Anal. Chem.</u>, <u>43</u>, 641 (1971).
- (8) G.E. Mieling, R.W. Taylor, L.G. Hargis, J. English, and H.L. Pardue, Anal. Chem., 48, 1686 (1976).
- (9) H.L. Pardue, H.T. Gaw, G.E. Mieling, V.L. Mathews, D.M. Fast, and M. Rubesch, Clin. Chem., 23, 1230 (1977).
- (10) H.V. Malmstadt, Analyst, 105, 1018 (1980).
- (11) H.V. Malmstadt, D.L. Krottinger, and M.S. McCracken, "Topics in Automated Chemical Analysis," vol. 1, Halsted Press, NY, 1979, p. 95.
- (12) R.W. Spillman and H.V. Malmstadt, <u>Anal. Chem.</u>, <u>48</u>, 303 (1976).
- (13) H.V. Malmstadt, D.L. Krottinger, and M.S. McCracken, Am. Lab., 9(3), 51 (1977).
- (14) H.V. Malmstadt, D.L. Krottinger, and M.S. McCracken, J. Autom. Chem., 1, 15 (1978).
- (15) F.J. Holler, Ph.D. thesis, MSU, 1977.
- (16) L.D. Rothman, Ph.D. thesis, MSU, 1974.
- (17) E. Bradt, Undergraduate project, MSU, 1976.

- (18) E.R. Johnson, unpublished work.
- (19) Model TCKA6201050A, Lee Co., Westbrook, Conn.
- (20) Model B6031V6A, Altex, Berkeley, CA.
- (21) Model 201-14, Altex.
- (22) Model Al506C, Velmex, Inc., Bloomfield, NY.
- (23) Model 23D-6102C, Computer Devices, Santa Fe Springs, CA.
- (24) Glenco Scientific, Inc., Houston, TX.
- (25) Model H13BI, General Electric, Syracuse, NY.
- (26) Model LM324, National Semiconductor, Santa Clara, CA.
- (27) Power One, Inc., Camarillo, CA.
- (28) Semiconductor Circuits, Haverhill, MA.
- (29) Model 6100, Intersil, Cupertino, CA.
- (30) Digital Equipment Corp., Maynard, MA.
- (31) M.D. Joseph, Ph.D. thesis, MSU, 1978.
- (32) D.R. Christmann, Ph.D. thesis, MSU, 1980.
- (33) Pacific Cyber/Metrix, Inc., San Ramon, CA.
- (34) Teledyne, Hawthrone, CA.
- (35) Scovill, Wake Forest, NC.
- (36) "Sigma Stepper Motor Handbook," Sigma Instruments, eds., Braintree, MA.
- (37) C.J. Patton, unpublished data.
- (38) D.A. Skoog and D.M. West, "Fundamentals of Analytical Chemistry," Holt, Rinehart, and Winston, NY (1976).
- (39) Model EU-701A, GCA McPherson Corp., Acton, MA.
- (40) Model 427, Keithley Instruments, Inc., Cleveland, OH.
- (41) L.D. Rothman, J.D. Ingle, Jr., and S.R. Crouch, <u>Anal.</u> <u>Chem.</u>, <u>47</u>, 1226 (1975).

- (42) W.C. Vosburgh and G.R. Cooper, <u>J. Amer. Chem. Soc.</u>, <u>63</u>, 437 (1941).
- (43) S.R. Crouch, F.J. Holler, P.K. Notz, and P.M. Beckwith, Appl. Spec. Rev., 13(2), 165 (1977).
- (44) P.M. Beckwith and S.R. Crouch, <u>Anal. Chem.</u>, <u>44</u>, 221 (1972).
- (45) Wai Tak Law, Ph.D. thesis, MSU, 1978.
- (46) R. Gall, Ph.D. thesis, MSU, 1978.
- (47) P.K. Notz, Ph.D. thesis, MSU, 1977.
- (48) A. Scheeline, B.S. thesis, MSU, 1974.
- (49) P.M. Beckwith, Ph.D. thesis, MSU, 1972.
- (50) Heath Co., Benton Harbor, MI.
- (51) Model EU 701-50, Heath Co.
- (52) Model EU 700/E, Heath Co.
- (53) Model 1P28A, RCA.
- (54) "Small Computer Handbook," DEC eds., 1972.
- (55) Model MM8, DATEL Systems, Inc., Canton, MA.
- (56) Model ADC-HZ12BGC, DATEL.
- (57) Model AD582, Analog Devices, Norwood, MA.
- (58) G. Gonzalez, University of Minnesota.
- (59) "Fundamentals of Clinical Chemistry," N.W. Tietz, ed., W.B. Saunders Co., Philadelphia, PA., 1976, p. 116.
- (60) B.G. Willis, J.A. Bittikofer, H.L. Pardue, and D.W. Margerum, Anal. Chem., 42, 1340 (1970).
- (61) G.E. Mieling, H.L. Pardue, Anal. Chem., 50, 1333 (1978).
- (62) A.C. Javier, S.R. Crouch, and H.V. Malmstadt, <u>Anal.</u> <u>Chem.</u>, <u>41</u>, 239 (1969).
- (63) DADE Division, American Hospital Supply.
- (64) M.I. Karayannis, Anal. Chim. Acta, 76, 121 (1975).

- (65) M.I. Karayannis, <u>Talanta</u>, <u>23</u>, 27 (1976).
- (66) H.V. Malmstadt, K.M. Walczak, M.A. Koupparis, <u>Amer.</u>
  <u>Lab.</u>, <u>12</u>, 27 (1980).
- (67) U. Isacsson and G. Wettermark, <u>Anal. Chim. Acta</u>, <u>83</u>, <u>227</u> (1976).
- (68) U. Isacsson and G. Wettermark, <u>Anal. Letters</u>, <u>11(1)</u>, 13 (1978).
- (69) D.F. Marino and J.D. Ingle, Jr., <u>Anal. Chim. Acta</u>, <u>87</u>, 163 (1976).
- (70) D.F. Marino and J.D. Ingle, Jr., <u>Anal. Chem.</u>, <u>53</u> 456 (1981).
- (71) W.R. Seitz and M.P. Neary, <u>Anal. Chem.</u>, <u>46</u>, 188A (1974).
- (72) H.O. Albrecht, <u>Z. Phys. Chem.</u>, <u>136</u>, 321 (1928).
- (73) F. Gorus and E. Schram, <u>Clin. Chem.</u>, <u>25</u>, 512 (1979).
- (74) W.R. Seitz, <u>J. Phys. Chem.</u>, <u>79</u>, 101 (1975).
- (75) U. Isacsson, J. Kowaleska, and G. Wettermark, J. Inorg. Nucl. Chem., 40, 1653 (1978).
- (76) C.J. Patton, Master's thesis, MSU, 1974.
- (77) A. Savitzky and M.J.E. Golay, <u>Anal. Chem.</u>, <u>36</u>, 1627 (1964).
- (78) #12,307-2, Aldrich Chemical Co., Milwaukee, WI.
- (79) "CRC Handbook of Chemistry and Physics," R.C. Weast, ed., CRC Press, Cleveland, OH., 1974, p. D-113
- (80) R.M. Chapin, <u>J. Amer. Chem. Soc.</u>, <u>56</u>, 2211 (1934).

